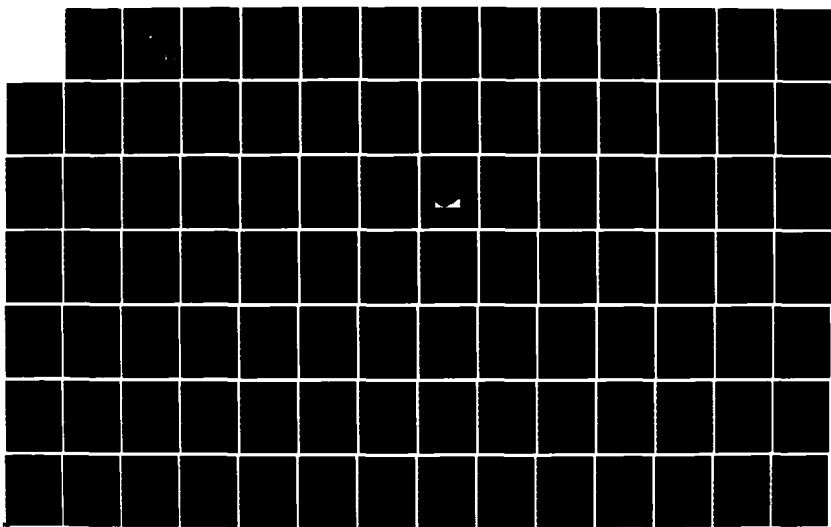


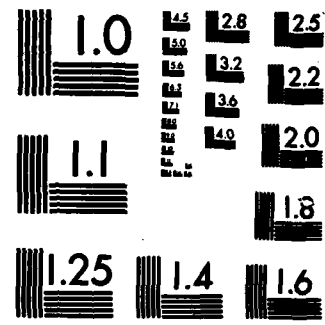
AD-A158 784 THE IMPLICIT FINITE-DIFFERENCE (IFD) ACOUSTIC MODEL IN 1/2
A SHALLOW WATER ENVIRONMENT(U) NAVAL POSTGRADUATE
SCHOOL MONTEREY CA M E KOSNIK JUN 84

UNCLASSIFIED

F/G 28/1

NL





MICROCOPY RESOLUTION TEST CHART
NATIONAL BUREAU OF STANDARDS-1963-A

(2)

NAVAL POSTGRADUATE SCHOOL

Monterey, California



AD-A150 784

DTIC FILE COPY

THESIS

THE IMPLICIT FINITE-DIFFERENCE (IFD)
ACOUSTIC MODEL
IN A SHALLOW WATER ENVIRONMENT

by

Mark E. Kosnik

June 1984

Thesis Co-advisors:

J.V. Sanders
C.R. Dunlap

Approved for public release; distribution unlimited

DTIC
ELECTED

MAR 4 1985

85 : 02 19 079

UNCLASSIFIED

SECURITY CLASSIFICATION OF THIS PAGE (When Data Entered)

REPORT DOCUMENTATION PAGE		READ INSTRUCTIONS BEFORE COMPLETING FORM												
1. REPORT NUMBER	2. GOVT ACCESSION NO.	3. RECIPIENT'S CATALOG NUMBER												
4. TITLE (and Subtitle) The Implicit Finite-Difference (IFD) Acoustic Model in a Shallow Water Environment		5. TYPE OF REPORT & PERIOD COVERED Master's Thesis June 1984												
7. AUTHOR(s) Mark E. Kosnik		6. PERFORMING ORG. REPORT NUMBER												
9. PERFORMING ORGANIZATION NAME AND ADDRESS Naval Postgraduate School Monterey, California 93943		10. PROGRAM ELEMENT, PROJECT, TASK AREA & WORK UNIT NUMBERS												
11. CONTROLLING OFFICE NAME AND ADDRESS Naval Postgraduate School Monterey, California 93943		12. REPORT DATE June 1984												
14. MONITORING AGENCY NAME & ADDRESS (if different from Controlling Office)		13. NUMBER OF PAGES 128												
		15. SECURITY CLASS. (of this report)												
		15a. DECLASSIFICATION/DOWNGRADING SCHEDULE												
16. DISTRIBUTION STATEMENT (of this Report) Approved for public release; distribution unlimited		<table border="1"> <tr> <td>Accession For</td> </tr> <tr> <td>NTIS GRA&I</td> </tr> <tr> <td>DTIC TAB</td> </tr> <tr> <td>Unannounced</td> </tr> <tr> <td>Justification</td> </tr> <tr> <td>By _____</td> </tr> <tr> <td>Distribution/</td> </tr> <tr> <td>Availability Codes</td> </tr> <tr> <td>Dist</td> <td>Avail and/or Special</td> </tr> <tr> <td>A-1</td> <td></td> </tr> </table>	Accession For	NTIS GRA&I	DTIC TAB	Unannounced	Justification	By _____	Distribution/	Availability Codes	Dist	Avail and/or Special	A-1	
Accession For														
NTIS GRA&I														
DTIC TAB														
Unannounced														
Justification														
By _____														
Distribution/														
Availability Codes														
Dist	Avail and/or Special													
A-1														
17. DISTRIBUTION STATEMENT (of the abstract entered in Block 20, if different from Report)														
18. SUPPLEMENTARY NOTES (+1 1472L)														
19. KEY WORDS (Continue on reverse side if necessary and identify by block number) Pressure Amplitude, Trapped Normal Mode Propagation, Shallow Water Acoustics, Ocean Modeling														
20. ABSTRACT (Continue on reverse side if necessary and identify by block number) In this thesis														
<p>An implicit finite-difference (IFD) computer model was developed by Jaeger to solve the parabolic equation. The model preserves continuity of pressure and the normal component of particle velocity at the ocean bottom where there is an interface between media with different sound speeds and densities. This feature was implemented to make the model more accurate.</p>														

(Cont.)

UNCLASSIFIED
SECURITY CLASSIFICATION OF THIS PAGE (When Data Entered)

in a shallow water environment. The IFD performance in a shallow water environment is analyzed. The IFD results are compared with those of two other models and analyzed in light of basic physical reasoning. In addition, a single sloping ocean bottom is modeled in an experimental tank so that the measured pressure field can also be compared to IFD model results.

Originator-Supplied Keywords include:

(to 1473A)

S N 0102-LF-014-6601

B

UNCLASSIFIED
2 SECURITY CLASSIFICATION OF THIS PAGE (When Data Entered)

Approved for public release; distribution unlimited.

The Implicit Finite-Difference (IFD)
Acoustic Model
in a Shallow Water Environment

by

Mark E. Kcsnik
Lieutenant, United States Navy
E.B.A., University Of Notre Dame, 1973

Submitted in partial fulfillment of the
requirements for the degree of

MASTER OF SCIENCE IN METEOROLOGY AND OCEANOGRAPHY

from the

NAVAL POSTGRADUATE SCHOOL
June 1984

Author: Mark E. Kcsnik

Approved by: James V. Sondes

Thesis Co-Advisor

Calvin P. Dunlap

Thesis Cc-Advisor

Christopher J. Kilwee

Chairman, Department of Oceanography

J.W. Dyer

Dean of Science and Engineering

ABSTRACT

An implicit finite-difference (IFD) computer model was developed by Jaeger to solve the parabolic equation. The model preserves continuity of pressure and the normal component of particle velocity at the ocean bottom where there is an interface between media with different sound speeds and densities. This feature was implemented to make the model more accurate in a shallow water environment. The IFD performance in a shallow water environment is analyzed. The IFD results are compared with those of two other models and analyzed in light of basic physical reasoning. In addition, a simple sloping ocean bottom is modeled in an experimental tank so that the measured pressure field can also be compared to IFD model results.

TABLE OF CONTENTS

I.	INTRODUCTION	10
II.	THE IFD COMPUTER MODEL	12
A.	BACKGROUND	12
B.	THE COMPUTER MODEL	13
C.	MODEL PROBLEMS/MODIFICATIONS	14
D.	MODEL VERIFICATION	18
1.	Comparison with Jaeger Model Run	18
2.	Comparison with Jensen and Kuperman Model Run	19
3.	Comparison with Coppens, Humphries and Sanders Model Run	28
4.	Comparison with Physical Reasoning	30
5.	Verification Summary	40
III.	LABORATORY MEASUREMENTS	42
A.	BACKGROUND	42
B.	EXPERIMENTAL DESIGN	42
1.	The Task	42
2.	Signal Generating/Receiving Equipment . .	44
C.	MEASUREMENT PROCEDURES	47
IV.	MODEL RESULT COMPARISONS WITH LABORATORY MEASUREMENTS	53
A.	INTRODUCTION	53
B.	THE GENERAL ANALYSIS	53
C.	THE DETAILED ANALYSIS	64
V.	CONCLUSIONS/RECOMMENDATIONS	75
A.	CONCLUSIONS	75

1. Performance of the IFD Model	75
2. Modeling/Measurement Procedures	76
B. RECOMMENDATIONS	76
APPENDIX A: REVISED IFD PROGRAM LISTING	78
APPENDIX E: TL CONTCUR PLOT PROGRAM LISTING	113
APPENDIX C: RUNNING THE CONTCUR PLOT ON THE NPS COMPUTER	115
A. INTRODUCTION	115
E. COPYING THE FILE FOR USE	115
C. RUNNING THE PROGRAM	115
APPENDIX D: SOURCE DEPTH SENSITIVITY ANALYSIS	117
BIBLIOGRAPHY	125
INITIAL DISTRIBUTION LIST	127

LIST OF FIGURES

2.1	Jaeger's Deep-to-Shallow Water Case	19
2.2	Jensen and Rberman Sloping Bottom Case	20
2.3	IFI and JKM Comparison at a Range of 2.5 Km . .	22
2.4	IFI and JKM Comparison at a Range of 5.0 Km . .	23
2.5	IFI and JKM Comparison at a Range of 7.5 Km . .	24
2.6	IFI and JKM Comparison at a Range of 10.0 Km . .	25
2.7	IFI and JKM Comparison at a Range of 12.5 Km . .	26
2.8	10 Degree Simple Sloping Bottom Case	29
2.9	IFI and CHSE Comparison at the Apex	31
2.10	IFI TL Contours(db) from the Source to 604 Meters	33
2.11	IFI TL Contours(db) from 600 to 1350 Meters . .	34
2.12	IFI TL Contours(db) from 1350 to 2100 Meters . .	35
2.13	IFI TL Contours(db) from 1550 to 2300 Meters . .	36
2.14	Normal Mode Propogation in a Wedge Shaped Ocean	39
3.1	Experimental Tank Set Up	43
3.2	Electronic Equipment Schematic	46
3.3	Pulse Length Analysis at 3.0X	49
3.4	Pulse Length Analysis at 10.4X	50
3.5	Pulse Length Analysis at 10.4X	51
4.1	Comparison of Results at 1.0X	54
4.2	Comparison of Results at 2.1X	55
4.3	Comparison of Results at 3.1X	56
4.4	Comparison of Results at 4.2X	57
4.5	Comparison of Results at 5.2X	58
4.6	Comparison of Results at 6.2X	59
4.7	Comparison of Results at 7.3X	60

4.8	Comparison of Results at 8.3X	61
4.9	Comparison of Results at 9.4X	62
4.10	Comparison of Results at 10.4X	63
4.11	Comparison of Results at 0.7X	65
4.12	Comparison of Results at 0.8X	66
4.13	Comparison of Results at 1.0X	67
4.14	Comparison of Results at 1.3X	68
4.15	Comparison of Results at 1.5X	69
4.16	Comparison of Results at 1.7X	70
4.17	Comparison of Results at 1.9X	71
4.18	Comparison of Results at 2.1X	72
4.19	Comparison of Results at 2.3X	73
I.1	Source Sensitivity Analysis at 1.0X	119
I.2	Measurements with Source Depth of 5, 7, and 9 Cm	120
I.3	Measurements with Source Depth of 11, 13, and 15 Cm	121
I.4	Measurements with Source Depth of 17, 19, and 21 Cm	122
I.5	Measurements with Source Depth of 23, 25, and 27 Cm	123
I.6	Measurements with Source Depth of 29 and 31 Cm	124

ACKNOWLEDGEMENTS

The author thanks LCDR James Nelson, USN, for his advice and assistance in developing many of the graphics plotting programs. Appreciation is also due LT Patrick LeSesne, USCG, for his many long hours spent assisting in the laboratory while compiling the experimental data. Thanks are also due to Professor Calvin Dunlap for his review of the thesis.

The author also expresses his appreciation to Dr. Alan E. Cappens for his advice and clarification given to the theoretical aspects of the thesis. Finally, the author thanks Dr. James V. Sanders for his time and effort in assisting in all aspects of research and thesis preparation. Without the knowledge, patience, and advice of the Cappens and Sanders team this thesis would not have been possible.

I. INTRODUCTION

A variety of acoustic models exist to predict transmission loss. Each of these models contain inherent strengths and weaknesses. All have shown poor results in a shallow water environment due to difficulties at the ocean bottom where there is an interface between media of different sound speeds and densities.

Since its introduction (Hardin and Tappert, 1973), the parabolic wave equation has been a widely accepted means of solution for acoustic propagation. The earliest programs used a split-step Fourier transform algorithm to solve the parabolic equation (FE). Several other solution techniques have been developed primarily to overcome difficulties that occur when the Fourier transform encounters an interface between different media (Lee and Botseas, 1982 and McDaniel and Lee, 1982).

An alternative solution technique that uses an implicit finite-difference (IFI) algorithm was developed by Lee and Papadakis (1979). This method incorporates appropriate interface conditions and allows solutions in shallow water. Starting with the IFI algorithm, Jaeger (1983) developed a computer model to predict transmission loss and acoustic pressure based on user specified bottom topography and a single sound speed profile. This computer model uses the mathematical treatment of the horizontal and sloping interfaces developed by McDaniel and Lee (1982) and Lee and McDaniel (1983). It also utilizes several design features and methods incorporated in an earlier computer program developed by Lee and Eoteas (1982), and a PE computer model developed by Brock (1978).

The IFD program preserves continuity of pressure and continuity of the normal component of particle velocity at an interface between media having different sound speeds and densities. This feature makes the program unconditionally stable and better able to handle the bottom boundary condition.

Since its development, the IFD program has not been rigorously tested. This thesis analyzes the program's performance in an idealized shallow water environment. The environment includes a simple sloping sand bottom beneath an isospeed water field. The analysis begins by comparing the IFD's predictions with predictions from Jenson and Kuperman's (1980) FE model and Coppens, Humphries and Sander's (1984) image model. The analysis also includes a comparison of the model's estimated transmission loss contours with expectations based on simple physical reasoning. Finally, the thesis describes an attempt to model a shallow sloping bottom in an experimental tank. The tank contains a sand bottom sculptured with a ten degree slope. Laboratory measurements of the pressure field are taken at a frequency of 100 kHz for comparison to the predicted pressure field generated by the IFD. These comparisons of the IFD predictions with other model estimates, theory, and laboratory measurements give an indication of the IFD's performance in a shallow water environment.

II. THE IFD COMPUTER MODEL

A. BACKGROUND

An implicit finite-difference solution technique to the parabolic equation has been studied and refined by many authors. The history of this development is explained in detail by Jaeger (1983), but merits review in order to gain a perspective on an analysis of the IFD computer model. The parabolic equation is an approximation to the elliptical wave equation. The first means of solving the PE used a split-step fast Fourier transform method as developed by Tappert and Hardin (1973). This method requires periodic boundary conditions in depth because of the finite Fourier transform and handles this constraint by introducing an artificial horizontal pressure release bottom below the actual physical bottom. This method of implementing an artificial bottom was incorporated into the earliest PE models developed by Jenson and Krol (1975) and Brock (1978).

Errors in this split-step Fourier transform method were found to be proportional to the horizontal range step and the second derivative of the index of refraction. The second derivative of the index of refraction tends to be large across the ocean bottom interface. Another problem with the split-step method is that it does not consider density differences between two different media at an interface, which influences the reflection coefficient. For these reasons the split-step Fourier transform method proved to be poorly suited for a shallow water environment.

The IFI solution method was introduced by Lee and Papadakis (1979) as an alternative to the split-step method. The IFD method employs a second order central difference

formula to solve the PE in the form of a tridiagonal matrix. Although the first version of the IFD did handle discontinuities in the sound speed profile, it did not consider density discontinuities. In 1982 McDaniel and Lee introduced a method to handle a horizontal interface of different densities. In 1983, they extended their treatment to include a sloping interface. It is this version of the IFD that is used in Jaeger's computer program.

E. THE COMPUTER MODEL

The IFD computer program consists of a main program and twenty subroutines. The program utilizes a modular construction so that each of the various subroutines are called from the main program to complete a specific calculation or function when required. The IFD is run interactively from a user generated input file that contains values for frequency, one sound speed profile, a bottom profile, source/receiver depths, attenuation coefficients for both the water and the bottom, and several other input parameters that tell the program where to obtain a solution within the field. The program initiates the calculations assuming an initial Gaussian pressure field and an artificial pressure release surface at a user specified depth.

Attenuation in both the water and the sediment is handled as complex indices of refraction. An artificial attenuation layer is established beneath the sediment to introduce attenuation above the artificial pressure release surface. The actual magnitude of this enhanced attenuation is calculated using an equation derived by Brock (1978) for use in his PE computer model.

The IFD program steps along the specified bottom profile and makes calculations down through the water/sediment column at each user specified horizontal range. The program

requires that the bctcm intersect exactly at a vertical grid point. As a result, for a sloping bottom the program automatically calculates the range step to fulfill this requirement. This computer generated range step is always less than or equal to the user provided range step. As the slope of the bottom increases, the range step must decrease and more calculations and computer time are required to solve the entire pressure field. In some situations an actual modification of the user inputted bottom is required. This occurs with a very gently sloping bottom when the required range step exceeds the user specified range step. Here, the program automatically models the bottom as a series of level and sloping sections in order to ensure the user generated range step is not exceeded. This modification of the bctcm is always less than or equal to one-half the vertical grid spacing and the model issues a warning to the user of the modification.

Both printed and graphical output are provided by the IFD. The printed output provides transmission loss and the real and imaginary components of the pressure field at each depth for a specified horizontal range. The graphical output is a plot of transmission loss versus range at the user specified receiver depth.

C. MODEL PROBLEMS/MODIFICATIONS

As this study of the IFD program progressed, it became necessary to modify certain aspects of the model. Most of these modifications were necessary to alter the program output into a more desirable form, but a few were implemented to correct programming deficiencies. Although this section of the thesis discusses the earliest model runs, these results are not presented in detail, but only discussed in general terms because they were obtained before

the computer model was fully modified. All modifications were made only after careful analysis of multiple model runs. It is important to realize that all results generated for comparison to other models and laboratory measurements came from a fully modified version of the IFD.

Since the ultimate objective of this study was to compare IFD model results with laboratory measurements the program was first run with input parameters which exactly modeled conditions in the tank. The experimental set up, explained later in great detail, consisted of a tank that is approximately two meters in length, one meter in depth, with a ten degree sloping sand bottom and a maximum water depth of 35 centimeters(cm). Based on a test case run by Jaeger (1983) of a simple sloping bottom, and by results shown by Jense and Kuperman (1980) for propagation in a wedge-shaped ocean, it was expected that there would be certain recognizable patterns in the predicted propagation patterns. Specifically, since the speed of sound in the bottom exceeds that in the water (fast bottom), the simple sloping bottom supports trapped normal mode propagation (Coppens and Sanders, 1981). As the acoustic energy travels up slope toward the apex, successively lower modes are cut off and the energy contained in these modes is transmitted into the bottom. The range from the apex at which energy of the lowest mode is transmitted into the bottom is referred to as the dump distance and is a function of wavelength, wedge angle, and the ratio of sound speed in the water to the sound speed in the sediment. An empirical equation that defines this dump distance was derived by Coppens, Sanders, Ioannou, and Kawamura (1978); and was used to identify the expected ranges of these dump distances for the given scenario described above.

The initial unmodified IFD run used the parameters taken from the tank and showed no recognizable patterns in the

acoustic field. There was no observable decrease in transmission loss at the various dump distances as expected. Rather, results indicated widely fluctuating patterns in the acoustic field that appeared inconsistent with both previous studies and simple physical reasoning. Upon closer analysis, it was discovered that although the program was designed to be independent of scale there are several logic statements that are not implemented if the user provided range step is less than one meter. Because the logic statements aren't satisfied, the NEWSEG and NEWMAT subroutines (Jaeger, 1983) are not called correctly. The NEWSEG subroutine initializes the kctcm slope and the NEWMAT subroutine computes matrix elements for the program. Obviously, errors in these two program functions seriously distort results. Because of this systematic error in the program it became necessary to scale up all tank parameters. All distances were scaled up by a factor of 1000, and frequency was scaled down by a factor of 1000. Careful analysis reveals that all input parameters are a function of either distance or frequency, so this scaling produces results that model those expected in the tank.

The second modification of the IFD was required to provide a three dimensional graphics display. As discussed earlier, the IFD provides a transmission loss plot versus range at a single depth. However, to study the model predictions in greater detail it was felt that a two dimensional analysis of the model estimates would be more meaningful. As a result a transmission loss contouring program was developed. The program (Appendix B) displays transmission loss contours for range versus depth. Use of the contour plot requires that transmission loss values generated by the IFD be sent to a data disk used by the contour routine. To facilitate this transfer a dummy variable (LIFD) was established in the PRINT2 subroutine to store the transmission loss values and then these values are written to the data disk at the end of the main program.

Another modification of the IFD output was required to change the real and imaginary components of the pressure to a single pressure amplitude magnitude. It was felt that dealing with the pressure magnitude was easier and more meaningful than with the real and imaginary components of the pressure field. This conversion was done in the PLINT2 subroutine and established a new variable (PRMAG) to represent the pressure magnitude.

A final modification in the computer program was made due to a suspected error in the computation of the attenuation in the artificial layer. Physical reasoning dictates that proper implementation of the artificial attenuation would result in a steady drop off in acoustic pressure with depth throughout the artificial layer, with pressure dropping to zero at the pressure release surface. IFD model results on the other hand showed wide fluctuations in pressure with depth in the layer and then only a minimal fall off at the pressure release surface. The equation in the IFD that actually computes the magnitude of the attenuation in the artificial layer was taken directly from Brock's (1978) PE model (Jaeger, 1983). However, Brock's equation was derived with feet as the unit of measurement while Jaeger's model is derived with meters as the unit of measurement. With this in mind, Jaeger's equation should be approximately a factor of three larger than Brock's equation to correct for the difference in units. To correct for this error the equation to calculate attenuation (ATT(I)) in the NEWMAT subroutine was increased by a factor of three. When this correction was implemented, the large fluctuations in pressure with depth were eliminated. The expected drop off in pressure with depth and the fall off of pressure to zero at the pressure release surface were noted.

A listing of the revised IFD computer program with all modifications can be seen in Appendix A.

L. MODEL VERIFICATIONS

1. Comparison with Jaeger Model Run

In light of the modifications to the IFD computer program just discussed, it was necessary to ensure that the changes themselves did not introduce errors into the model. So as a first step the modified IFD program was run for one of the test cases used by Jaeger in his original work. This case analyzes propagation in an environment that moves from deep to shallow water. This particular environment is depicted in Figure 2.1 and was chosen because it was very similar to the simple sloping bottom in the tank experiment. A solution is obtained for a bottom with an upslope of 8.5 degrees. An isospeed water field is used with sound speed set at 1500 m/s. Source frequency is 25 Hz. The scenario has a maximum depth of 350 meters and a range of 40 kilometers. Both the source and the receiver are set at 25 meters.

The results using the modified IFD program were the same as Jaeger's for this test case above the artificial attenuation layer. As explained earlier, the program was modified to reflect higher attenuation in the artificial layer, so as to properly reflect the effect of attenuation in this region. The modified program results did not show the large fluctuations in pressure with depth in the artificial layer but rather the gradual decline in pressure towards a value of zero at the pressure release surface. But above the artificial layer the modified program results were identical with those achieved by Jaeger with the original program. Apparently, the minor changes in the program designed to improve on the form of the program output does not hinder the model's ability to achieve a solution in the upper sediment and water column.

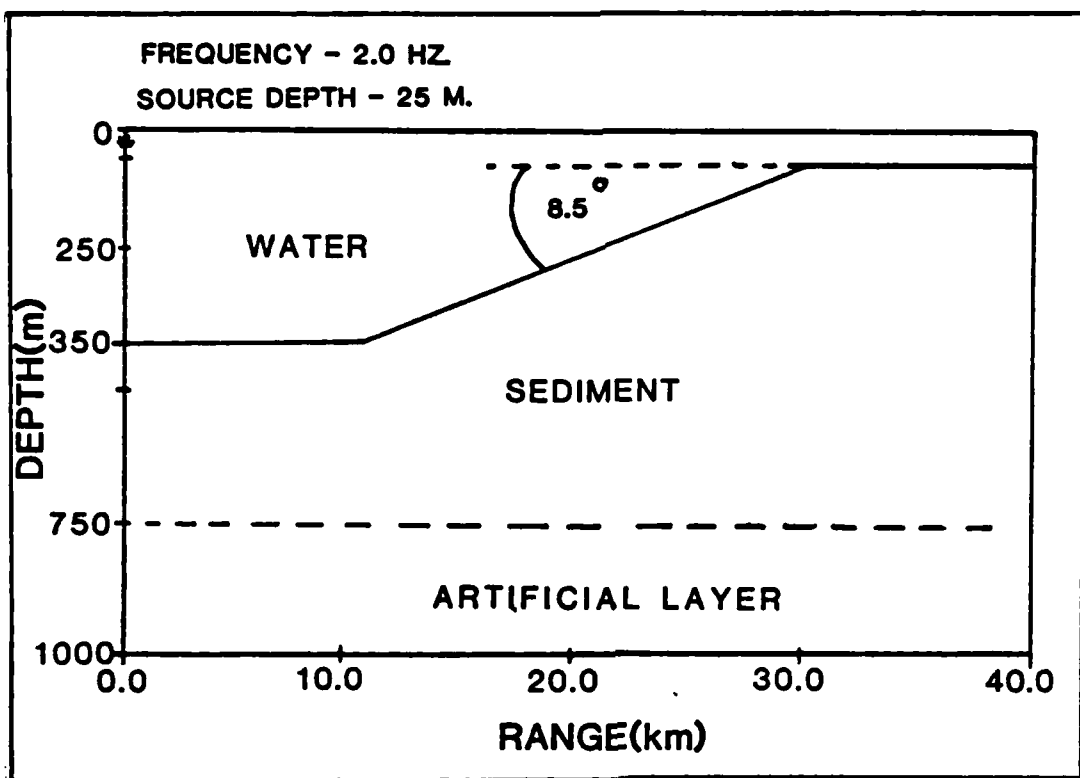


Figure 2.1 Jaeger's Deep-to-Shallow Water Case.

2. Comparison with Jensen and Kuperman Model Run

The second attempt at verifying the IFD model involved a comparison of model results with those achieved with a FE model designed by Jensen and Kuperman (1980). The Jensen and Kuperman Model (JKM) uses a split-step solution technique. Comparison with this particular model was chosen because it is one of the few that obtains a solution in two dimensions. Most acoustic models obtain a solution at only a single depth. In addition, Jensen and Kuperman made their model runs in a simple sloping ocean bottom environment very similar to the scenario of interest modeled in the task. This environment is depicted in Figure 2.2 and features a gently sloping bottom of 2.2 degrees. The water column has a

uniform speed of 1500 m/s. The source is placed just below the midpoint in the channel at 112 meters and is driven at a frequency of 25 Hz. The maximum depth in this scenario is 200 meters and has a maximum range of 12.5 kilometers.

The Jensen and Kuperman results were expressed as

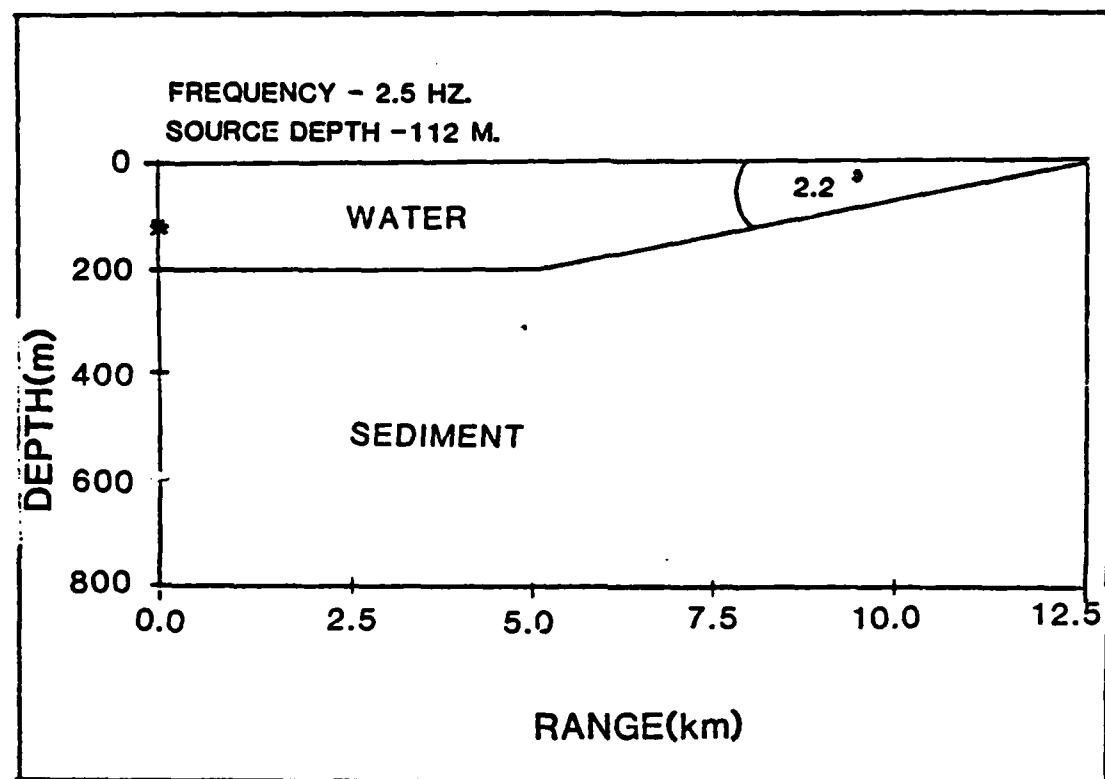


Figure 2.2 Jensen and Kuperman Sloping Bottom Case.

transmission loss contours for range versus depth. Their study concentrated on transmission loss patterns in the sediment, but results were obtained both in the sediment and in the water. These results are compared to the IFD results at ranges of 2.5, 5.0, 7.5, 10.0, and 12.5 kilometers. These ranges were chosen for analysis because the JKM results showed the greatest variation in transmission loss with

depth and thus, makes for a more meaningful comparison with the IFL results.

The IFD and JKM results can be seen in Figure 2.3 through Figure 2.7. In all the figures, the IFD estimates are shown as a solid curve while the Jensen and Kuperman results are depicted as circular points. The first analysis is at a range of 2.5 kilometers. From Figure 2.2, it can be seen that the depth at this range is 200 meters and is in a flat bottom region. From the results shown in Figure 2.3, it is obvious that both models obtained almost identical results from the surface down to a depth of about 300 meters. There are differences between the two sets of predictions from the ocean bottom to a depth of 100 meters below this point. Below 300 meters the Jensen and Kuperman results show a very slight increase in transmission loss (IL) with depth. The IFD also shows an overall increase in transmission loss with depth but with several fluctuations in transmission loss and a marked peak at about 300 meters. So in general, the results from the two models have the same general tendencies although the IFD appears to show greater detail in results near the water/sediment boundary.

Figure 2.4 shows results at 5.0 km in range. Here, the water depth is still 300 meters and marks the very beginning of the sloping bottom section. For this range the JKM predictions are only available to a depth of 300 meters. The results are nearly identical with those obtained by the IFD. Both models show a relative minimum in transmission loss at a depth of 100 meters and then a gentle increase in IL with depth.

The model results at a range of 7.5 km are seen in Figure 2.5. At this range the bottom depth is about 150 meters and the bottom is sloping. The models show the greatest difference at this range. Both models produce nearly identical results in the water column, but beneath

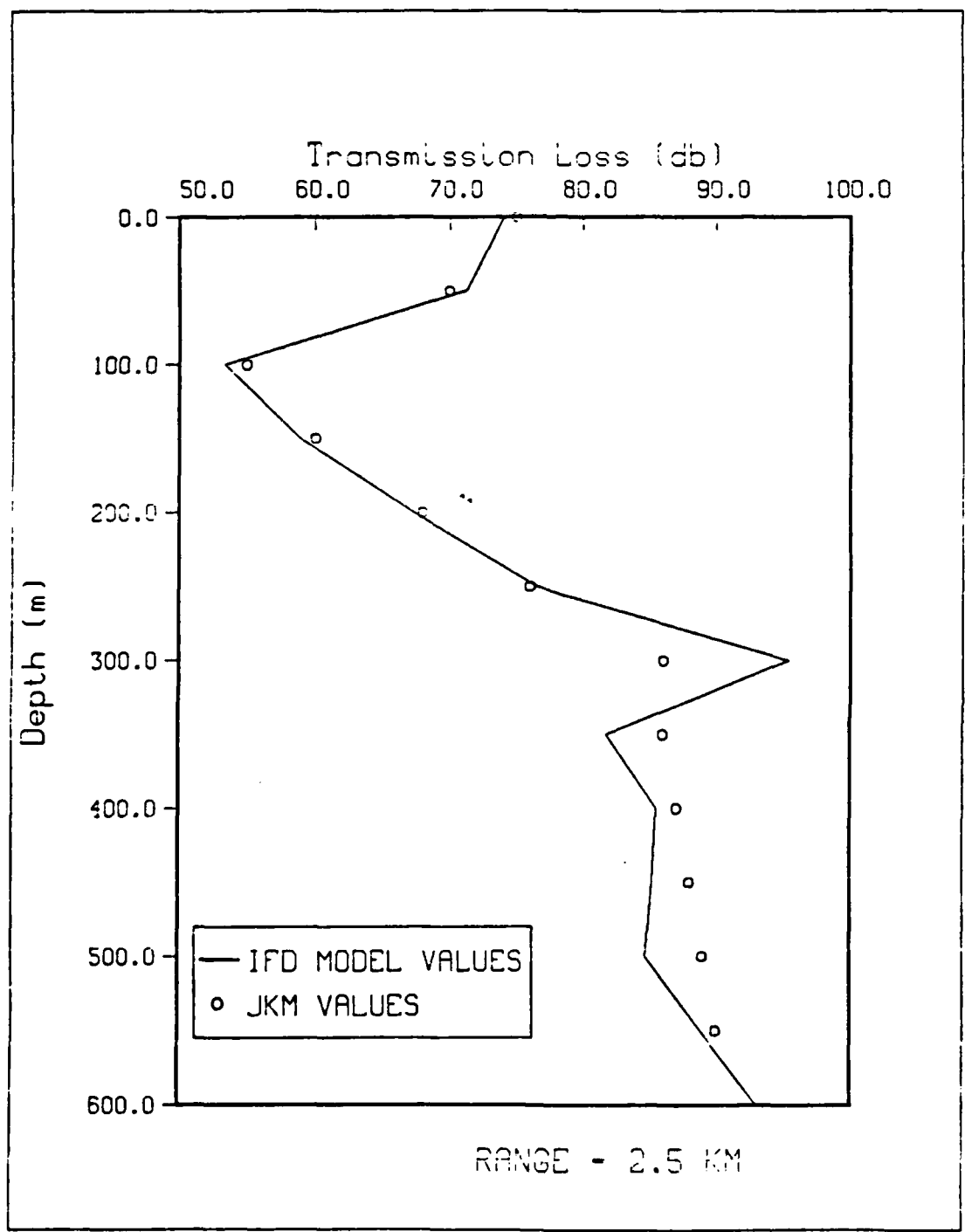


Figure 2.3 IFD and JKM Comparison at a Range of 2.5 Km.

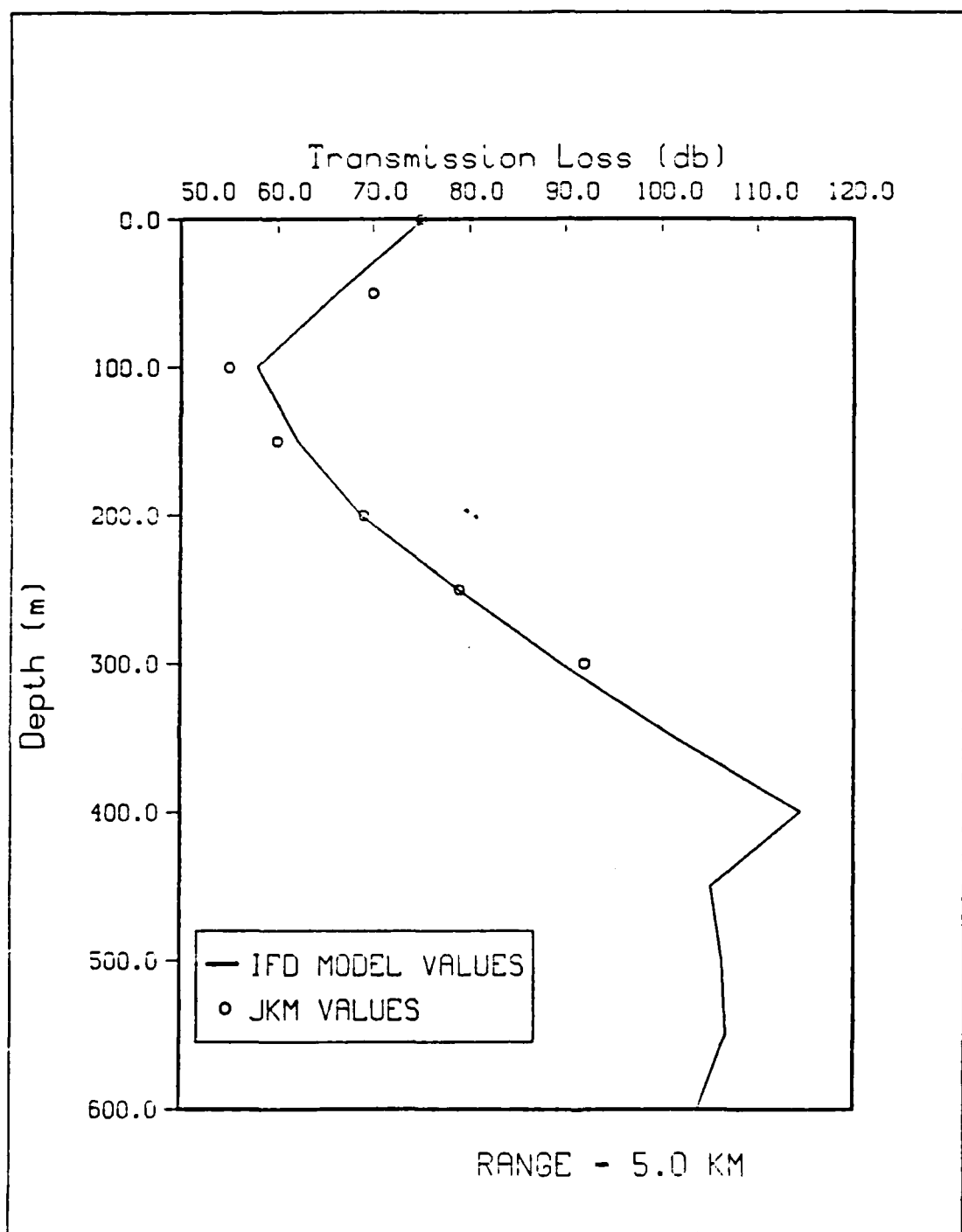


Figure 2.4 IFD and JKM Comparison at a Range of 5.0 Km.

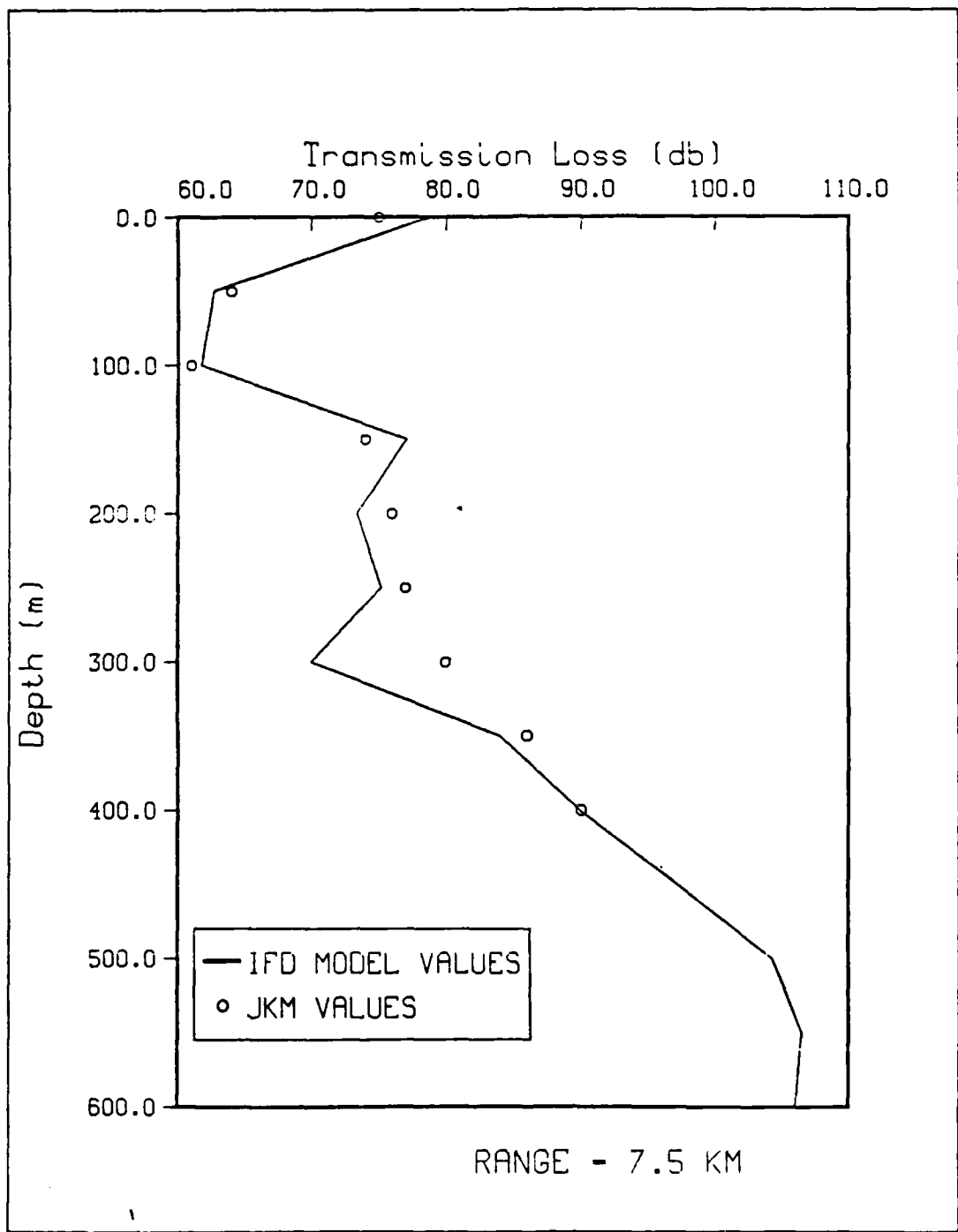


Figure 2.5 IFD and JKM Comparison at a Range of 7.5 Km.

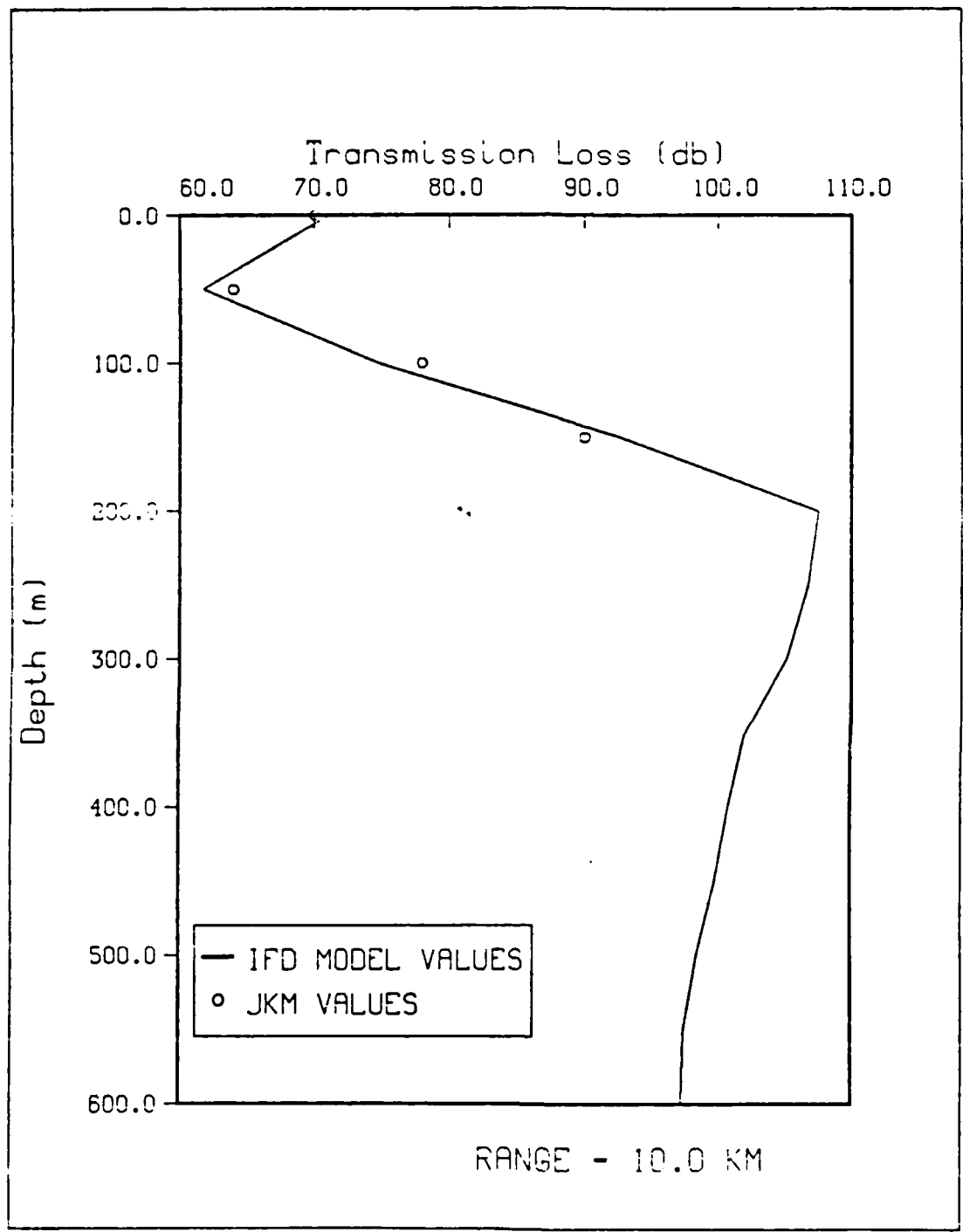


Figure 2.6 IFD and JKM Comparison at a Range of 10.0 Km.

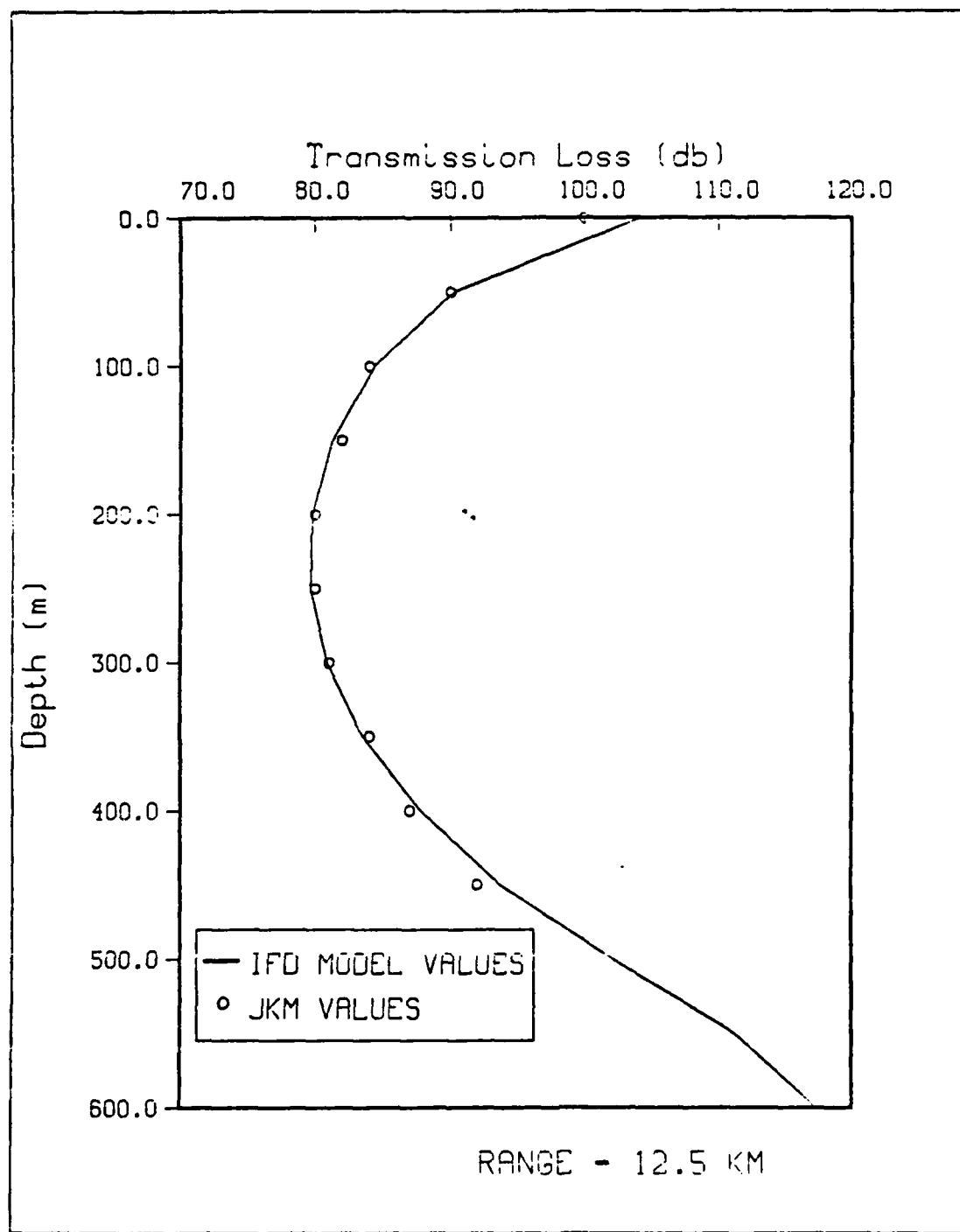


Figure 2.7 IFO and JKM Comparison at a Range of 12.5 Km.

150 meters in depth the model estimates begin to show differences. The Jensen and Kuperman results show a gradual increase in TL with depth below the ocean bottom. The IFD results on the other hand, show a gradual decrease in transmission loss from 150 meters to 300 meters, with a relative minimum at 300 meters and then an increase in TL beneath this depth. Although there are some differences in model estimates near the boundary in the flat bottom sections previously discussed, the differences appear to be greater at the boundary in this sloping bottom case. In those regions away from the boundary in either the water column or in the sediment, however, both models produce similar results. The JKMs difficulty in obtaining an accurate solution at the sediment boundary is not totally unexpected. The model uses a variation of the straight split-step solution technique similar to Brock's computer model (Jensen and Kuperman, 1980), that has characteristically been unsuccessful in obtaining a reliable solution near a boundary.

The results at a range of 10.0 km are seen in Figure 2.6. At this range the water depth is approximately 100 meters and the bottom is again in a sloping region. At this range Jensen and Kuperman results are only available to about 150 meters in depth. For the data available, the models produce nearly identical results. Both models predict a minimum at about 50 meters in depth and then an almost linear increase in TL with depth. The IFD results also reflect a transmission loss maximum at about 200 meters, and then a slight decrease of TL beneath this depth. Data at these depths are not available from the Jensen and Kuperman run. In light of the results obtained at 7.5 km for a sloping bottom case one might expect that the results for the two models would show differences near the ocean bottom. However, since there is only one Jensen and Kuperman prediction available near the bottom for this range, it is

difficult to make any definite conclusions regarding differences in model performance at the boundary.

Results at the apex (range equal to 12.5 km) can be seen in Figure 2.7. Since all estimates are made in the sediment at this range, there is no boundary to contend with. At this range the two models show the best agreement. Both models show a gradual decrease in transmission loss to a depth of about 300 meters and then a gradual increase of TL with depth.

In general, there appears to be good agreement between the IFD and the JKM model results in regions not influenced by a boundary. In both the water and the deep sediment the two models produce similar results. Although this is not conclusive evidence, these similarities suggest that the IFD can successfully model acoustic propagation in these regions. Near the water/sediment boundary however, the Jenser and Kuperman and IFD predictions show marked differences. These differences appear to intensify as the bottom becomes more sophisticated. In general, the Jenser and Kuperman results do not seem to show the detail the IFD results do. Considering the different solution techniques employed by the two models, these differences in results are expected.

3. Comparison with Coppens, Humphries and Sanders Model Run

The third attempt at verifying the IFD performance was done by comparing results with an image theory model derived by Coppens, Humphries, and Sanders (1984). This Coppens, Humphries, and Sanders Model (CHSM) uses a saddle point approximation to an image model to solve for the acoustic field. Both programs were run for the scaled scenario modeled in the tank experiment. This scenario is depicted in Figure 2.8 and features a ten degree sloping

bottcs. The maximum water depth for the run is 350 meters and the maximum range is two kilometers. The source generates a 100 Hz signal and is set at a depth of 175 meters.

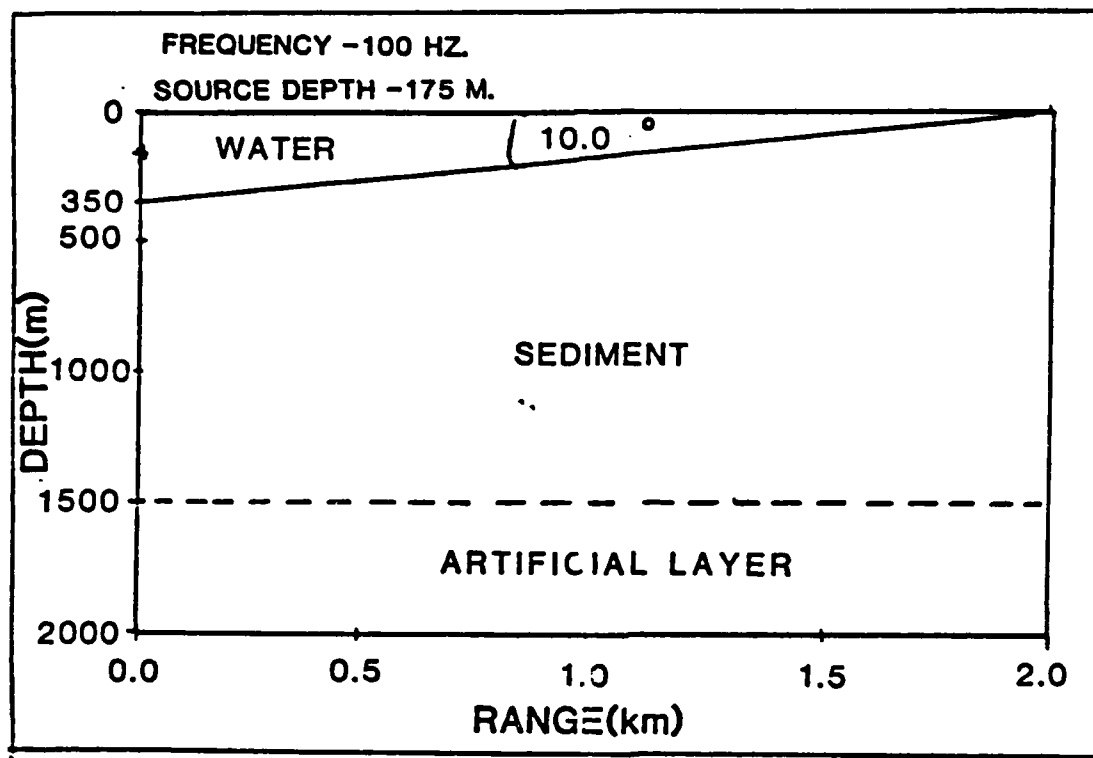


Figure 2.8 10 Degree Simple Sloping Bottom Case.

The image model provides solutions only at the apex. The comparison of predictions at the apex (range equal to 2 kilometers), can be seen in Figure 2.9. In the Figure, the IFD values are plotted as the solid curve while the image model values are shown as circular points. The predictions are given as values of normalized pressure amplitude for a given depth. The different models produce pressure amplitude values in different units, and thus, had to be normalized to make a comparison of values possible. This normalization was

done for each model by dividing the pressure amplitude by the maximum amplitude predicted by the model.

The results suggest that even though the models predict similar large scale trends in pressure amplitude with depth, there are several differences in detail. The plot shows that both the IFD and the image model predict an almost linear increase in amplitude with depth down to a specific maximum and then a slow decrease in amplitude beneath this maximum. The IFD however, shows the maximum at about 15.5 meters in depth while the image model maximum is deeper at 19 meters. Beneath this maximum the IFD shows a much sharper decrease in amplitude than the image model. The trend in the image model data appears smooth, while the IFD curve reflects several small scale fluctuations.

It appears that both models predict similar large scale trends in pressure amplitude for this scenario. It is difficult, if not impossible, to account for the differences in detail. As a minimum, however, this comparison indicates that the two sets of predictions are consistent with one another and can be considered reasonable in this shallow water environment.

4. Comparison with Physical Reasoning

From model comparisons it appears that the IFD at least makes a reasonable estimation of acoustic fields in a shallow water environment. IFD results are also analyzed in comparison with basic physical reasoning and theory as a fourth attempt at model verification. This analysis examines IFD transmission loss contours for the simple ten degree sloping ocean scenario seen in Figure 2.8. The scenario is two kilometers in range with a maximum depth of 350 meters. The source generates a signal at 100 Hz and is placed at 175 meters in depth.

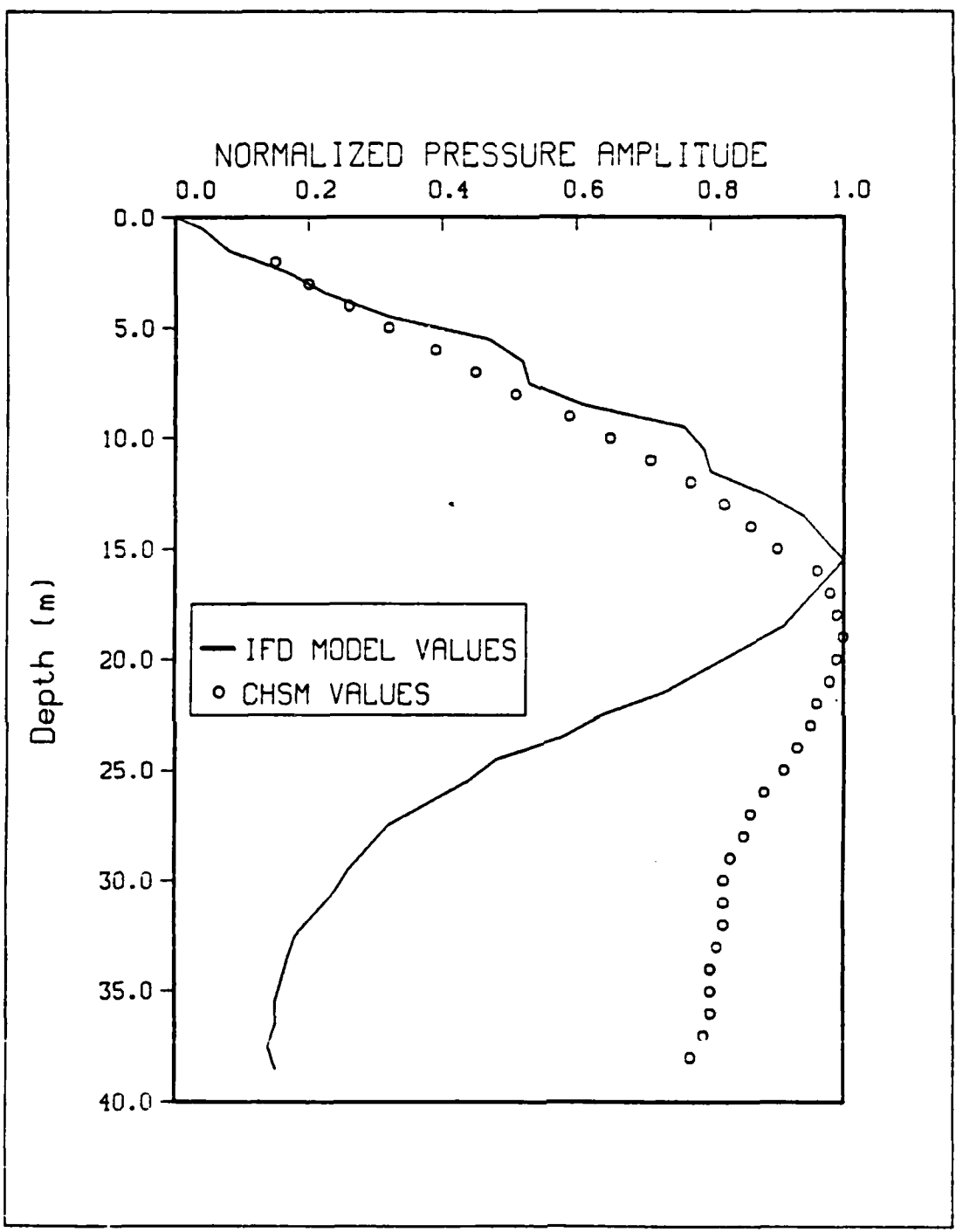


Figure 2.9 IFI and CHSM Comparison at the Apex.

Transmission loss contour plots are displayed in Figure 2.10 through Figure 2.13. All TL contours are expressed in decibels(db) and are shown as a function of depth versus range. In all figures, the ten degree sloping bottom is shown as a solid unlabeled line. The contour plots are displayed over four range subsections due to computer graphics limitations and to emphasize different significant features in the field.

The first figure shows transmission loss contours from the source to a range of 600 meters. The contours in the first 250 meters appear very symmetric, increasing outward from the source in a pattern that resembles spherical spreading. Since the IFI program assumes a Gaussian starting field this early pattern is expected.

From a range of about 300 meters to 600 meters the field in the water appears to be dominated by a surface reflection pattern. From the spotty appearance of the TL contours in this region there is an indication of an interaction of surface reflection and bottom reflection on the contours. It is possible to compare transmission loss maxima with nodes in the surface interference pattern. Based on surface interference theory these nodes should occur where (Kinsler, Frey, Coppers, and Sanders, 1982):

$$\sin(khd/r) = 0$$

or in other words;

$$khd/r = n\pi$$

where:

$$n = 0, 1, 2 \dots$$

r = Range

k = Wavenumber ($2\pi/\lambda$)

d = Source Depth

h = Depth of Node

λ = Wavelength.

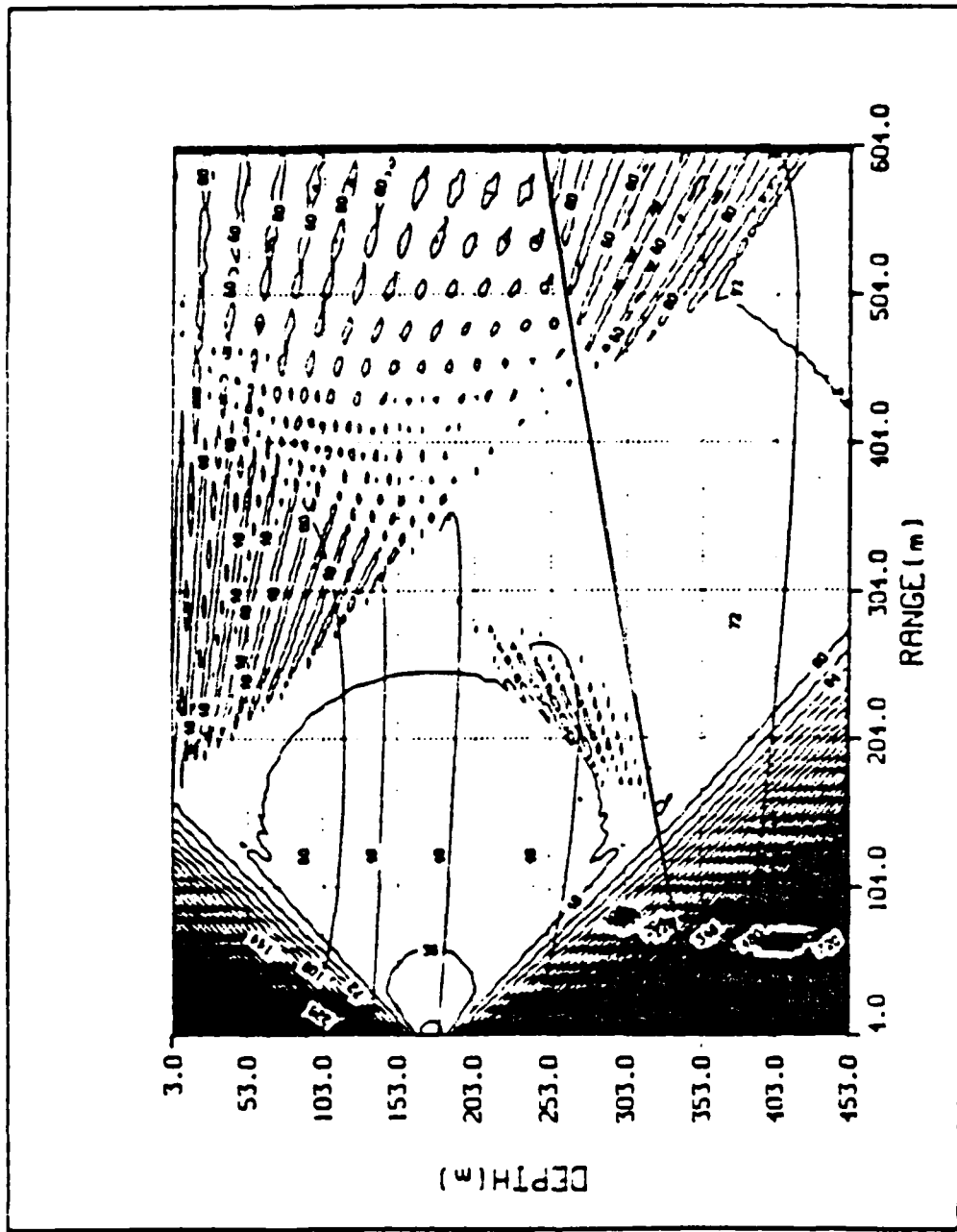


Figure 2.10 IFD TL Contours (dB) from the Source to 604 Meters

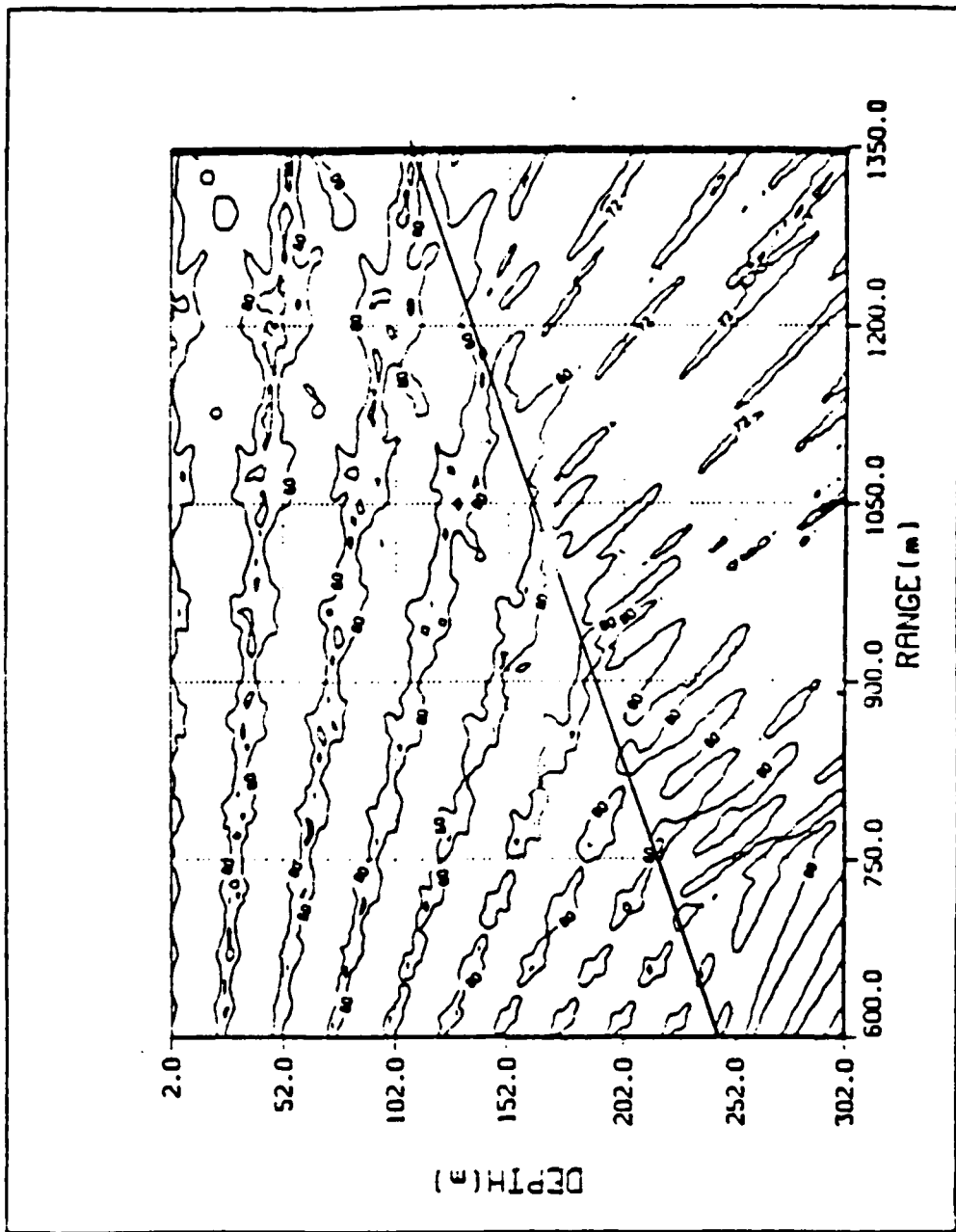


Figure 2.11 IPD TI Contours (db) from 600 to 1350 Meters.

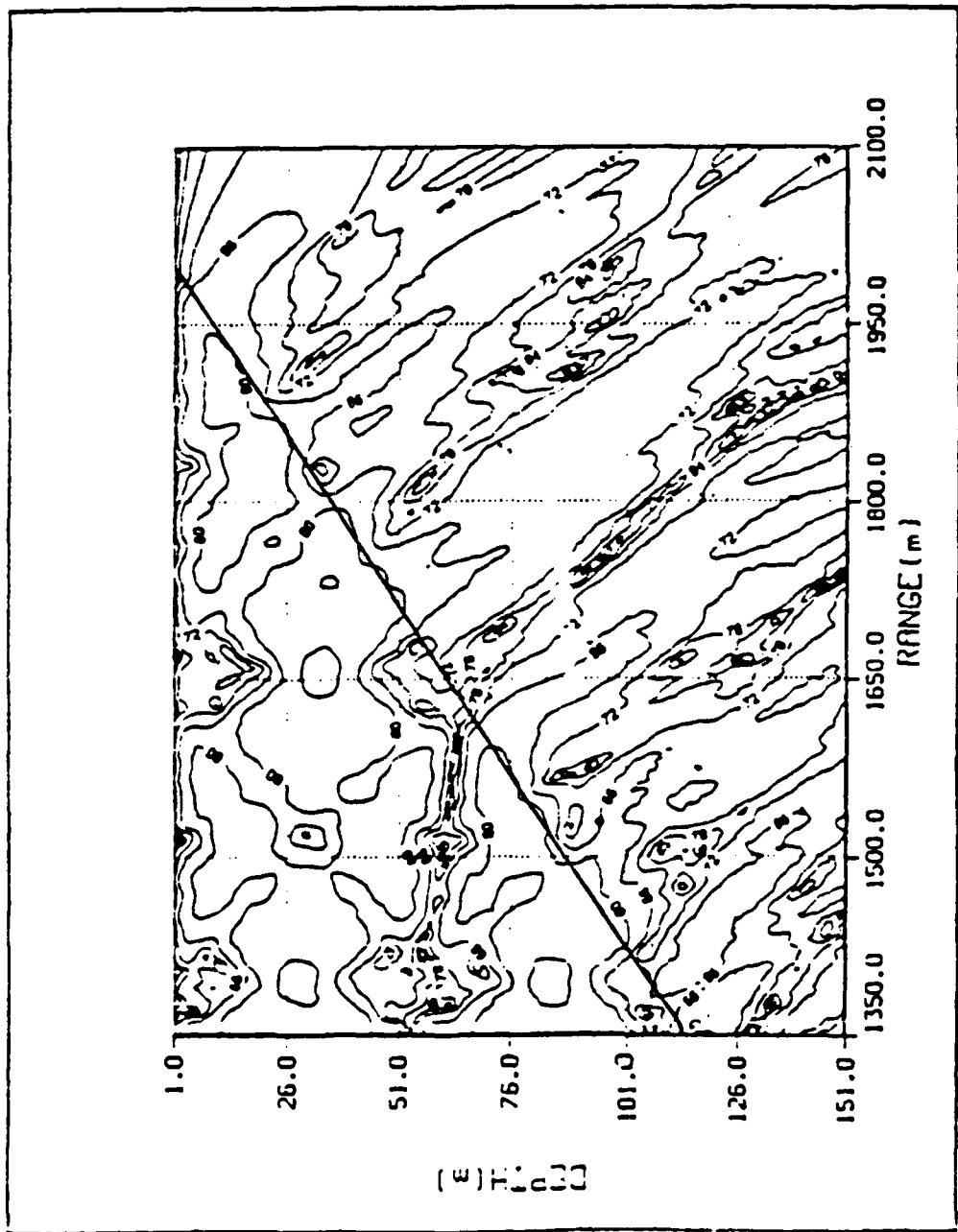


Figure 2.12 IFD TL Contours (db) from 1350 to 2100 Meters.

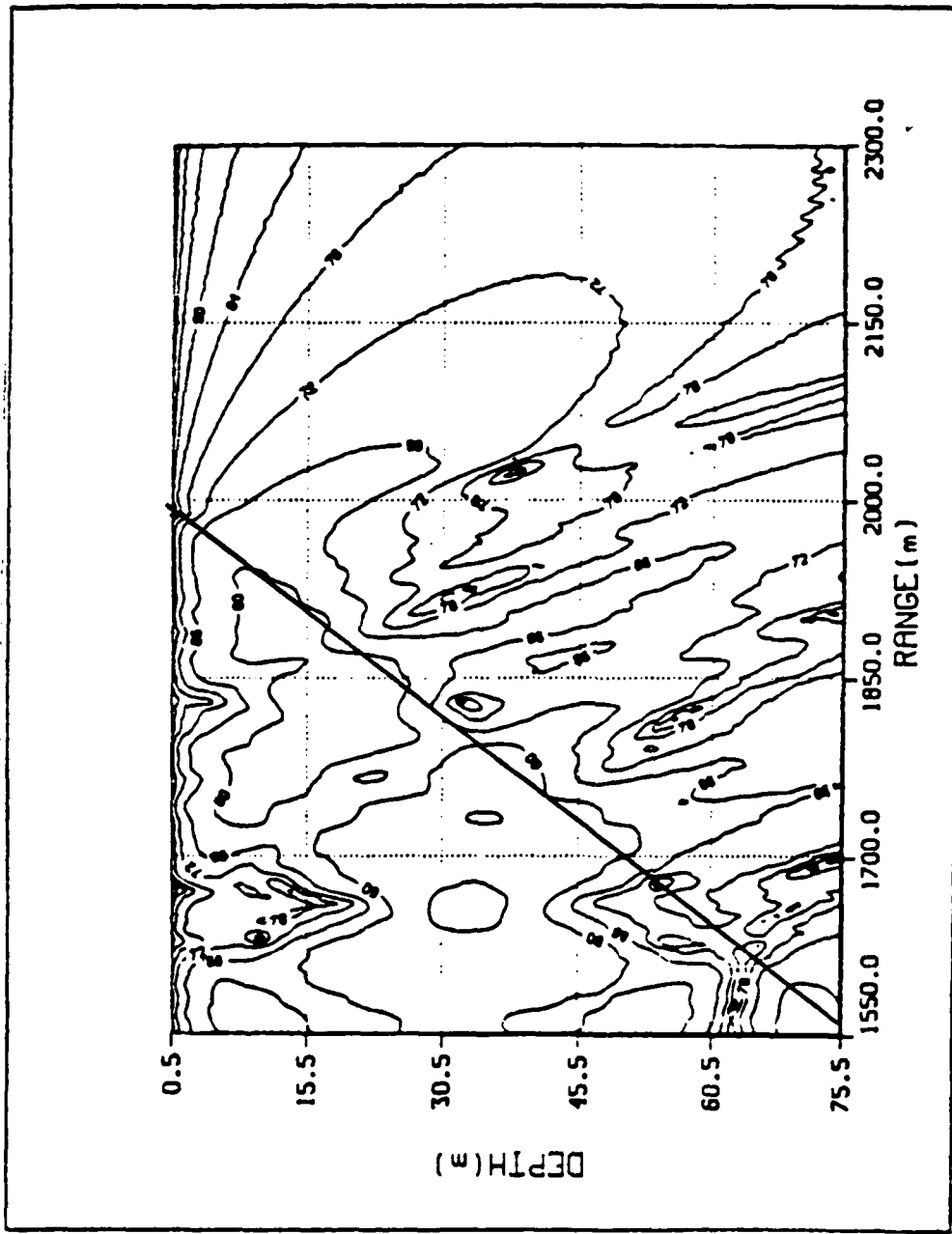


Figure 2.13 IFD TL Contours (db) from 1550 to 2300 meters.

By manipulating the above equation it is possible to solve for the depth at which the nodes should be observed. For this particular scenario at a range of 604 meters, nodes should occur at integer multiples of 25 meters in depth (25n). Figure 2.10 shows that these transmission loss maxima do exist as expected, every 25 meters in depth at the stated range.

Based on simple physical reasoning one would expect refractive bending along the ocean bottom due to density differences between the water and the sediment. The current plot reflects a change in basic pattern at the interface. There is a bending of the TL contours that suggest a refractive influence.

Figure 2.11 shows transmission loss contours from a range of 600 meters to 1350 meters. Again in this region the water appears to be dominated by surface reflection. Solving for the nodes in this surface interference pattern at a range of 1350 meters, it is found that these nodes should appear every 55 meters in depth. From the figure it is again seen that TL maximums do occur every 55 meters in depth as anticipated. As in the first figure there is a change in the basic TL pattern at the ocean bottom. The bending appears more accentuated than in the previous figure, but still suggests the influence of refraction at the ocean bottom.

Figure 2.12 displays transmission loss from 1350 meters to past the apex at a range of 2100 meters. In this figure, the dominance of the surface reflection mechanism is less obvious and the TL patterns become more complicated. It is in this region that the influence of trapped normal mode propagation can be seen. As discussed earlier, as acoustic energy travels up the slope toward the apex, normal modes are cut off and energy is transmitted into the bottom. According to adiabatic normal mode theory, modal separation

is range dependent (Graves, Nagel, Uberall, and Zaur, 1975 and Coppens and Sanders, 1980). The range from the apex at which the lowest mode is transmitted into the bottom, can be calculated using the following equation (Coppens, Sanders, Iannucci, and Kawamura, 1978):

$$X = \lambda/4 \sin\theta_c \tan\beta$$

where:

X = Dump Distance Of The Lowest Mode

λ = Wavelength

θ_c = Critical Angle

β = Wedge Angle.

According to adiabatic normal mode theory (Kinsler, Frey, Coppens, and Sanders, 1982), in deep water (near the source) the lower normal modes are far above cutoff and the adiabatic eigenfunctions consist of an integer number of half sine waves with zero pressure at both the top and bottom surfaces. At the cutoff of each mode, the pressure at the bottom must be maximized, resulting in an adiabatic eigenfunction that contains 1/4, 3/4, and 5/4 wavelengths at the respective cutoff distances of 1X, 3X, and 5X for the three lowest modes. From Figure 2.14 it can be seen that as the normal modes travel up the sloping bottom, successive modes are forced into the bottom at distances where a particular mode reaches a depth at which it can no longer propagate. Also from the figure it is obvious that a source set at mid-depth can not excite the second mode. Since this particular geometry is present in the tank scenario it is expected that the energy associated with this second mode should not be seen. Based on this line of physical reasoning, modes should be dumped into the sediment at the first dump distance, fifth dump distance, ninth dump distance and so on. If these modes are dumped as described

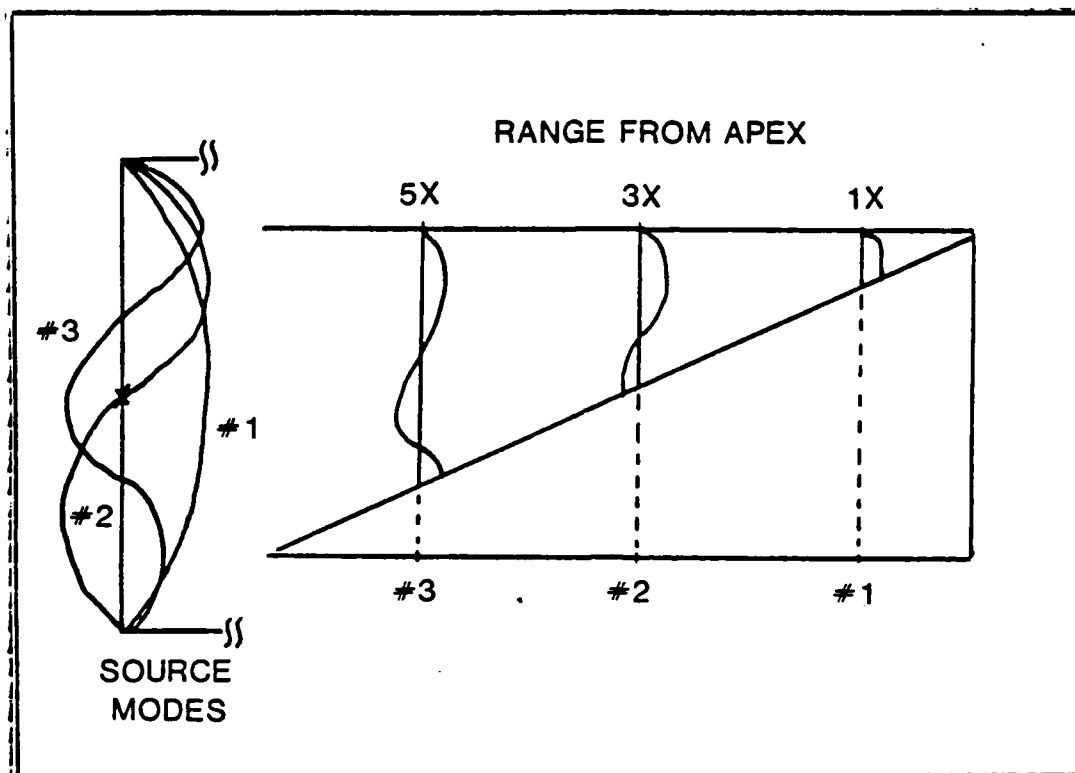


Figure 2.14 Normal Mode Propagation in a Wedge Shaped Ocean.

then they should be seen in the contour plot as reductions of transmission loss in the bottom at ranges of 1952 meters, 1760 meters, 1568 meters, and so on.

From Figure 2.12 it can be seen that there is an obvious decrease in transmission loss at approximately 1950 meters (dump distance #1) and 1760 meters (dump distance #5). There is also a less clearly defined reduction in TL along the bottom at 1565 meters (dump distance #9).

The final contour plot (Figure 2.13) shows transmission loss contours from 1550 meters to 2300 meters. This figure is an extension of Figure 2.12, intended to emphasize how clearly the bear at the first dump distance is defined in the plots. The bear at the fifth dump distance is also

visible but is not nearly as well defined. From this figure, one can also see an indication of a very narrow beam in the sediment at about 1860 meters. This distance corresponds to the third dump distance (second normal mode). Based on adiabatic mode theory the second mode is not expected to be excited. However, adiabatic mode theory is only an approximation of normal mode behavior. This approximation of normal mode behavior becomes less exact as the bottom slope increases and the closer the source is to the apex. The appearance of a narrow beam at the third dump distance indicates that there is a strong possibility that the second mode is present and that the adiabatic approximation is not exact with a ten degree bottom slope.

The basic features of the IFD contour plots are consistent with both physical reasoning and theory. Basic surface reflection and bottom refraction occur where expected and behave as anticipated. In the far field, trapped normal mode propagation is observed and can be verified with simple dump distance calculations. The location of beams dumped into the bottom appear consistent with basic mode theory. In short, the transmission loss contours indicate that the IFD is making reasonable predictions of the acoustic field in a shallow water environment.

5. Verification Summary

It is difficult to say how exact the IFD predictions are for a shallow water environment based on these simple verification techniques. As a minimum it can be said that the model results are at least consistent with other model predictions and expectations based on simple physical reasoning. Model estimates are virtually the same as the Jenser and Kuperman FF model in regions not influenced by a water/sediment boundary. Close to the boundary the IFD results appear to show greater detail and variation than

this IF model. The IFD results also appear consistent with the general trends in pressure amplitude predicted by the Coppens, Murphries, and Sanders image model. Again differences were noted in the small scale structure. Finally, the IFD II contours verify well with basic expectations based on physical reasoning and theory. Surface reflection and bottom refraction patterns are observed as anticipated. Far field normal mode propagation can be verified in the plots using simple dump distance calculations. In short, all verification methods attempted, fail to uncover any inconsistency in IFI performance in a shallow water environment.

III. LABORATORY MEASUREMENTS

A. BACKGROUND

The major attempt at appraising IFD performance involved comparing model results with laboratory measurements. The shallow water environment modeled in the tank is very idealized; a ten degree sloping sand bottom with an isovelocity water column. Although this scenario appears extremely simplistic, it is one that can be reasonably modeled in the laboratory and still approximate conditions in an actual shallow water ocean environment. The methods used to model and measure the acoustic field are relatively untested. Indeed, this attempt at laboratory modeling was performed not only to verify IFI predictions, but also to see if the environment could be successfully modeled in the laboratory.

E. EXPERIMENTAL DESIGN

1. The Tank

A fiberglass coated wooden tank was used. The tank is 304 centimeters in length, 117 centimeters wide and 95 centimeters deep. Sand filling the bottom of the tank was shaped to form the ten degree sloping bottom, and measurements were taken over a range of two meters. Maximum water depth in the tank was 35 centimeters. A 100 kHz source was placed at mid-channel depth (17.5 centimeters). The layout of the tank is depicted in Figure 3.1.

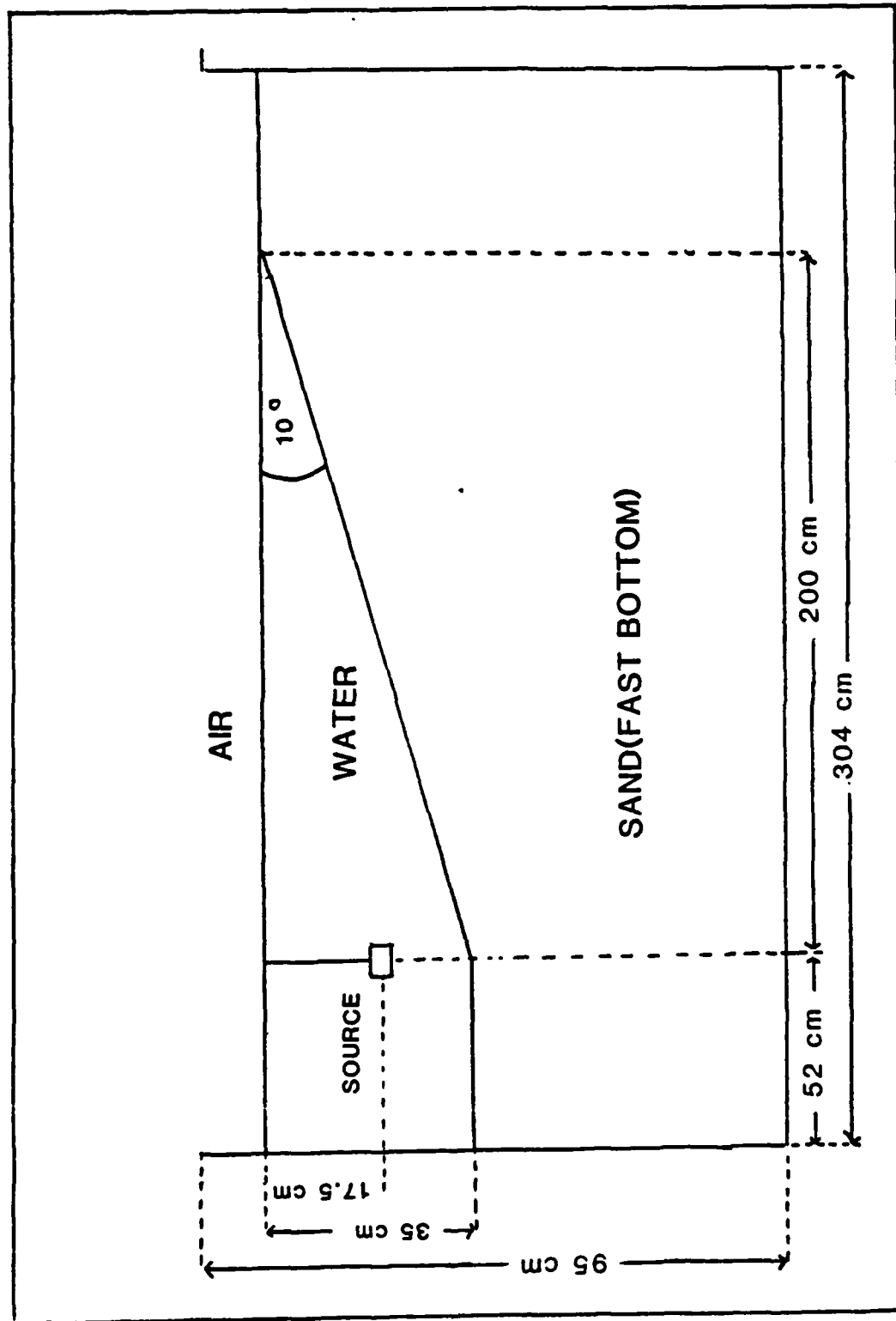


Figure 3.1 Experimental Tank Set Up.

A slope of ten degrees was selected for several reasons. To begin with, even though a ten degree slope is greater than most ocean bottom slopes, it is still small enough to be considered realistic. Perhaps most important, the ten degree slope was selected because given the frequency limitations (discussed later in this chapter) and range limitations, this wedge angle allowed the source to be placed many (41.6) dump distances from the apex. A large number of dump distances was necessary to simulate a distant source.

The bottom material used in the experiment was #30 fine grade sand. The grain size ranged from 0.15 millimeters to 0.70 millimeters. The sand was treated with a technique used by Faek (1984) to remove air from the sediment. This technique used a high speed jet to agitate the sand/water mixture to remove the bubbles and then allowed the sand to settle for several days before the experiment was initiated.

Fresh(tap) water served as the medium in the tank. To remove air bubbles, the water was allowed to settle in a settling tank before being transferred to the experimental tank for use. The water in the tank was periodically treated with chlorine bleach to prevent the growth of biological material.

2. Signal Generating/Receiving Equipment

The acoustic signal used for the measurements was produced by a function generator, sent through an amplifier and then transmitted into the water by a directional transducer resonant at 100 kHz. The dimensions of the active face of the transducer were 7.0 cm in width and 2.0 cm in height. These dimensions resulted in an approximate beamwidth (angle from the acoustic axis to the first theoretical null) of 11.9 degrees in the horizontal and 46.3 degrees in the vertical. The narrow horizontal beam minimized reflections

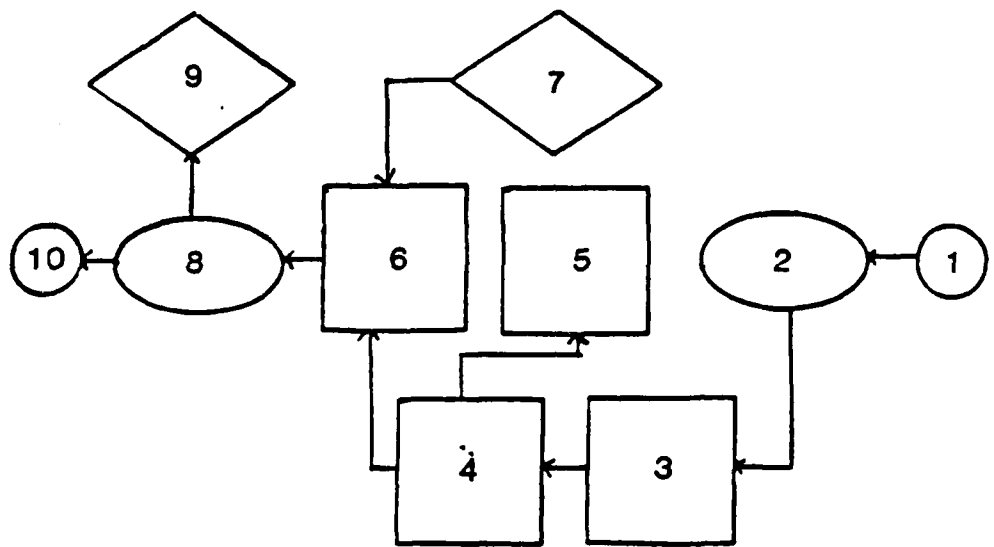
from the sidewalls of the tank, while the wide vertical beam allowed complete ensonification of the channel in the vertical dimension.

The signal was received by an LC-5 omni-directional hydrophone, sent through an amplifier and filter, and then displayed on an oscilloscope and voltmeter. A schematic showing the electronic setup is shown in Figure 3.2.

A frequency of 100 kHz was selected for two practical reasons. First, to avoid particle scattering by the sediment, the acoustic wavelength must be at least three times larger than the grain size of the sediment (Anderson and Liebermann, 1968). The largest grain size in the sand was 0.07 cm, so that a wavelength of 1.45 cm(100 kHz) was sufficiently large enough to be immune to this effect. Second, the 100 kHz frequency and the properties of the sand provide a dump distance that is small enough to allow the source to be positioned many dump distances from the apex.

Shaping the sand bottom into a ten degree wedge with a uniform and smooth interface proved to be a long and tedious process. To facilitate this modeling, wooden supports (two-by-fours) were mounted along the length of both sides of the tank. These supports were elevated at one end of the tank to achieve the required ten degree slope. A scraping device was constructed with wooden supports and a metal scraping blade that extended across the width of the tank. This scraping device consisted of wooden supports along the top that reached across the tank and could be pulled along the elevated wooden supports on both side of the tank. This scraping device was pulled along the supports repeatedly until a smooth slope of ten degrees was sculptured from the sand.

Holes had to be drilled into the metal scraping blade because when a solid blade was used in the shallow portion of the slope, water trapped behind the blade was



- 1.) LC-5 HYDROPHONE.
- 2.) AMPLIFIER (HP 465A).
- 3.) ELECTRONIC FILTER (SK 302).
- 4.) OSCILLOSCOPE.
- 5.) VOLTMETER (HP 400D).
- 6.) FUNCTION GENERATOR WAVETEK 116.
- 7.) FREQUENCY OSCILLATOR (GR 1310).
- 8.) AMPLIFIER (HP 467A).
- 9.) FREQUENCY COUNTER (HP 5233L).
- 10.) 100 KHZ TRANSDUCER.

Figure 3.2 Electronic Equipment Schematic.

forced beneath the scraper gouging the smooth bottom. This bottom modeling technique was slow because, once a pass was made over the bottom, the water became turbid and it was then impossible to see the bottom. When the bottom was not visible, it was impossible to see where further scratching was necessary until the water settled several hours later. In addition, as this smoothing process continued a silty residue became separated from the sand and settled cut on top of the sand. This residue would be easily resuspended and eventually had to be removed using a water syphon.

C. MEASUREMENT PROCEDURES

Measurement of the pressure field within the water was done by lowering the receiver in depth at specific ranges of interest. The receiving hydrophone was attached to a pair of micrometers at right angles to one another, that was in turn bolted to a board which spanned the width of the tank. Once the board was placed close to a range of interest, one micrometer was used to give fine adjustments in range and the other in depth.

The measurements were subject to both an accuracy and a precision error. On a given day, with the water level fixed and the cross-tank support set at a particular place in the tank, it was possible to position the receiving hydrophone with an accuracy in depth and range of plus or minus 0.06 centimeters (one turn of the micrometer). To prevent the sand 'inland' of the apex from drying out when not taking measurements, enough water was added to the tank after each data run to keep the sand completely submerged. The next time measurements were taken, water had to be removed from the tank to reestablish the beach. Because of these small changes in the water level the horizontal position of the beach was subject to a precision error estimated to be within plus or minus one centimeter.

The final decision associated with the measurements centered on whether to use a triggered pulse or a continuous wave (CW) signal. With a triggered pulse it was possible to distinguish the received signal from interference caused by reflections off the side of the tank. On the other hand, by using a triggered pulse there was a possibility that the pulse length was not long enough for the acoustic energy associated with paths reflecting off the top and bottom of the water column to overlap the direct path from the source to receiver. A CW signal would avoid potential pulse length problems, but it would be impossible to distinguish between the actual signal and interference. The use of a source with a narrow horizontal beam reduced the effects of reflections from the side walls, but there was still the possibility of interference from side lobes reflected from the sides.

It was necessary to determine the best means to take measurements. This was done by taking measurements at the same location with different pulse lengths to determine the required pulse length to give consistent results and then comparing these results to those obtained with a CW signal. The third dump distance (14.4 cm from the apex) and just past the tenth dump distance (50.0 cm from the apex) were chosen, and measurements were taken for pulsed signals of 64 and 256 cycles, and a CW signal. These measurements can be seen in Figure 3.3 through Figure 3.5. In the figure depicting results at the third dump distance, the CW measurements are shown as the solid curve, the 64 trigger cycle results are displayed as circular points, and the 256 trigger cycle results are depicted as triangular points. For clarity, the measurements taken just past the tenth dump distance are shown in two figures. Figure 3.4 compares CW results (solid curve) with the 64 trigger cycle signal (circular points). Figure 3.5 compares CW measurements (solid curve) with the 256 cycle results (circular points).

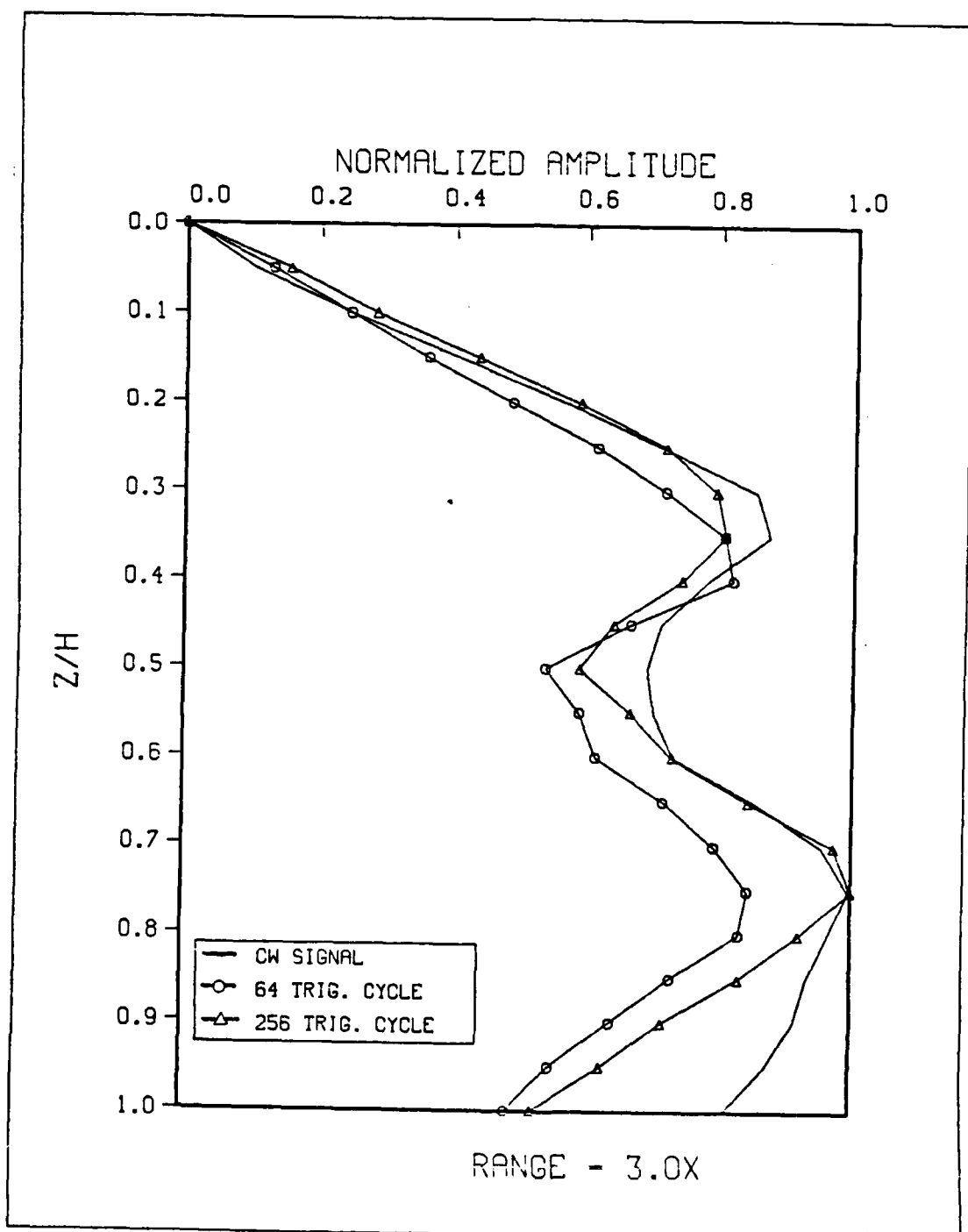


Figure 3.3 Pulse Length Analysis at 3.0X.

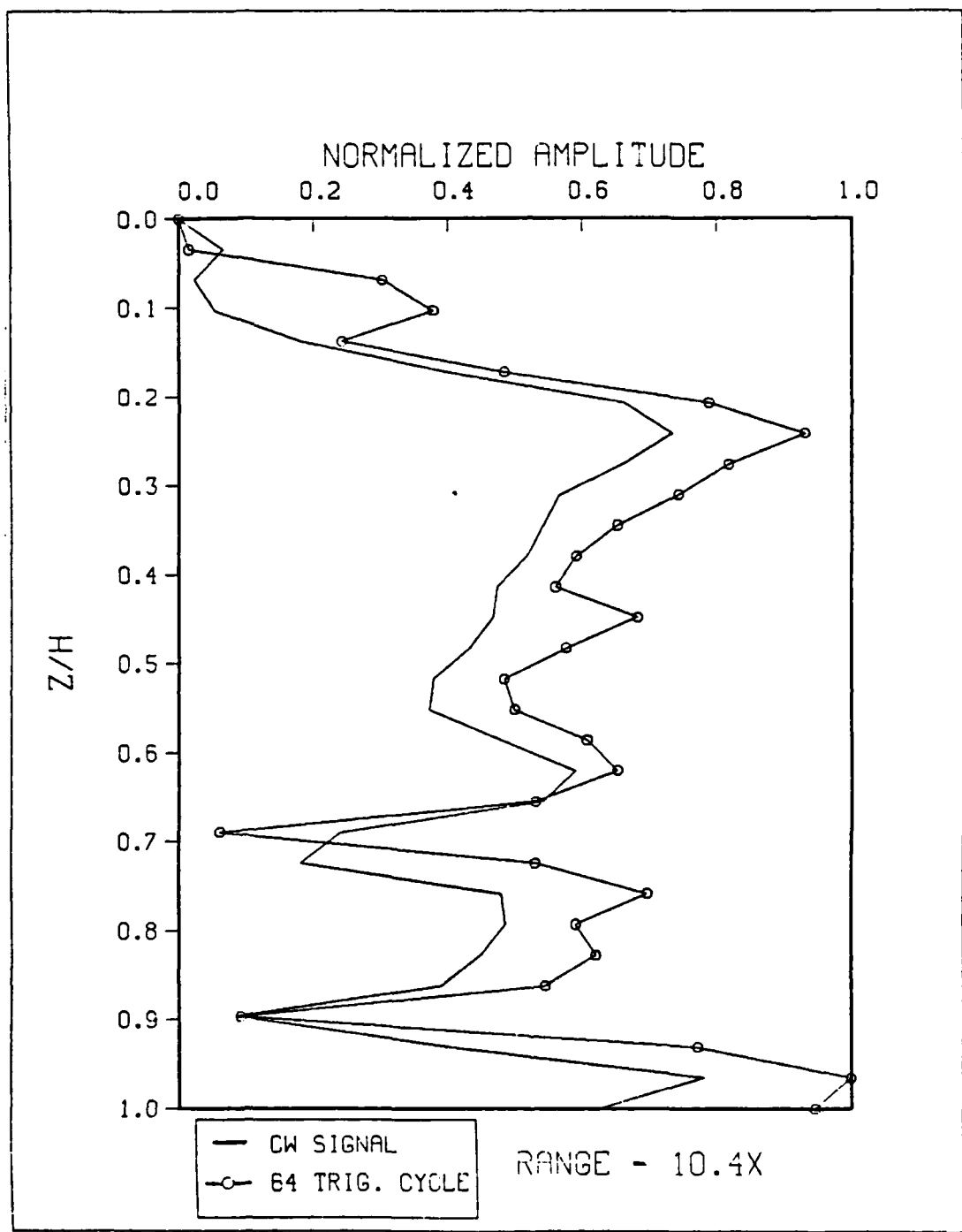


Figure 3.4 Pulse Length Analysis at 10.4X.

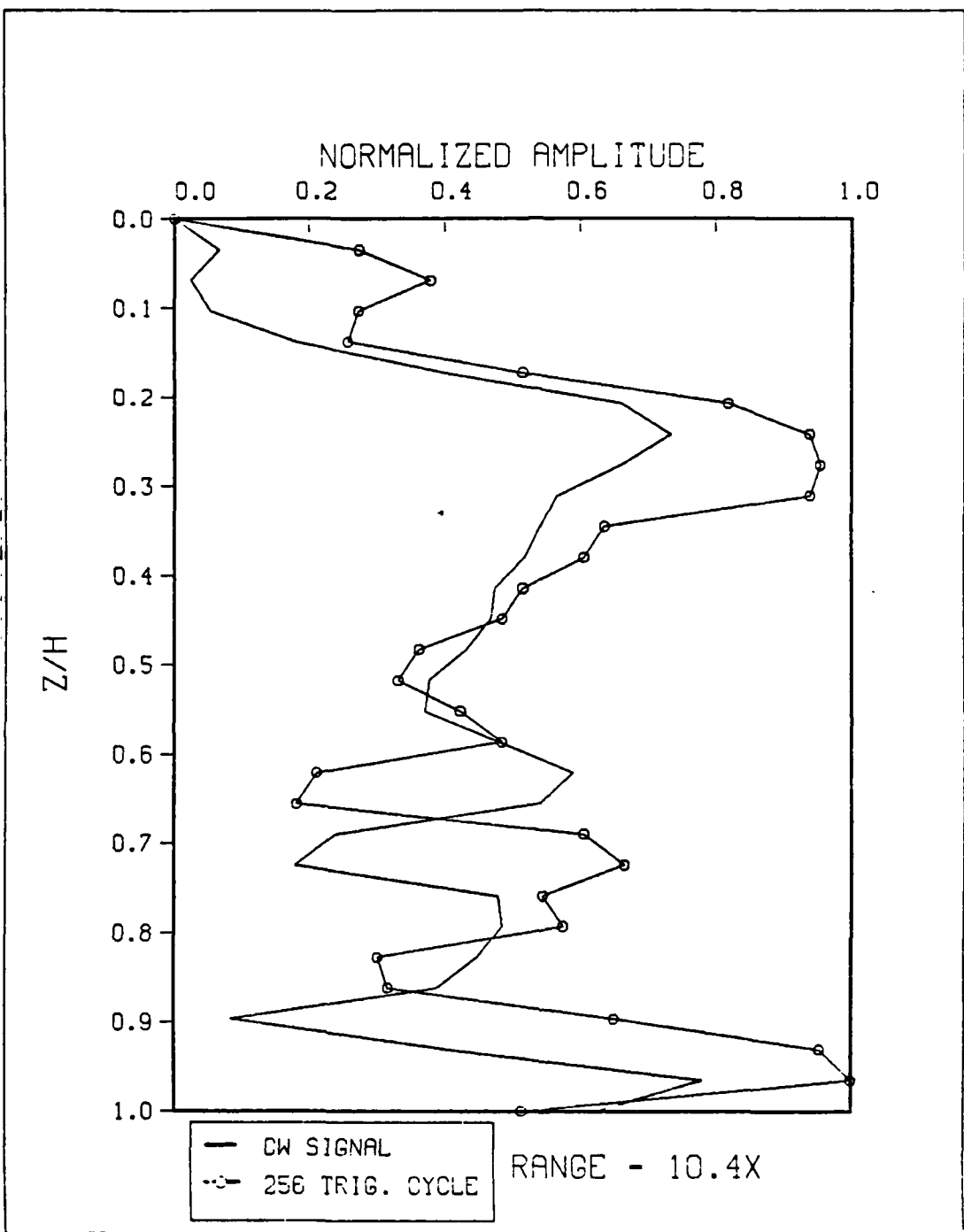


Figure 3.5 Pulse Length Analysis at 10.4X.

The pressure amplitude values were normalized by dividing each pressure value by the maximum pressure value in the field. The depth values were also normalized by dividing each depth by the maximum depth.

The results in Figure 3.3 show good agreement between the three curves. In particular, the results for the CW signal and the 256 cycle signal are very similar. The 64 cycle signal shows the same behavior as the CW signal, but differs in magnitude below mid-depth.

The results at 50.0 cm from the apex appear much more complicated than at the third dump distance. Figure 3.4 compares results achieved with the CW signal and the 64 cycle signal. From the figure it can be seen that the two sets of results show good agreement. The measurements depicted in Figure 3.5, which compares the 256 cycle signal and the CW signal show poorer agreement, although the general shapes of both curves remain similar.

These results indicate that interference from the side walls is sufficiently small so that it is possible to make measurements with a CW signal to at least ten dump distances from the apex. Long pulses could also be used, but the difficulty of making voltage measurements with an oscilloscope compared to reading a voltmeter, dictates that measurements should be made with a CW signal.

IV. MODEL RESULT COMPARISONS WITH LABORATORY MEASUREMENTS

A. INTRODUCTION

IFD model predictions and laboratory measurements were obtained for comparison in both a general and detailed analysis. The general analysis compared results every five centimeters from the beach to a range of 50.0 cm from the beach. The measurements were spaced to give results at approximately each of the first ten dump distances. The detailed analysis compared results every centimeter from 3.0 to 11.0 cm from the apex. These measurements were taken to observe the sensitivity of the pressure field to small changes in range.

B. THE GENERAL ANALYSIS

The general analysis compared IFD results and laboratory measurements at approximately each of the first ten dump distances (every five centimeters from the beach). These measurements were obtained by fixing the receiving hydrophone with respect to the cross board and then moving the board out in increments of five centimeters to measure the desired field as a function of depth at each range. The received CW signal was read on the voltmeter.

The comparisons are shown in Figure 4.1 through Figure 4.10. In the figures, the IFD predictions are displayed as a solid line while the experimental measurements are shown as circles connected by a dashed line. Each pressure value was normalized to unity by dividing it by the maximum pressure value for the respective curve. The depth values were also normalized by dividing each depth by the maximum depth in the water column.

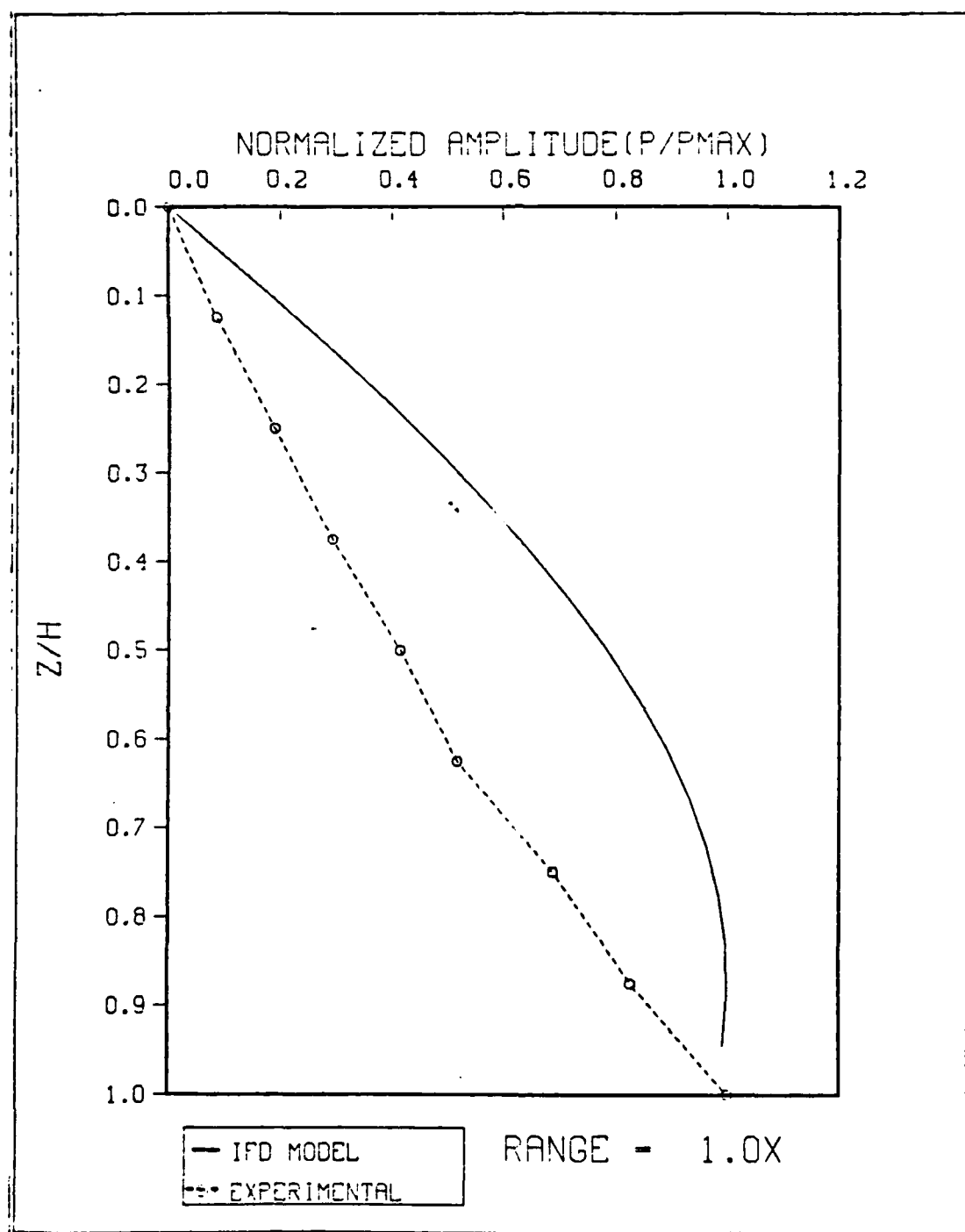


Figure 4.1 Comparison of Results at 1.0X.

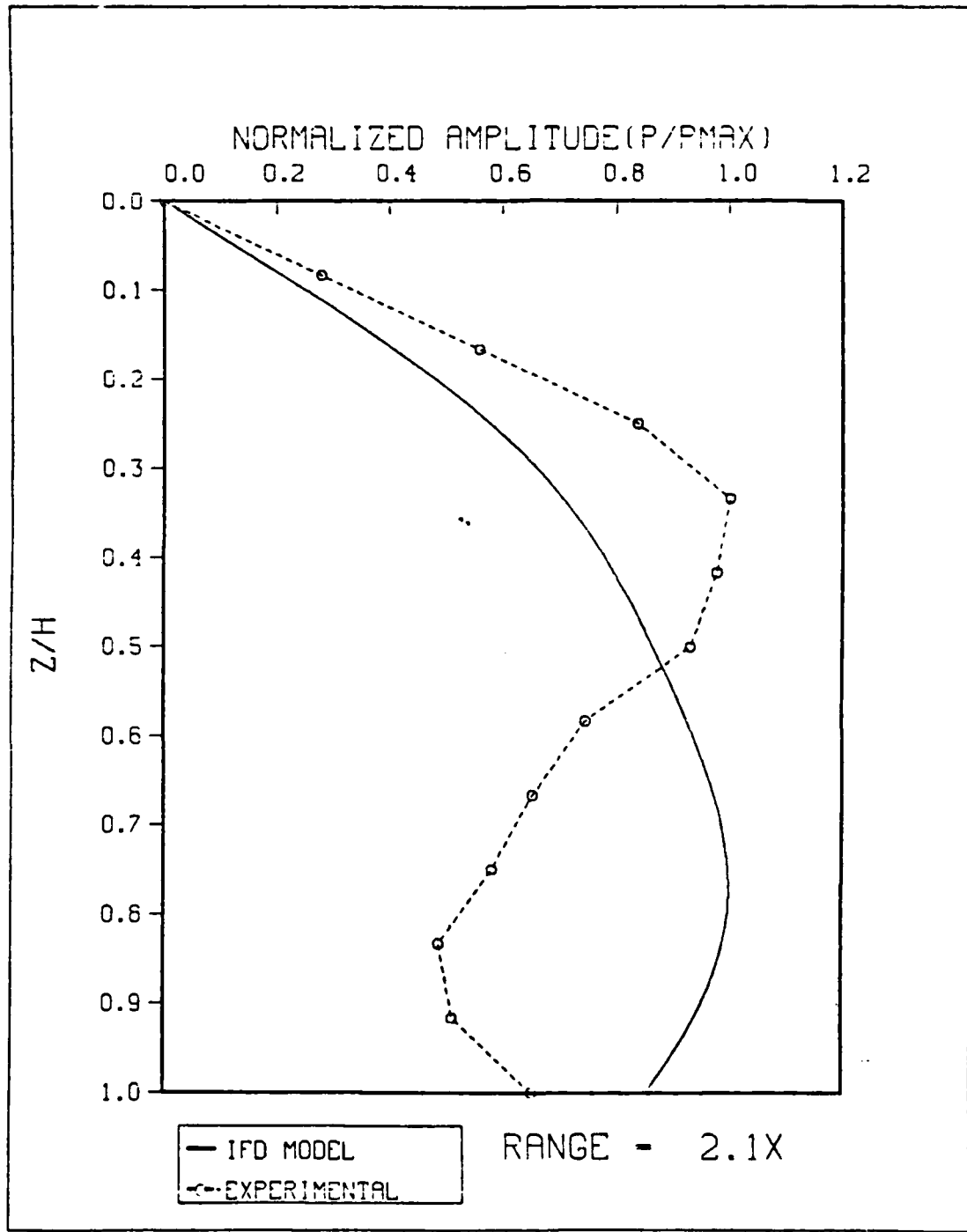


Figure 4.2 Comparison of Results at 2.1X.

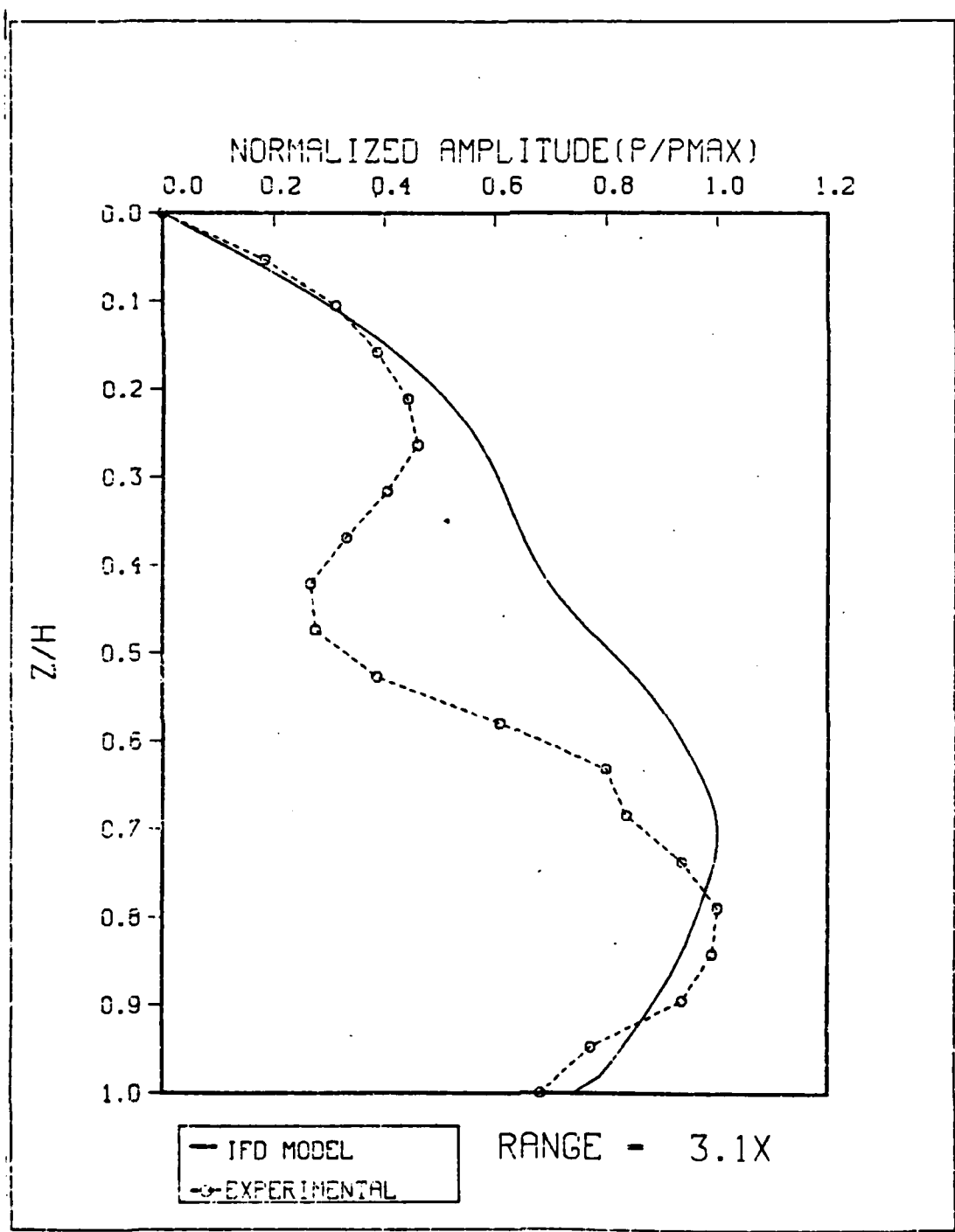


Figure 4.3 Comparison of Results at 3.1X.

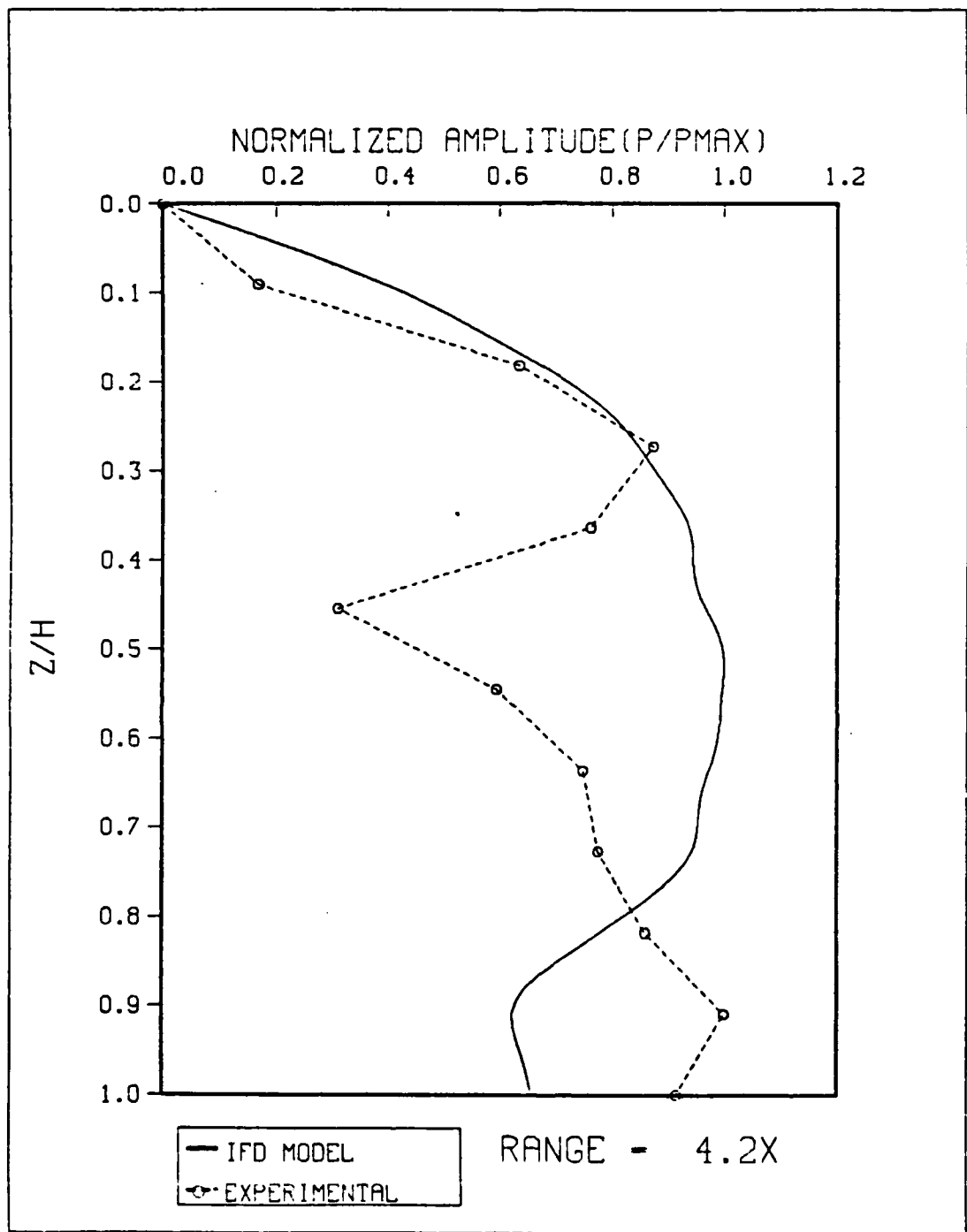


Figure 4.4 Comparison of Results at 4.2X.

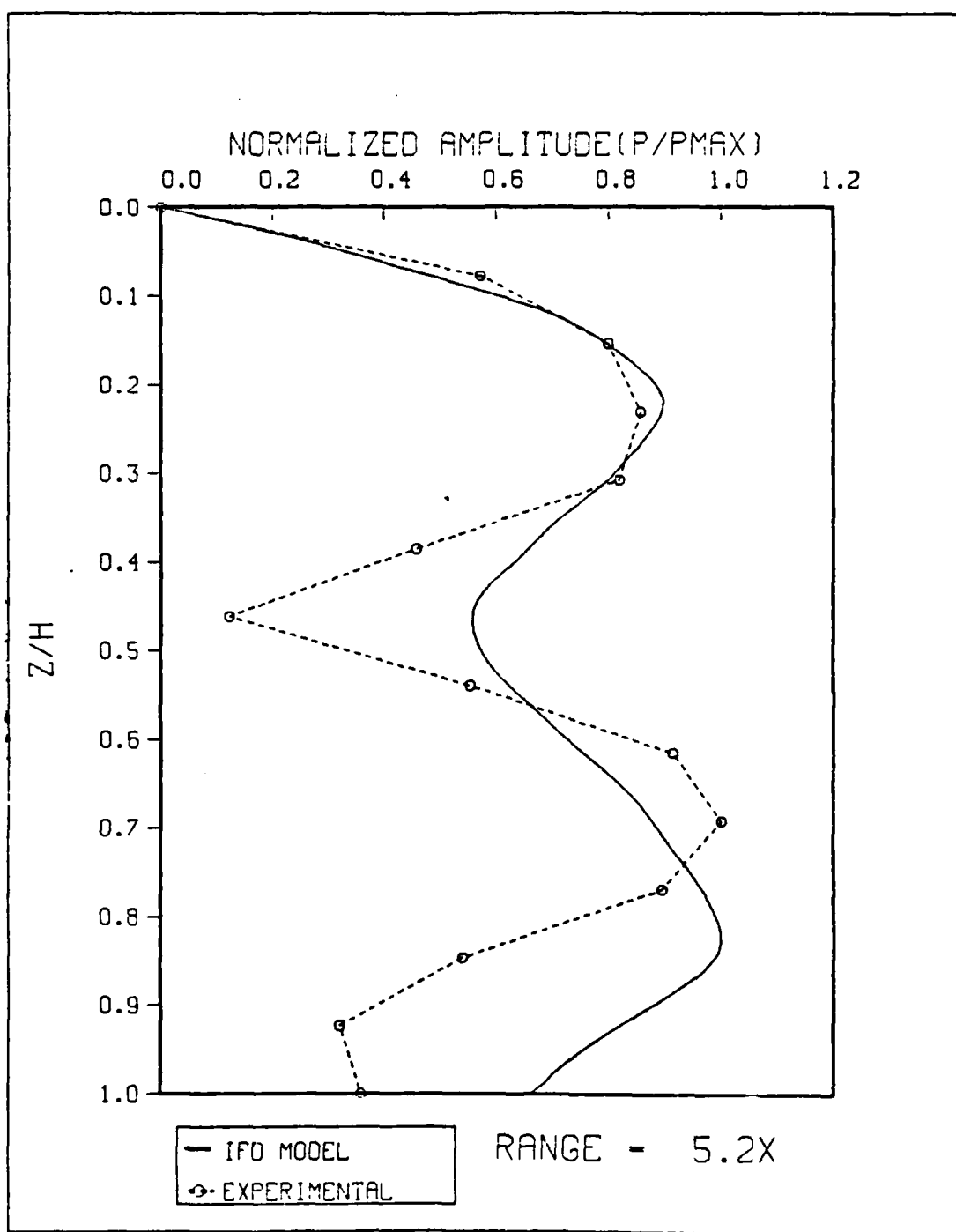


Figure 4.5 Comparison of Results at 5.2X.

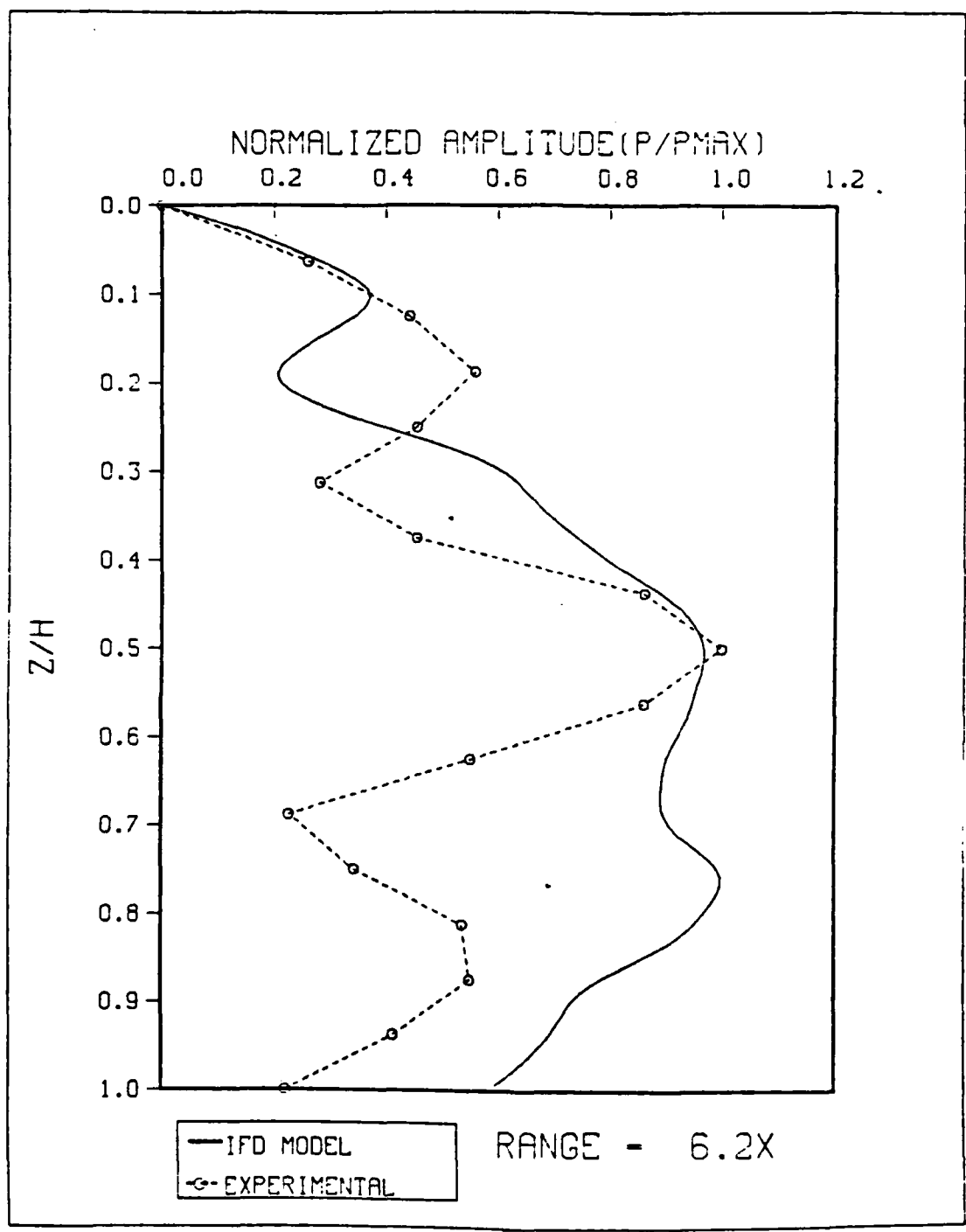


Figure 4.6 Comparison of Results at 6.2X.

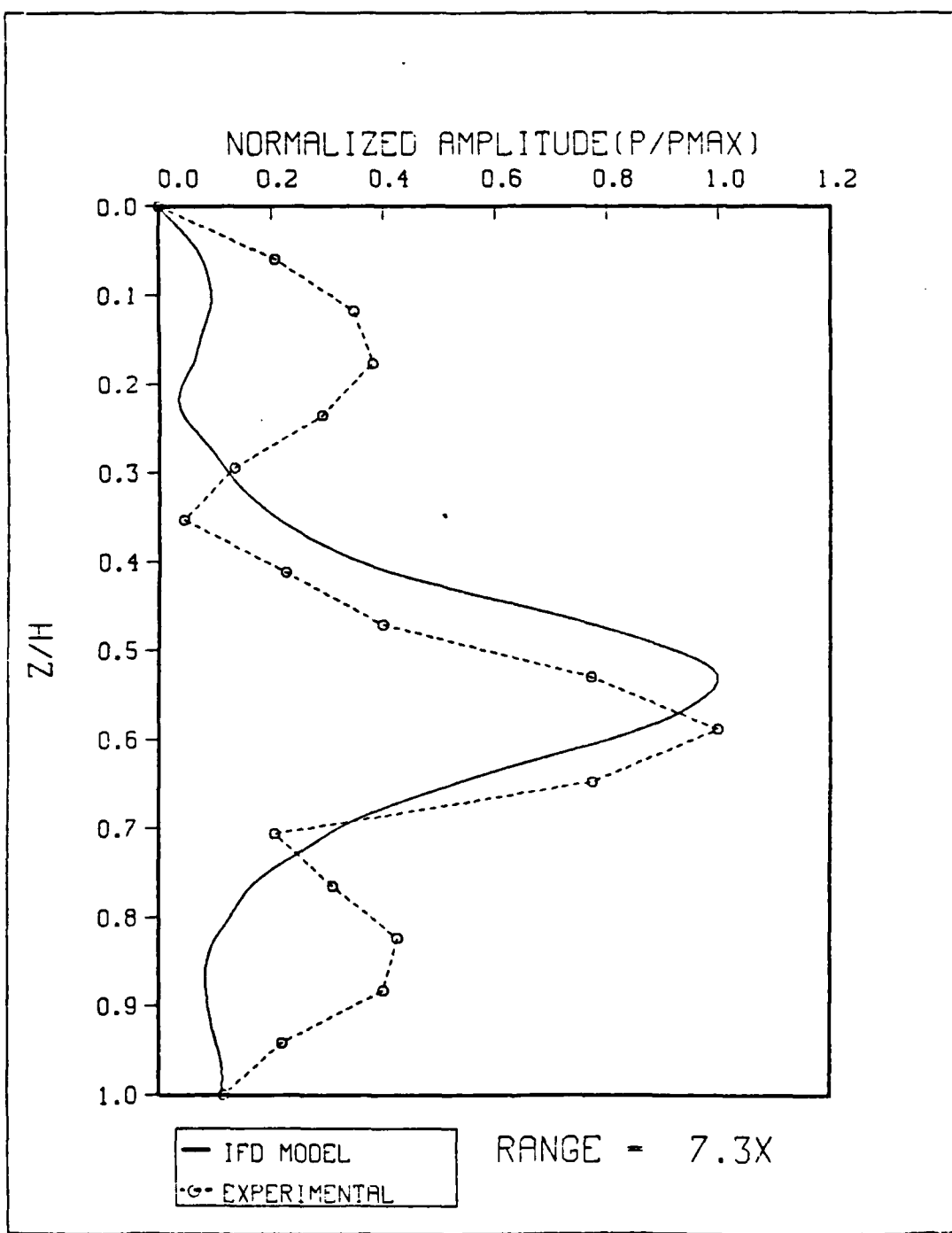


Figure 4.7 Comparison of Results at 7.3X.

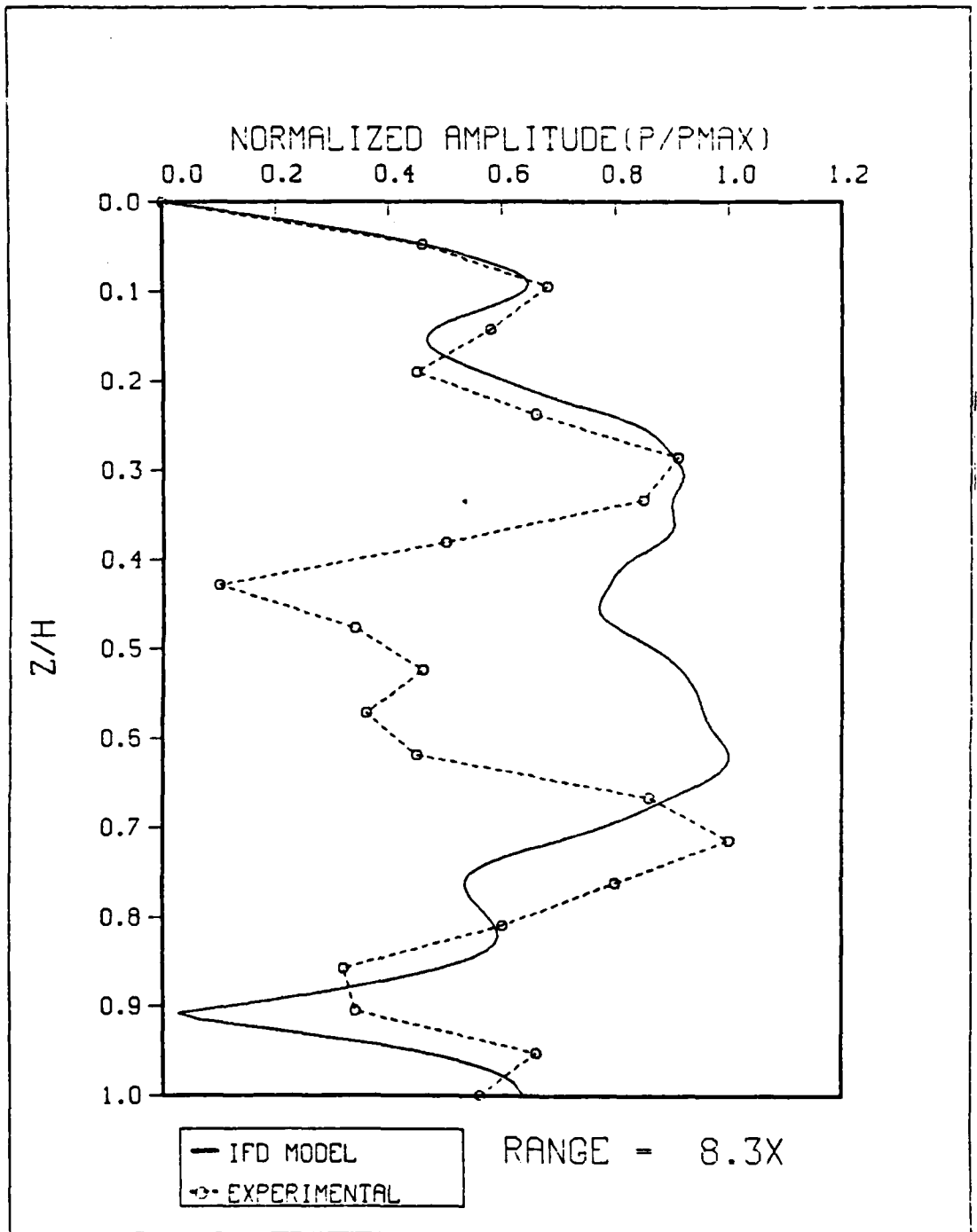


Figure 4.8 Comparison of Results at 8.3X.

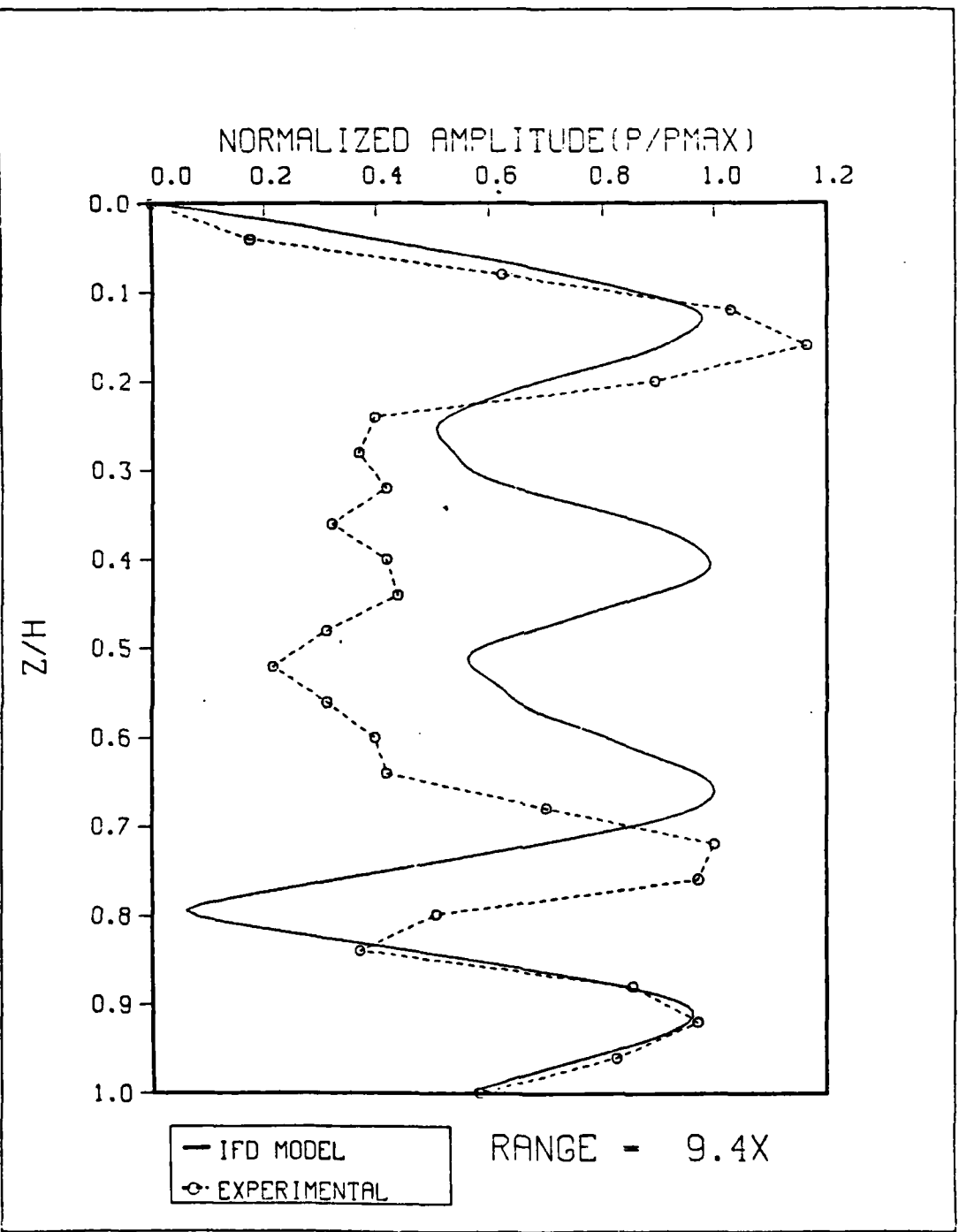


Figure 4.9 Comparison of Results at 9.4X.

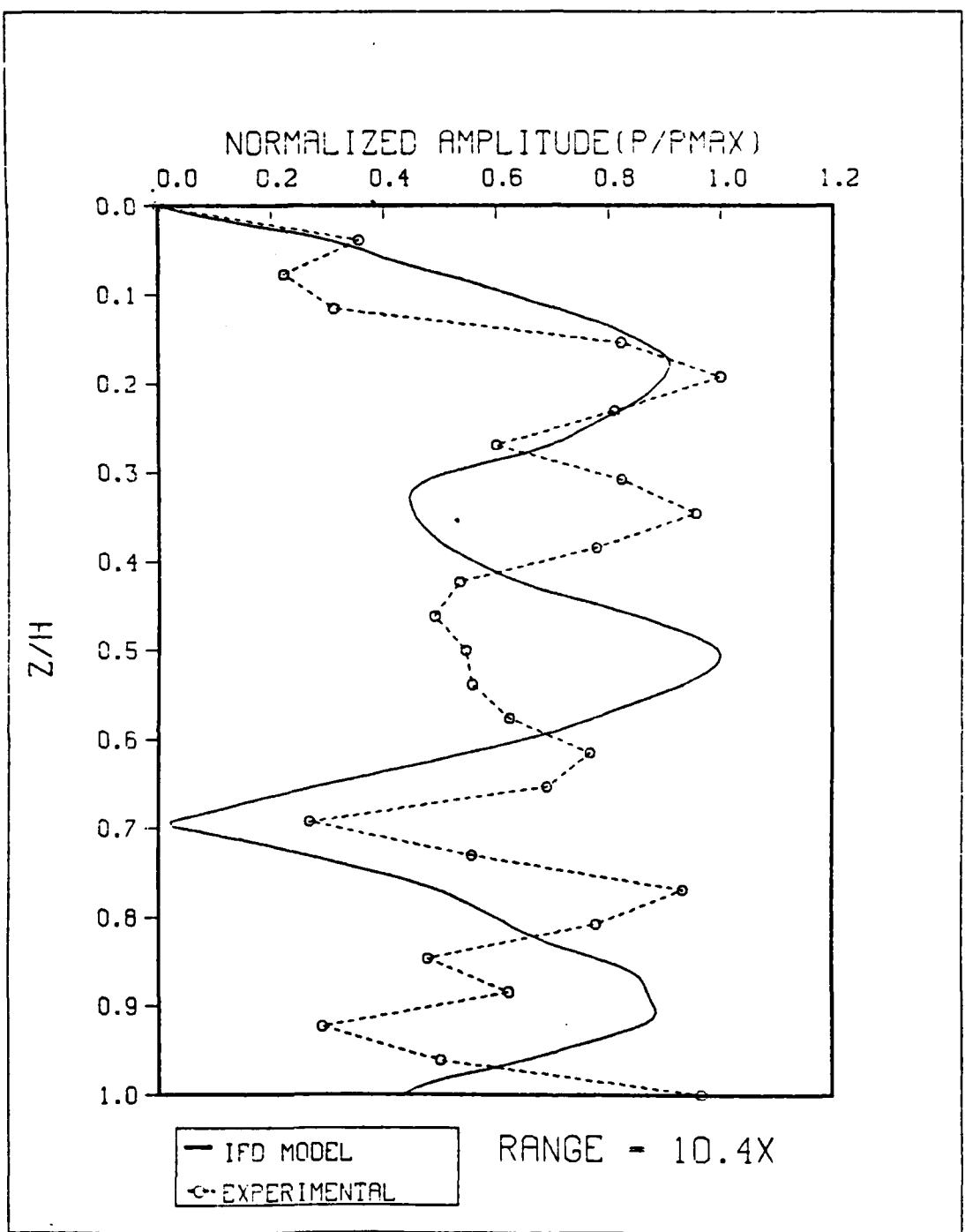


Figure 4.10 Comparison of Results at 10.4X.

In general, the pressure patterns predicted by the IFD and those measured, both become more complicated as the range from the beach increases. At all ranges, there is qualitative agreement in the scale of the predicted features and the scale of the measured features. Quantitative agreement is lacking. This agreement in scale but not detail, suggests that the phases among the normal modes predicted by the model do not accurately reflect the experimental situation.

C. IFF DETAILED ANALYSIS

The detailed analysis compared IFD values with experimental measurements every centimeter from 3.0 cm to 11.0 cm from the beach (0.7X to 2.3X). The laboratory measurements were taken by fixing the board at one location and then using the micrometer to adjust the receiver to the desired range. The received CW signal was read from the voltmeter.

These results are depicted in Figures 4.11 through 4.19. In the figures, the IFD predictions are shown as a solid line and the experimental measurements are displayed as circles. Each pressure value was normalized to unity by dividing it by the maximum pressure for the respective curve. The depth values were normalized by dividing each depth by the maximum depth at the particular range.

There is qualitative agreement in the scale of the basic features for all ranges, but quantitative agreement is not observed. The IFD patterns change very little throughout the analysis, while the measured values change more rapidly (especially past 2.0X). The results at 2.1X and 2.3X (Figure 4.18 and Figure 4.19) show that the pressure field can change fairly significantly over a range as short as one centimeter. At those ranges where there is poor agreement between results, there is an indication of phase

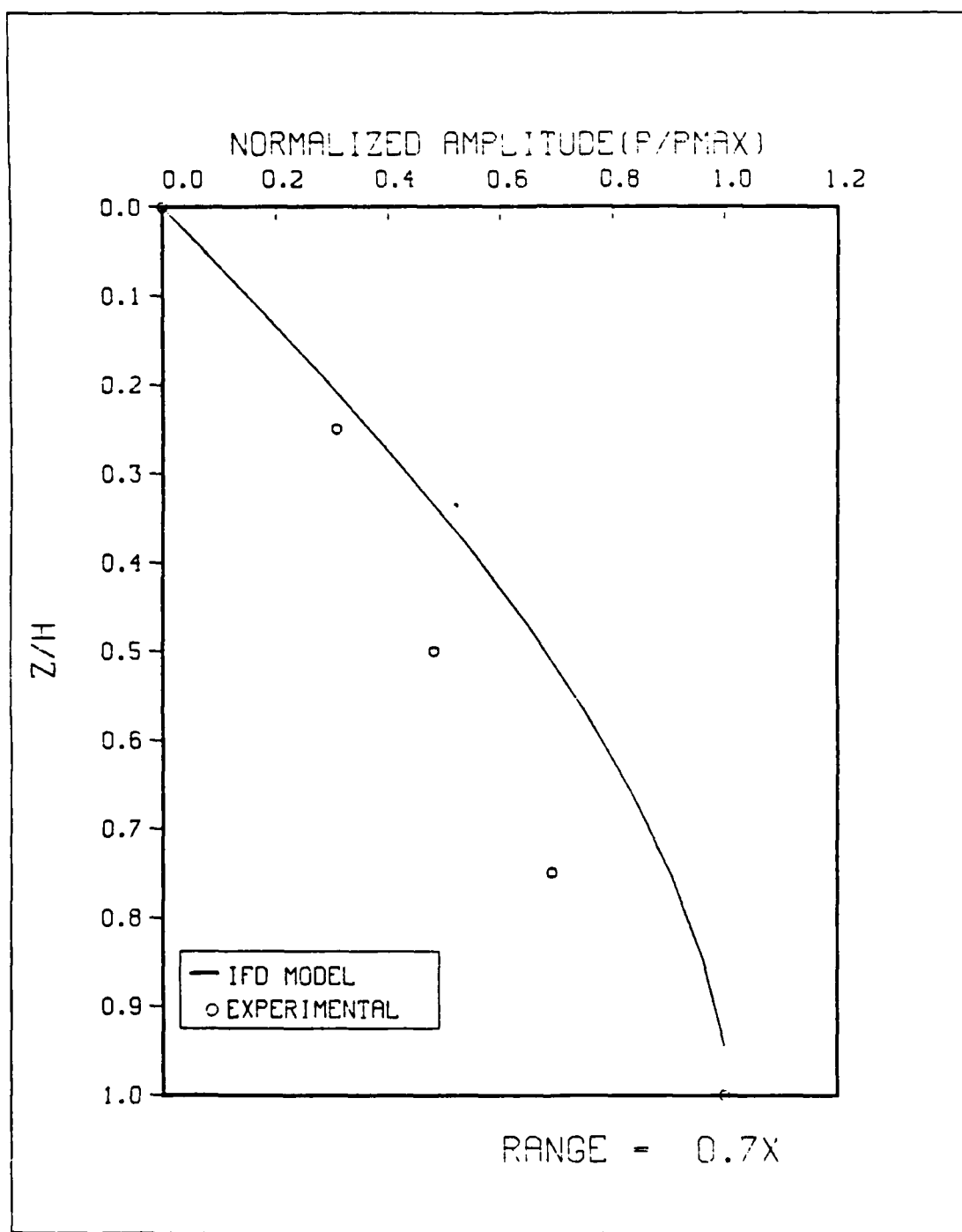


Figure 4.11 Comparison of Results at 0.7X.

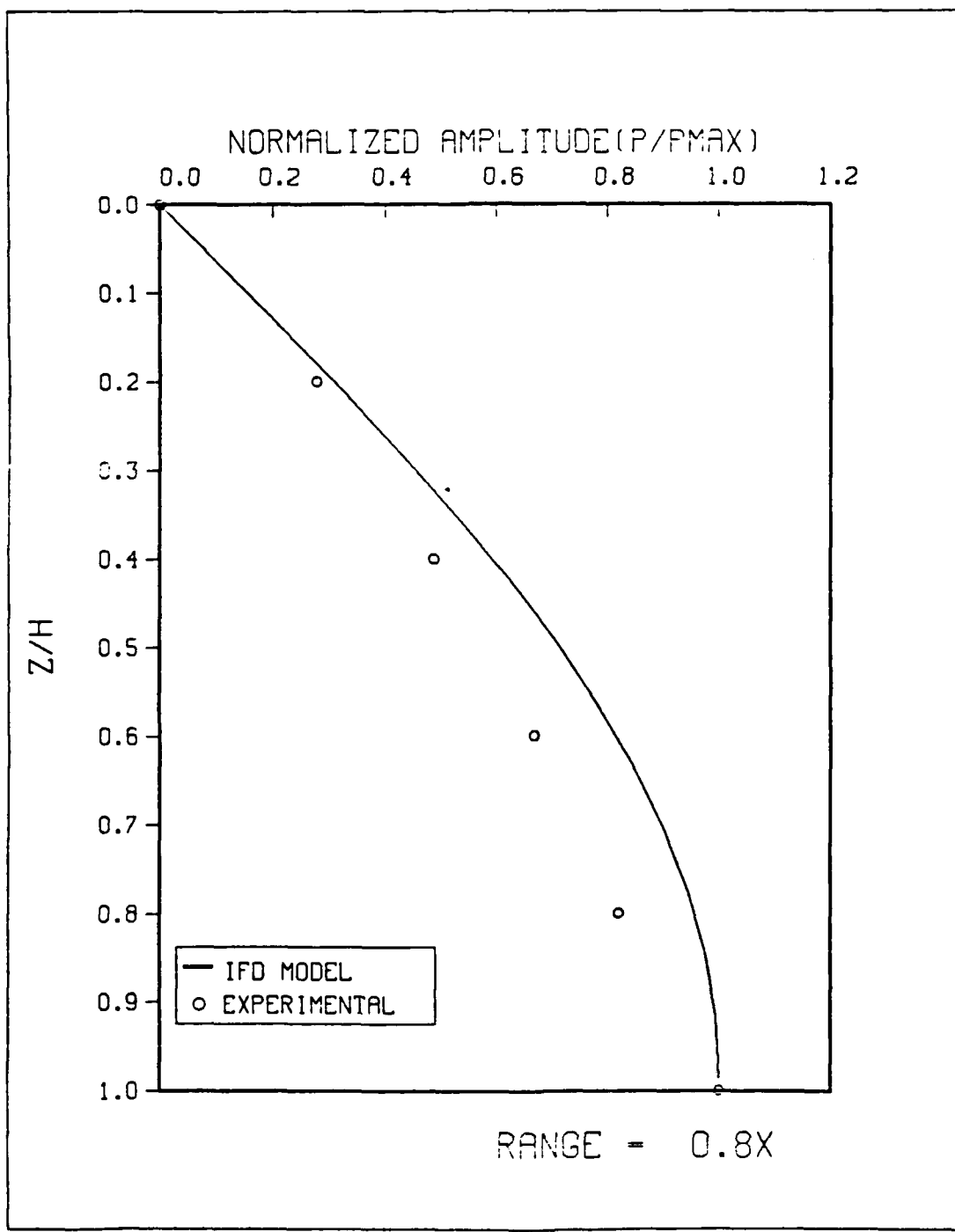


Figure 4.12 Comparison of Results at 0.8X.

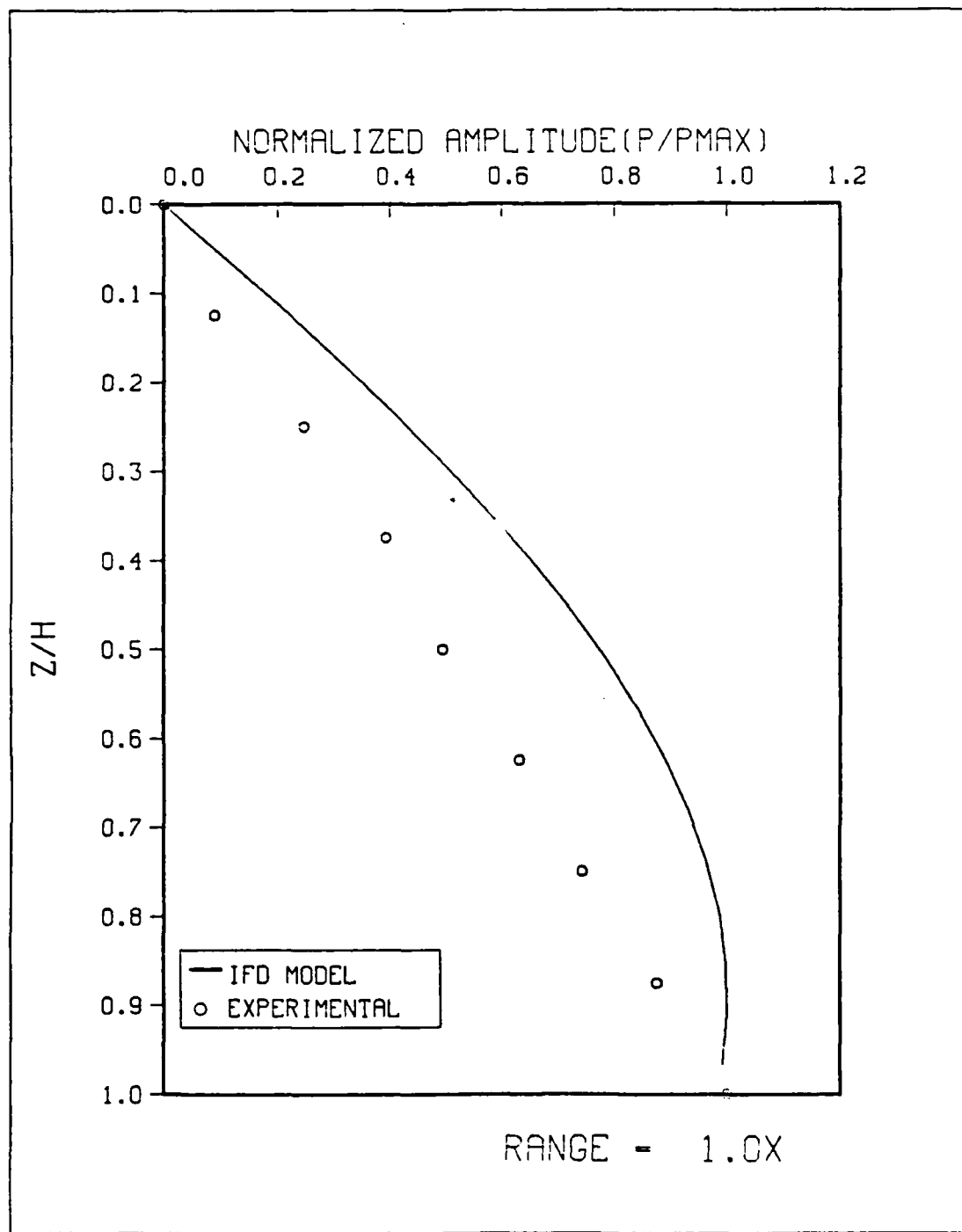


Figure 4.13 Comparison of Results at 1.0X.

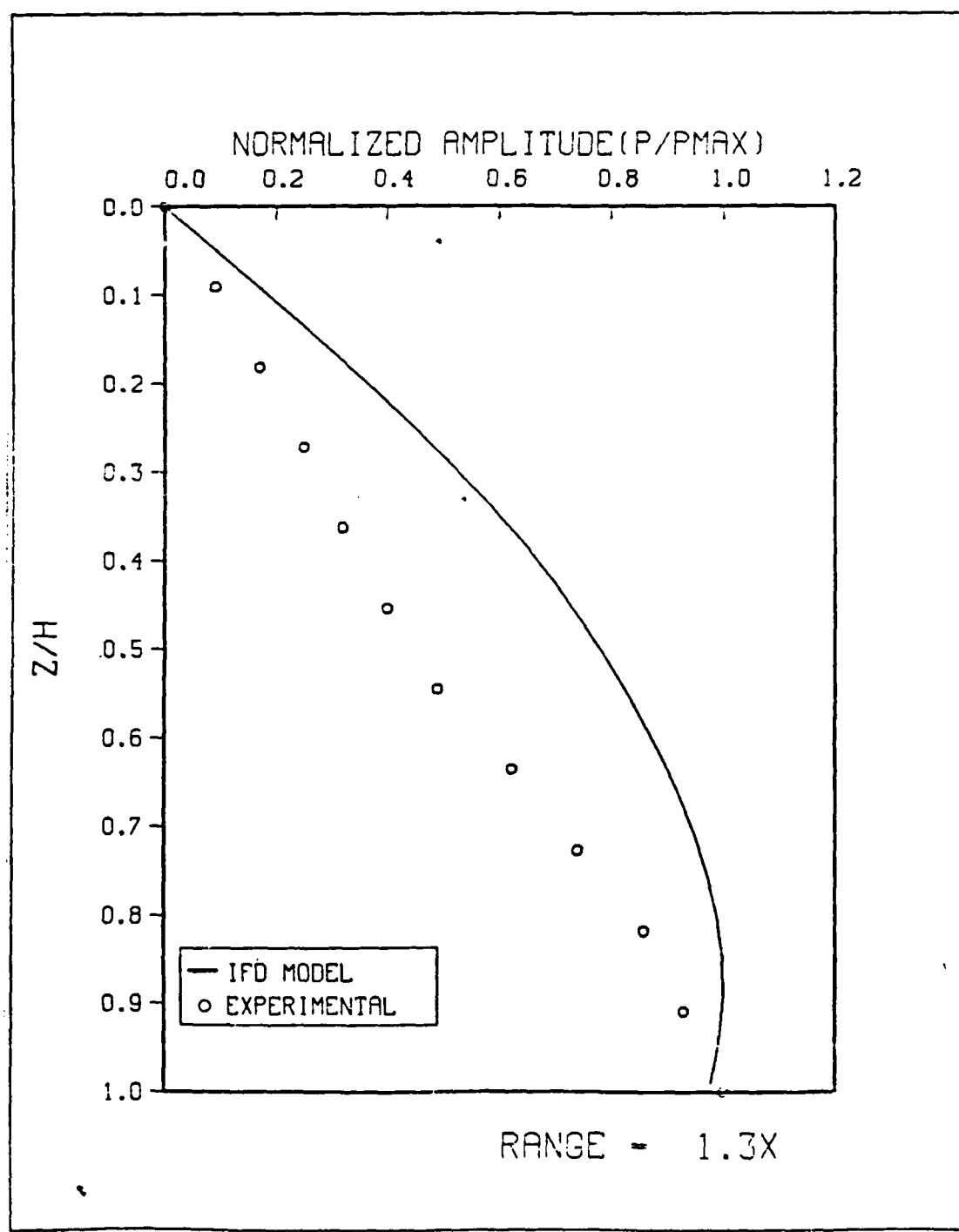


Figure 4.14 Comparison of Results at 1.3X.

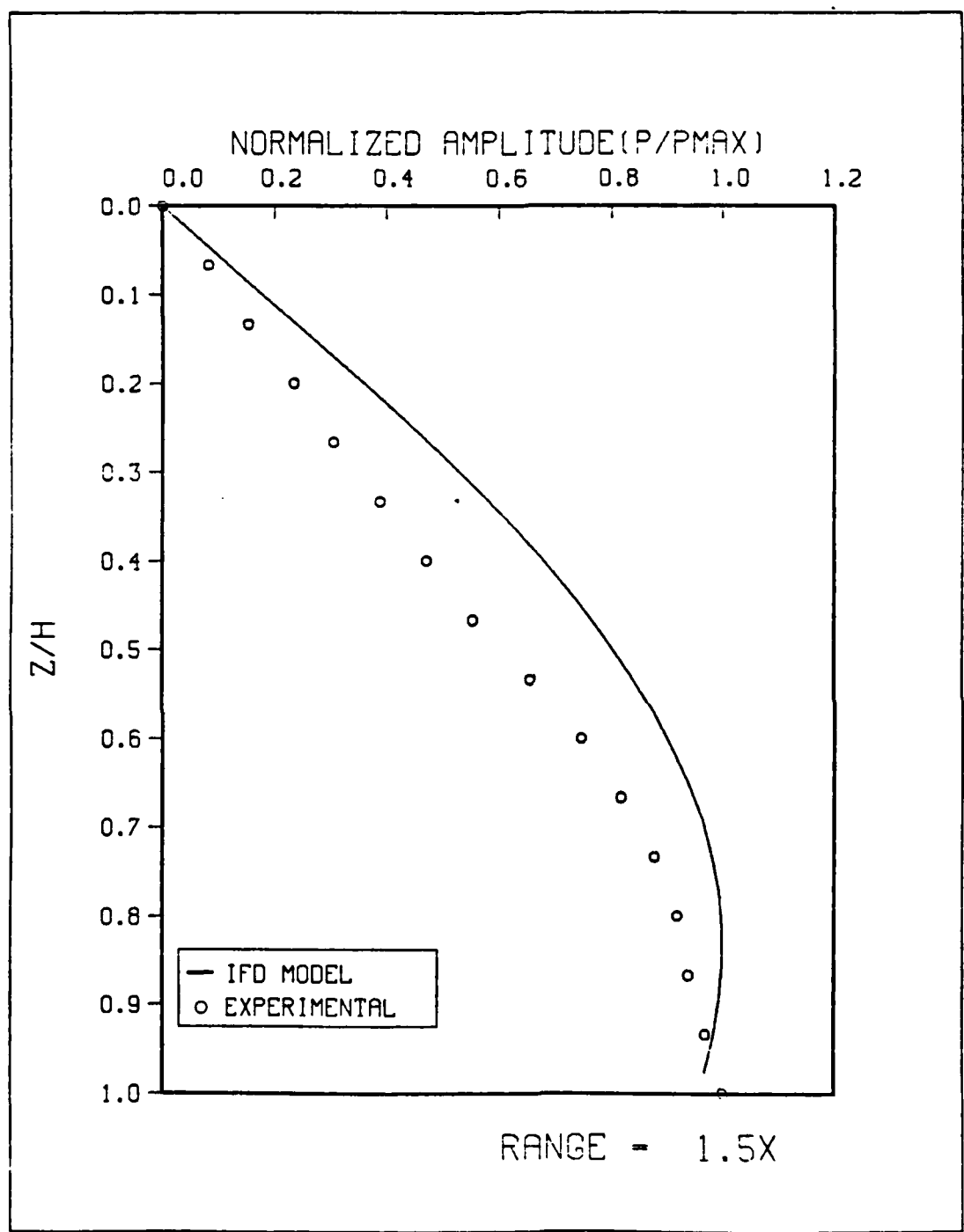


Figure 4.15 Comparison of Results at 1.5X.

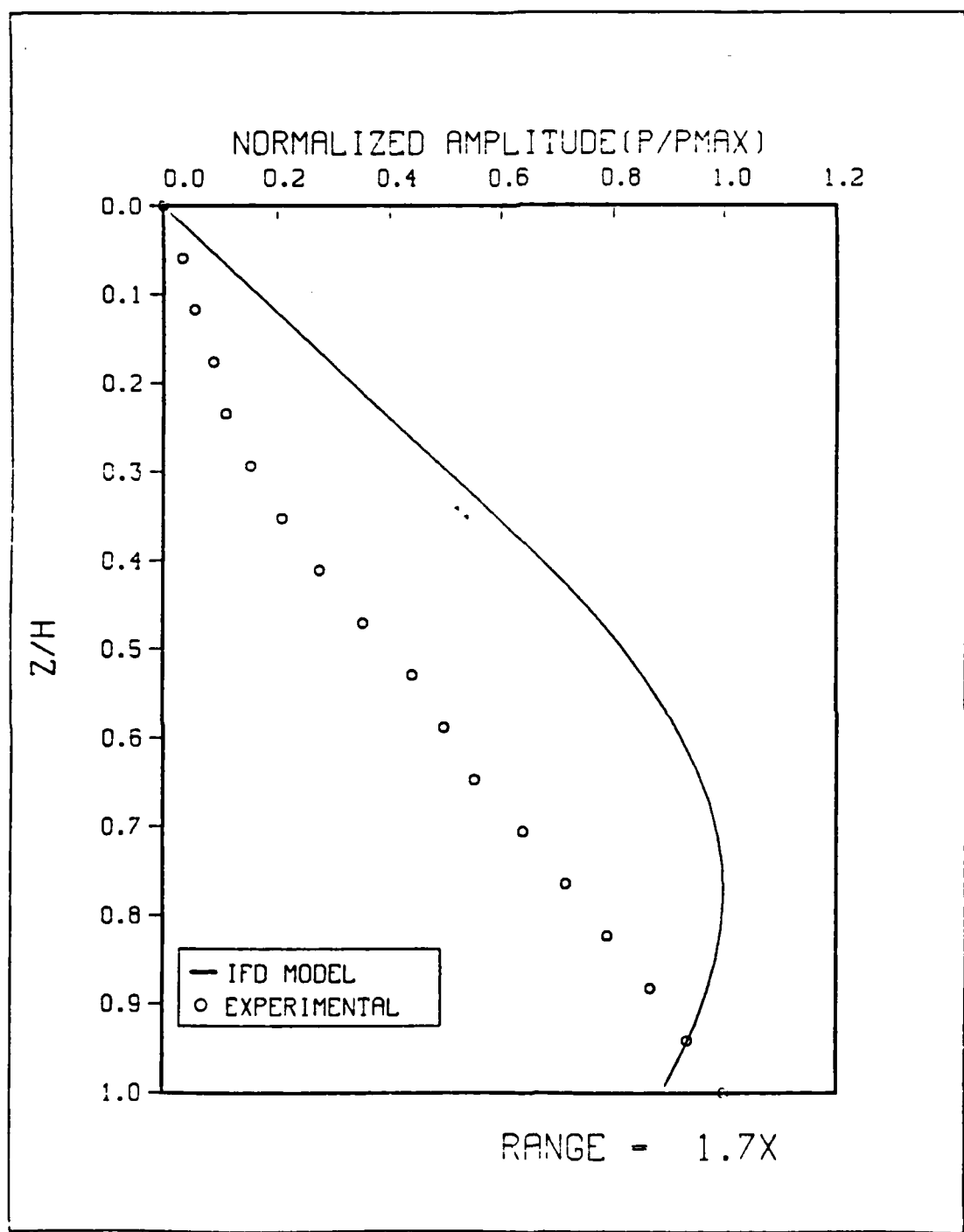


Figure 4.16 Comparison of Results at 1.7X.

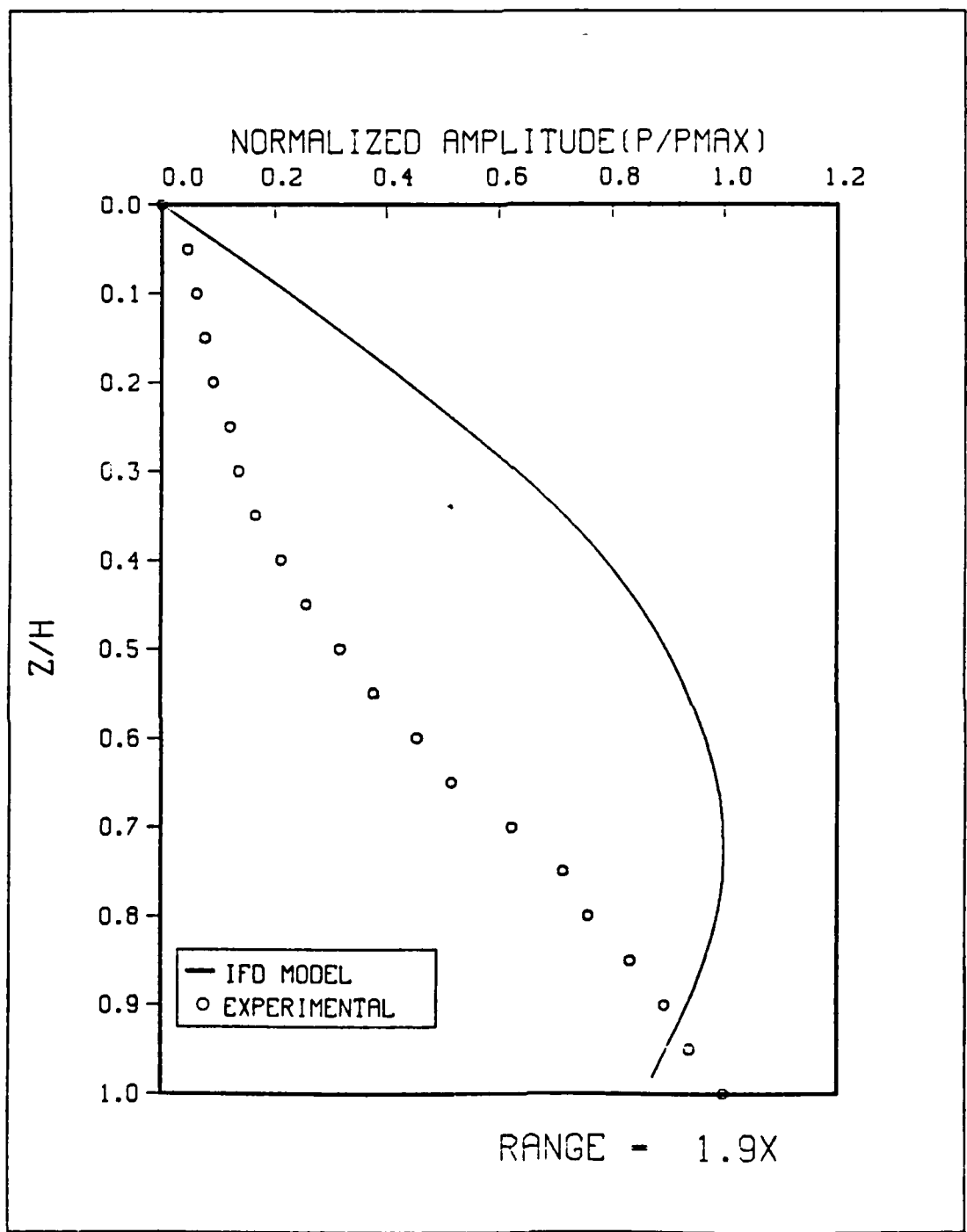


Figure 4.17 Comparison of Results at 1.9X.

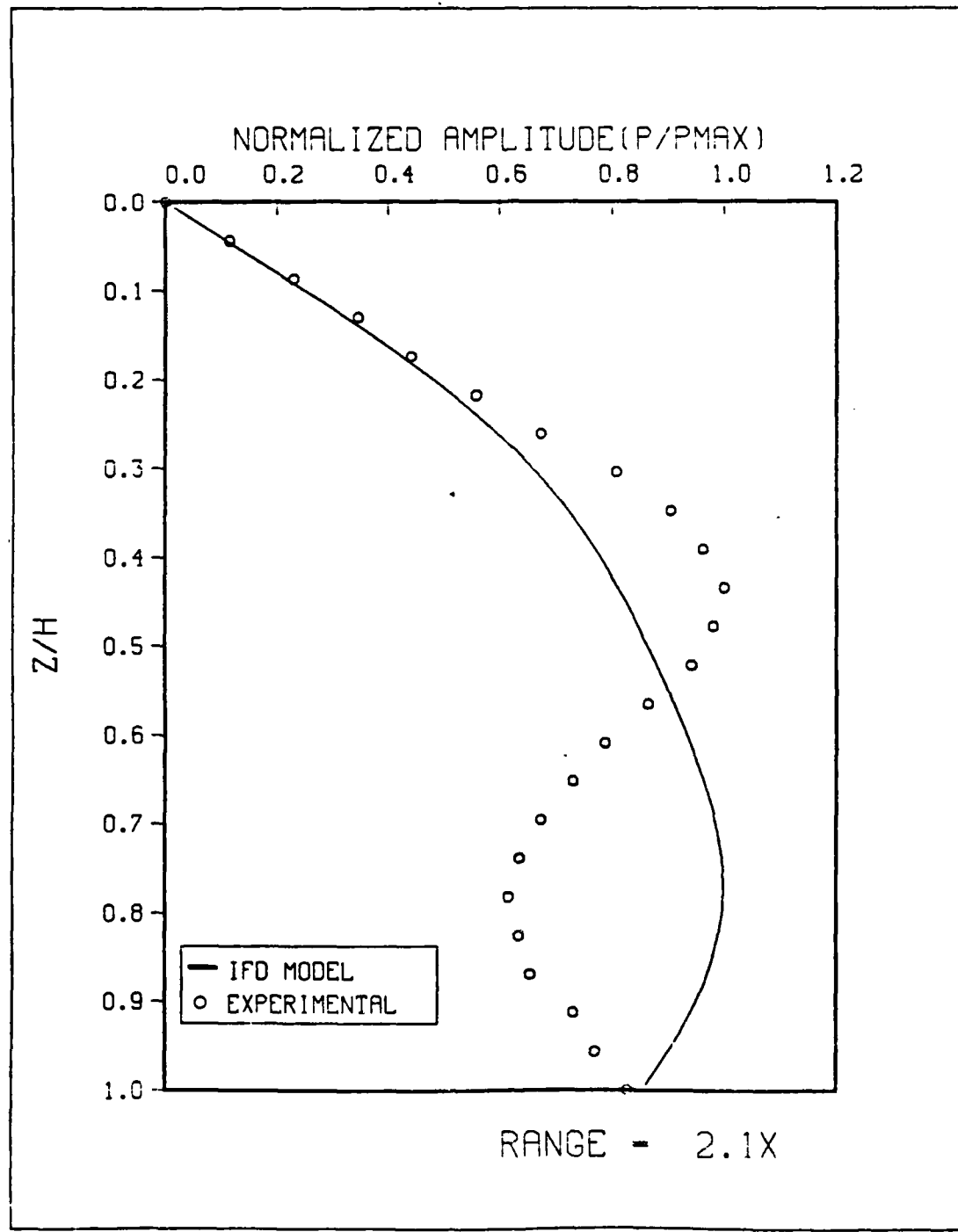


Figure 4.18 Comparison of Results at 2.1X.

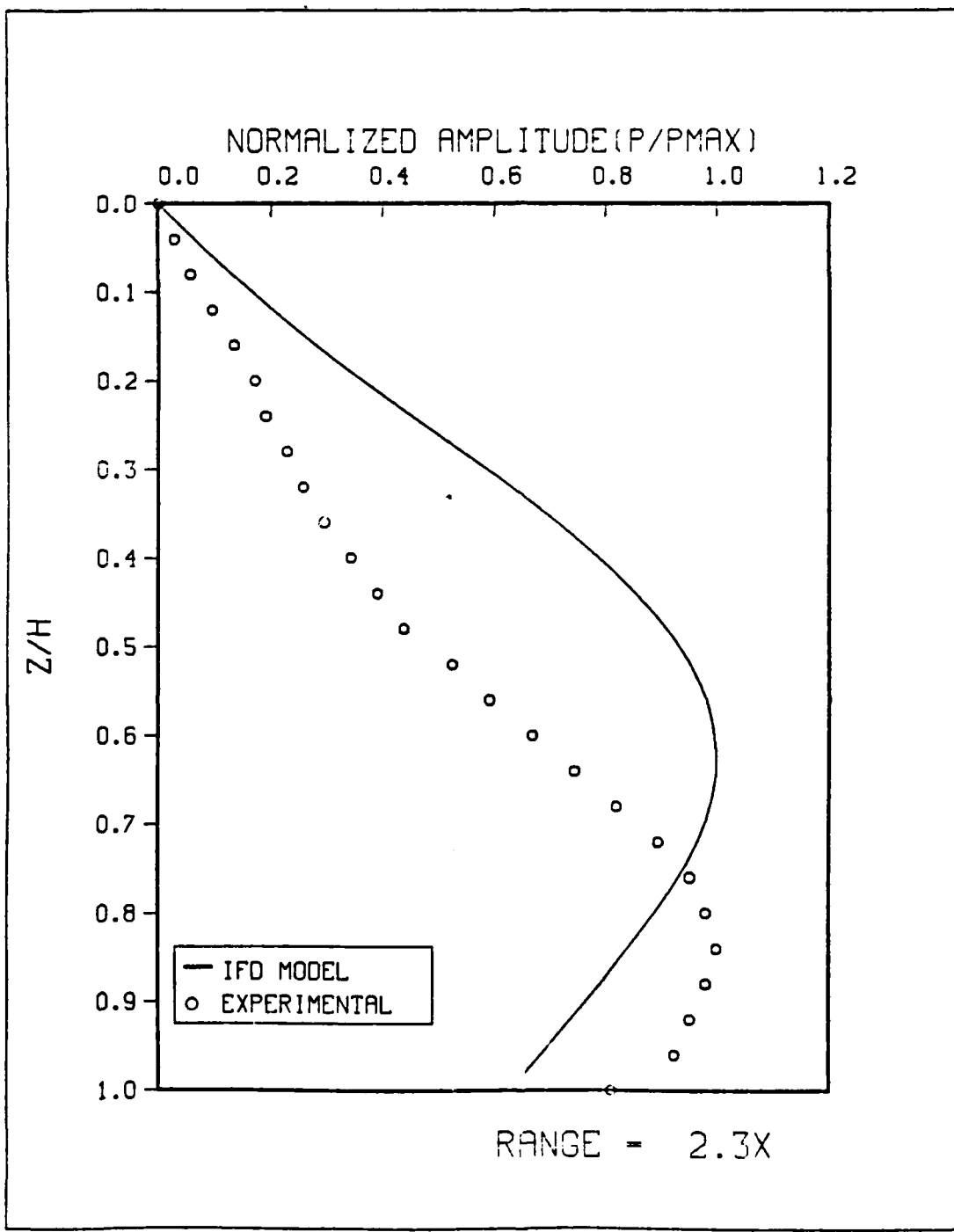


Figure 4.19 Comparison of Results at 2.3X.

interference (Figure 4.18). For distances less than $5X$, theory predicts that for a source at mid-depth, the lowest propagating mode should experience interference from only the evanescent tails of higher modes. Therefore, in the region of the detailed analysis, one expects small interference effects. The experimental results in this region however, show rather significant interference. The interference suggests unsuspected propagating modes are present, or that the evanescent tails are larger than expected. From the trend in the curves it appears as if the phase interference is not a factor from $1.5X$ inward toward the beach (Figures 4.11 through 4.15).

V. CONCLUSIONS/RECOMMENDATIONS

A. CONCLUSIONS

1. Performance of the IFD Model

This analysis of the IFD acoustic model did not uncover any major failures of model performance in a simplified shallow water environment. But this is not to say that the model consistently and accurately performs in such an ocean scenario. Although comparison of IFD predictions with two other models and with simple physical reasoning did not uncover any inconsistencies in performance, the agreement between IFD values and laboratory measurements is insufficient to give complete confidence in the performance of either the model or the experiment.

There is reasonable agreement between the scale of the features predicted by the IFD model and the experiment. Both the model and the measurements show increasing complexity as range is increased from the beach. But despite the similarities, there is poor quantitative agreement in results. One possible cause for the differences may be that the phases of the normal modes predicted by the model are extremely sensitive to minor irregularities in the shape of the interface and the acoustic properties of the bottom. Preliminary work (LeSesne, 1984), suggests that the phase relationships between modes is strongly dependent on the distance of the source from the apex even at great ranges. Consequently, it appears that the collective influence of the normal modes is dependent upon careful geometric control of the experiment.

The detailed analysis around 2X, reveals that large phase interferences occur where only one propagating mode is

expected. This indicates the existence of an extended evanescent tail within cutoff of the higher modes. Kawamura and Iannou (1978), noted that the apparent phases of the evanescent tails are extremely sensitive to the details of the environment. The results indicate that the tail does not decay quickly, and its influence is pervasive (Figures 4.2 and 4.3). From the trend in the curves, it appears this phase interference is not a factor any closer to the beach than 1.5% (Figures 4.11 through 4.15).

2. Modeling/Measurement Procedures

The laboratory measurements represent an initial attempt at modeling an idealized shallow water environment. The experimental techniques are not without problems. All sets of measurements were repeated and showed good agreement. The reproducibility of the measurements suggest that random errors have been minimized. However, systematic errors remain which also contribute to the discrepancies between predicted and measured values. Some of these errors derive from equipment, such as the fact that the size of the hydrophone is of the same order of magnitude as the scale of variations in the pressure field. In addition, the environment in the tank may not be sufficiently close to the ideal environment assumed by the model.

E. RECOMMENDATIONS

Further study and verification of the IFD computer model is recommended. A comparison of IFD predictions with other models not analyzed in this study, may uncover the cause of the inconsistency when compared to measured values. A detailed study of the phase interaction of the normal modes, although extremely complex, may also offer insight into the IFD performance.

It appears that the modeling of an idealized shallow water environment in the laboratory is of value in acoustic model verification. Despite the experimental difficulties, there was qualitative agreement in the basic features between model predictions and laboratory measurements. But the experiment represents only an initial probe into the modeling/measurement techniques of a shallow water environment. Further refinement of these techniques and the experimental equipment may result in better quantitative agreement between model predictions and laboratory measurements.

APPENDIX A
REVISED IFD PROGRAM LISTING

```
*** IMPLICIT FINITE-DIFFERENCE PROGRAM FOR          *IFD00010
*** SOLVING THE PARABOLIC EQUATION - REVISED VERSION    *IFD00020
***                                *IFD00030
***                                *IFD00040
***                                *IFD00050
***                                *IFD00060
***                                *IFD00070
***                                *IFD00080
***                                *IFD00090
*** REVISED BY LT MARK E. KOSNIK (JUNE 1984)      *IFD00100
***                                *IFD00110
***                                *IFD00120
***                                *IFD00130
*** ALPHABETICAL LIST OF PROGRAM VARIABLES FOLLOWING: *IFD00140
***                                *IFD00150
*** A - ARRAY - COEFFICIENT A IN PARABOLIC EQUATION    *IFD00160
***                                (IN WATER)
*** A2 - COEFFICIENT A IN PARABOLIC EQUATION (IN SEDIMENT) *IFD00170
*** ALPHA - VOLME ATTENUATION - DB/METER                *IFD00180
*** ATT - AREAAY - ATTENUATION COEFFICIENT FOR ARTIFICIAL *IFD00190
***                                *IFD00200
*** BETA1 - BETA1 AS DEFINED IN LEE AND MC DANIEL (1983) *IFD00210
*** BETA2 - BETA2 AS DEFINED IN LEE AND MC DANIEL (1983) *IFD00220
*** BETA1 - ATTENUATION IN WATER - LB/WAVELENGTH            *IFD00230
*** BETA2 - ATTENUATION IN SEDIMENT - DB/WAVELENGTH        *IFD00240
*** BE - AREAAY - RANGE FOR BOTTOM PROFILE - METERS      *IFD00250
*** BZ - ARRAY - DEPTH FOR BOTTOM PROFILE - METERS        *IFD00260
*** C - ARRAY - COUNTAINS TRIDIAGONAL MATRIX SYSTEM THAT NEEDS *IFD00270
***                                *IFD00280
***                                *IFD00290
*** CO - TOEFL SOLVE SCUND SPEED - METERS/SEC           *IFD00300
***                                *IFD00310
*** C2 - SOUND SPEED IN SEDIMENT                         *IFD00320
*** CCSE - COS ( THETA ) - STORAGE SPACE USED IN SUBROUTINES *IFD00330
*** CF - ARRAY - TRILL - SCUND SPEED IN SOUND SPEED FILE - *IFD00340
*** CSVP - ARRAY - METERS/SEC - AREAY - STORAGE SPACE USED IN SUBROUTINES TRILL AND *IFD00350
***                                *IFD00360
*** CTRO - TRILL - SCUND SPEED IN SOUND SPEED FILE -     *IFD00370
***                                *IFD00380
```

CC

*** CWTER - AREAY - SCUND SPEED AT GRID POINTS IN WATER COLUMN
 *** DELTA - DELTIA AS DEFINED IN LEE AND MC DANIEL (1983)
 *** DELIN - /DELTIA -
 *** DIFD - ARRAY - STORAGE SPACE FOR TI VALUES USED TO CONTOUR
 *** PLCT -
 *** D5LVL - RANGE STEP - METERS
 *** DEHAX - MAXIMUM ACHALMENGE RANGE STEP - METERS
 *** D2 - DEPTH INCREMENT "I"
 *** EYE - COFFLEX "I"
 *** FREQ - FREQUENCY - HZ
 *** GAHA1 - GAHA1 AS DEFINED IN LEE AND MC DANIEL (1983)
 *** GAHA2 - GAHA2 AS DEFINED IN LEE AND MC DANIEL (1983)
 *** IETOT1 - POINTER THAT POINTS TO BOTTON PROFILE PCINT AT START
 *** IETOT2 - COFFLEX SEGMENT OF SOLUTION "I"
 *** IETOT2 - POINTER THAT POINTS TO BOTTON PROFILE PCINT AT END
 *** ID - ARRAY - RUN IDENTIFICATION
 *** IFACE1 - POINTER THAT POINTS TO INTERFACE AT RANGE RA1
 *** IFACE2 - INTERFACE + 1
 *** IFACEP - COUINTER INDEX FOR DEPTH VALUES PRINTED
 *** IFZ - COUINTER IPZ, THE VALUE IN DEPTH IS PRINTED
 *** IIS - COUINTER INDEX FOR RANGE VALUES
 *** ISLOPE - SLCICE FLAG:
 *** ISICEE - BOTTOM SLOPES DJ WN
 *** ISICEE = 2 - BOTTOM LEVEL
 *** ISICEE = 3 - BOTTOM SLOPES UP
 *** ISICEE = 4 - BOTTOM SLOPES DOWN
 *** ISICEE = 5 - BOTTOM SLOPES UP, BOTTON MODIFIED
 *** ITEMP - TBLICARY VARIABLE CORRESPONDING TO RECEIVER DEPTH
 *** ITZ - NUMBER OF ECUT-SPONT POINTS IN
 *** INCUDIES BOTTON POINT - DOES NOT INCLUDE SURFACE PCINT
 *** NAOI - NUMBER OF POINTS IN ARTIFICIAL ATTENUATION LAYER
 *** NEOT - NUMBER OF POINTS IN BOTTON PROFILE (BF AND EZ)
 *** NIJ - UNIT NUMBER FOR INPUT DATA
 *** NH1 - UNIT NUMBER FOR OUTPUT PLOTTER FILE
 *** NCOUT - UNIT NUMBER FOR OUTPUT PRINTER FILE
 *** NOUT - NUMBER OF RANGE STEPS ALONG A BOTTON SEGMENT
 *** NSTEP - NUMBER OF RANGE STEPS CORRESPONDING TC CNE VERTICAL
 *** NSTEP1 - GRILL STEP FC MODIFIED BOTTON
 *** NSVP - POINTS IN CSVP AND ZS VP
 *** NMAX - NUMBER OF GRID POINTS IN WATER AT MAX DEPTH
 *** NMLPS - NUMBER OF NEAT LEVEL SECTION FOLLOWING A SLICING
 *** SECTION FOR A MODIFIED BOTTON

*** PER - RANGE INCREMENT AT WHICH SOLUTION IS PASSED TO
 CUTLINE PRINTERT FILE - METERS IFD00870
 DEPTH INCREMENT AT WHICH SOLUTION IS PRINTED - METERS IFD00880
 THE VALUE OF PISS - DB IFD00890
 PROPAGATION LOSS - DB IFD00900
 ABSAY - MAGNITUDE OF REAL AND IMAGINARY PRESSURE
 RANGE AT WHICH BOTTOM DEPTH IS AVAILABLE - METERS IFD00910
 NEXT RANGE AT WHICH BOTTOM DEPTH IS AVAILABLE - METERS IFD00920
 INCREMENT AS SOLUTION IS MARCHED OUT IN RANGE.
 IFD00930
 IFD00940
 IFD00950
 IFD00960
 IFD00970
 IFD00980
 IFD00990
 IFD01000
 IFD01010
 IFD01020
 IFD01030
 IFD01040
 IFD01050
 IFD01060
 IFD01070
 IFD01080
 IFD01090
 IFD01100
 IFD01110
 IFD01120
 IFD01130
 IFD01140
 IFD01150
 IFD01160
 IFD01170
 IFD01180
 IFD01190
 IFD01200
 IFD01210
 IFD01220
 IFD01230
 IFD01240
 IFD01250
 IFD01260
 IFD01270
 IFD01280
 IFD01290
 IFD01300
 IFD01310
 IFD01320
 IFD01330
 IFD01340

*** PEZ - CUTLINE INCREMENT AT WHICH SOLUTION IS PASSED TO
 PRINTERT FILE - METERS
 *** FI - DEPTH INCREMENT AT WHICH SOLUTION IS PRINTED - METERS
 *** EEMAG - PROPAGATION LOSS - DB
 *** R1 - RANGE AT WHICH BOTTOM DEPTH IS AVAILABLE - METERS
 *** R2 - NEXT RANGE AT WHICH BOTTOM DEPTH IS AVAILABLE - METERS
 *** RA1 - INCREMENT AS SOLUTION IS MARCHED OUT IN RANGE.
 *** RA2 - RANGE AT WHICH SOLUTION IS KNOWN - METERS
 *** RA2 = RA1 + DR
 *** RH01 - DENSITY IN WATER - GM/CM**3
 *** RH02 - DENSITY IN SEDIMENT - GM/CM**3
 *** ENAX - MAXIMUM RANGE CP SOLUTION - METERS
 *** SINE - SIN (THETA)
 *** TEMP - STEEPLY VARYING VARIABLE
 *** TETTA - SLICE OF SECTION - RADIAN
 THETTA = 0 - LEVEL INTERFACE DCWN
 THETTA > 0 - INTERFACE SLOPES UP
 ARRAY - COMPLEX ACOUSTIC PRESSURE FIELD
 PICTURE FILE AT WHICH SOLUTION IS WRITTEN TO OUTPUT
 *** U_RR - REFERENCE WAVE NUMBER
 *** XK0 - REFERENCE ELEMENT X MATRIX. LOWER DIAGONAL, ON INTERFACE
 *** YI1 - X MATRIX FOR SIOFING BOTTOM
 *** XI1Z - REFERENCE WAVELENGTH - METERS
 *** XIANDA - MATRIX ELEMENT. X MATRIX, OFF-DIAGONAL, IN WATER AND
 SEDIMENT
 *** XIWS - MATRIX ELEMENT. X MATRIX, MAIN DIAGONAL, ON INTERFACE
 *** YH1 - MATRIX ELEMENT. X MATRIX, MAIN DIAGONAL, IN SEDIMENT
 *** YHS - MATRIX ELEMENT. X MATRIX, MAIN DIAGONAL, IN
 *** YHN - WATER - MATRIX ELEMENT. X MATRIX, MAIN DIAGONAL, IN
 *** XN - REAL INDEX OF REFRACTION SQUARED
 *** YN1 - COMPLEX INDEX OF REFRACTION SQUARED - METERS
 *** XER - RANGE AT WHICH SOLUTION IS WRITTEN TO OUTPUT
 *** XER - RANGE AT WHICH SOLUTION IS WRITTEN TO OUTPUT
 *** XX... - VARIABLES THAT BEGIN WITH XX HAVE NO SPECIAL PHYSICAL
 SIGNIFICANCE BUT THEY CONTRIBUTE TO COMPUTATION
 EFFICIENCY. ALL XX VARIABLES ARE CALCULATED IN
 SUFFICIENT INITIAL VALUES INDEPENDENT OF RANGE STEP
 AND INTERFACE SLOPE, AND ALL ARE USED TO CALCULATE
 MATRIX ELEMENTS.
 *** YI1 - MATRIX ELEMENT X MATRIX. LOWER DIAGONAL, ON INTERFACE
 *** YIIV - YI1 FOR LEVELING INTERFACE
 *** YIZ - YI1 FOR SIOFING INTERFACE

*** YIRWS - MATRIIX ELEMENT, Y MATRIIX, OFF-DIAGCNAL, IN WATER AND IFDO1350
 *** YMI - MATRIIX ELEMENT, Y MATRIIX, MAIN DIAGCNAL, ON INTERFACE IFDO1360
 *** YMS - MATRIIX ELEMENT, Y MATRIIX, MAIN DIAGONAL, ON INTERFACE IFDO1370
 *** YMH - MATRIIX ELEMENT, Y MATRIIX, MAIN DIAGONAL, IN SEDIMENT IFDO1380
 *** YMR - MATRIIX ELEMENTS, Y MATRIIX, MAIN DIAGCNAL, IN IFDO1390
 *** YWT - MATRIIX ELEMENT, Y MATRIIX, UPPER DIAGCNAL, ON INTERFACE IFDO1400
 *** YF1 - YR1 FOR SLOPING INTERFACE IFDO1410
 *** YF2 - DEPTH OF WATER AT RANGE R1 - METERS IFDO1420
 *** YF3 - DEPTH OF WATER AT RANGE R2 - METERS IFDO1430
 *** YF4 - DEPTH OF WATER EDGE OF ARTIFICIAL ATTENUATION IFDO1440
 *** ZABLYR - DEPTH OF WEFER LAYER - METERS IFDO1450
 *** Z1YR1 - DEPTH OF GRID POINT - METERS IFDO1460
 *** Z1YR2 - MAXIMUM WATER DEPTH - METERS IFDO1470
 *** ZE - DEPTH OF FREESURE RELEASE SURFACE - METERS IFDO1480
 *** ZE - RECEIV ER DEPTH - METERS IFDO1490
 *** ZS - SOURCE DEPTH - METERS IFDO1500
 *** ZSVP - ARRAY THAT FOR SOUND SPEED PROFILE - METERS IFDO1510
 *** Z2... - BEGIN WITH ZZ HAVE SPECIAL PHYSICAL IFDO1520
 *** Z2... - SIGNIFICANCE BUT THEY CONTRIBUTE TO COMPUTATIONAL IFDO1530
 *** Z2... - EFFICIENCY. ALL ZZ VARIABLES ARE CALCULATED IN IFDO1540
 *** Z2... - SUBROUTINE NEWMAT ALI DEPEND ON RANGE STEP AND OR IFDO1550
 *** Z2... - INTERFACE SLOPE, AND ALL ARE USED TO CALCULATE MATRIX IFDO1560
 *** Z2... - ELEMENTS. IFDO1570
 *** Z2... - ****
 *** INPUT IFDO1580
 *** UNIT NUMBER = NIU IFDO1590
 *** INPUT FILENAME AND FILETYPE = IFDIN DATA IN IFDO1600
 *** CONTENTS: CARD IMAGES IN FREE FORMAT IFDO1610
 CARD 1 : EQN ZSR, CO N IFDO1620
 CARD 2 : ER{1} DRIVL, DRMAX, WDR, PDR, PLZ IFDO1630
 CARD 3 : ER{1}, B2{1} IFDO1640
 CARD 4 : ER{2}, B2{2} IFDO1650
 IFDO1660
 IFDO1670
 IFDO1680
 IFDO1690
 IFDO1700
 CARD N : IFDO1710
 CARD N+1 : -1 -1 RHC1, BETA1 ** IFDO1720
 CARD N+2 : ZSVP{1}, CSVP{1} ** IFDO1730
 CARD N+3 : ZSVP{2}, CSVP{2} ** IFDO1740
 CARD N+4 : IFDO1750
 IFDO1760
 IFDO1770
 IFDO1780
 IFDO1790
 IFDO1800
 IFDO1810
 IFDO1820

CC

WHERE:

PERC
2S = FREQUENCY (HZ) (M)
2R = RECEIVED DEPTH (M)
CO = REFERENCE SOUND SPEED (M/S). IF CO = 0.0, CO IS SET TO AVERAGE SCOUND SPEED IN WATER COLUMN.
N = NUMBER OF GRID POINTS

RMAX = MAXIMUM RANGE (M) OF SOLUTION
DRVL = RANGE STEP (M) ALONG LEVEL INTERFACE. IF DRVL = 0.0, DRVL SET TO 1/2 WAVELENGTH. IF DRVL GREATER THAN DRMAX, DRVL SET TO DRMAX.
DRMAX = MAXIMUM ALLOWABLE RANGE STEP (M). IF DRMAX = 0.0, DRMAX IS SET TO ONE WAVELENGTH.
WDR = RANGE STEP (M) AT WHICH SOLUTION IS WRITTEN TO FILE USED BY PLOTTING ROUTINE.
PDR = ROUNDED TO NEAREST DR WHICH SOLUTION IS PRINTED.
PDZ = ROUNDED TO NEAREST DR WHICH SOLUTION IS PRINTED.
PDZ = DEPTH INCREMENT AT WHICH SOLUTION IS PRINTED.
BR = RANGE (M) OF BOTTOM PROFILE
BZ = DEPTH (M) OF BOTTOM PROFILE

ZLYR1 = MAXIMUM WATER DEPTH (M)
RHO1 = DENSITY IN WATER (GM/CH**3)
BETA1 = ATTENUATION (DB/WAVELENGTH) IN WATER. IF BETA1 NEGATIVE THEN ATTENUATION COMPUTED.

ZSVP = DEPTH (M) ARRAY FOR SOUND SPEED PROFILE
CSVP = SOUND SPEED (M/S) ARRAY FOR SCOUNT SPEED PROFILE

ZLYR2 = DEPTH (M) OF PRESSURE RELEASE SURFACE
RHC2 = DENSITY (GM/CH**3) IN SEDIMENT
BETA2 = ATTENUATION (DB/WAVELENGTH) IN SEDIMENT
C2 = SOUND SPEED (M/S) IN SEDIMENT

ZAEYL = DEPTH (M) OF UPPER SURFACE OF ARTIFICIAL ATTENUATION LAYER

*** CPUTPUT *****
*** OUTPUT UNIT NUMBER FOR FILE USED BY PLOTTING ROUTINE = NOU
FILENAME AND FILETYPE FOR OUTPUT PLCTER FILE = IFDCUT ELCITER IFD02280
CUTPUT UNIT NUMBER FOR PRINT FILE = NPOUT
IFD02300


```

20      CALL DCNN
       GO TO 70
*** EOTOM IS LEVEL
       CALL LEVEL
       GO TO 70
*** EOTOM SLOPES UP
       CALL UP
       GO TO 70
*** EOTOM SLOPES DOWN SLOWLY, 3 CTCH MODIFIED
       CALL SLOPE
       GO TO 70
*** EOTOM SLOPES UP SLOWLY, BOTOM MODIFIED
       CALL SSLOPE

C70     CONTINUE
       CALL ATINU(U,ATT,IA,NA)
       RA2F = FA2+0.5
*** TIME TO WRITE?
       IF (FA2P.GE.XER) CALL WRITE2
*** TIME TO PRINT?
       IF (FA2P.GE.XER) CALL PRINT2
* -* TIME TO TERMINATE?
       IF (FA2.GE.RMAX) GO TO 90
CONTINUE

C80     *** GC BACK AND CONTINUE WITH NEXT LINEAR BOTTOM SEGMENT
       GC TO 10

C90     *** TIME TO TERMINATE
       CCBTIME
       WRITE(21,190) (FLFD(I,J),I=1,151),J=1,151)
       C00    FCENH(16F7,2)
       WRITE(27,101) (FLFD(I,J),I=1,121),J=1,121)
       101   FCENH(16F7,2)
       CALL END(FA2)
       STCF
       FINL

CCCCC  SUBROUTINE READ
CCCCC  {1} THIS SUBROUTINE READS ALL INPUT DATA.
CCCCC  {2} THE DATA IS READ FROM INPUT UNIT NUMBER: NIU = 51
CCCCC  {3} INPUT FILENAME AND FILETYPE ARE: IFLIN: DATAIN
CCCCC  {4} DATA IS READ IN FREE FORMAT.
CCCCC  {5} DATA IS TRANSFERRED BACK TO MAIN PROGRAM VIA COMMON BLOCK IFDO3260

```

```

C      CCEMCN /IN/ IABOT1, LEAVE IPZ4 ISLOPE, 1STEP, IN2.N, NA, NBCI, NN1.
C      * CCEMCN /NSTEP, ALEPHAAIT(5000) BETA1B(1C1) BZ(101) CO
C      * REAL, ALEPHAAIT(5000) BETA1B(1C1) BZ(101) CO
C      * CSVP(C1) C2CMATER(5000) DREIVL DEMAX(ZFRQ) EDR EIZ
C      * R1RA1EA2BRHC1EHO2RMAYTHETAXXK0 XLAHSAAPR W4, XX10.
C      * X11, X5EDRZLYR1, ZLYR2, ZR, ZS, ZSVP(101), ZAEFLR
C      * DATA NIU/5/, NEOUT/5/, /

C      *** READ INPUT PARAMETERS
C      READ(NIU,*END=100) ERCPY, ZSLVL, CO_N
C      READ(NIU,*END=100) BMAY, DRMAX, WDE, EDE, PRZ

C      *** READ BCTTC PROFILE - RANGE, DEPTH
C      DC 10 I=11C1
C      READ(NIU,*END=100) BR(I), BZ(I)
C      NBO1=I
C      *** END OF PROFILE?
C      IP(ER(I)-LT.0.0) GO TO 20
C      *** NO
C      CCNTINUE

C      CCNTINUE
C      *** EXTEND LAST DEPTH BEYOND MAX RANGE
C      ER(NBOT)=1.0E+10
C      EZ(NBOT)=EZ(NBOT-1)

C      *** FIRST LAYER IS WATER, SECOND IS SEDIMENT
C      READ(MAXDEPTH,DENSITY AND ATTENUATION OF FIRST LAYER
C      READ(NIU,*END=100) ZLYR1, RHO1, BEIA1
C      *** READ SCUND SPEED PROFILE IN FIRST LAYER
C      DC 25 I=1, 1C1
C      NSVP=I
C      READ(NIU,*END=100) ZSVP(I), CSVE(I)
C      *** IF ANOTHER PROFILE POINT?
C      IF(ZSVP(I)-LT.ZLYR1) GO TO 25
C      *** NO
C      *** WAS THAT THE LAST PROFILE POINT?
C      IF(ZSVP(I)=EC:ZLYR1) GO TO 30
C      *** NO, THERE IS ERROR.
C      GO TO 101
C      CCNTINUE

C      *** DOES THE SCENE SPEED PROFILE START AT THE SURFACE?
C      IF( ZSVP(1).NE.0.0 ) GO TO 102
C      *** YES

```

```

C *** READ DEPTH, DENSITY, ATTENUATION AND SPEED IN SECOND LAYER
C   READ (NIU*,IND=100) ZLYR2,RHO2,BETA2,C2
C   READ (DEPTH,CF,IND=100) EDGE_OF_ARTIFICIAL_ATTENUATING_LAYER
C   READ (NIU*,IND=100) ZAEYL
C   RETURN

C *** ERROR EXITS
100  WRITE(6,900)
      WRITE(NPOUT,900)
      STOP
      WRITE(6,901)
      WRITE(NPOUT,901)
      STOP
      WRITE(6,902)
      WRITE(NPOUT,902)
      STOP

C 900  *FCFMAT // EXECUTICA TERMINATED. //*
      *FCFMAT // EXECR: FINAL DEPTH IN SOUND SPEED PRCFILE DOES NOT *
      *          EXECUTICA TERMINATED. //*
      *FCFMAT // EXECR: FIRST DEPTH IN SOUND SPEED PRCFILE*
      *          PRCFILES NOT EQUAL. ZERO. //*
      *EXECUTICA TERMINATED. //*
      ENI

C SUPERCLINE SVPL
C {1} THIS SUBROUTINE CALCULATES THE VERTICAL SIZE: DZ
C     EACH OF THE VERTICAL GRID POINTS. THE SPEED OF SOUND AT
C     SOUND SPEED VALUES ARE DETERMINED BY LINEAR INTERPOLATION.
C {2} SOUND SPEEDS ARE STORED IN CWATER(I)
C {3} THE INDEX I RANGES FROM 1 TO NMAX.
C {4} CWATER(I) CORRESPONDS TO THE GRID FCINT DZ EELCW
C     THE SURFACE.

CCMNCN /IN/LIBOT1,IFACE,IPZ,IISLOPE,ISTEP,INZ,N,NA,NBCT,NN1,
* CCMNCN /NSTEP,NSTEP,NSVE,NMAX,NXNFS
* CCMNCN /REAL/AIFHA/AT(5000),BETA1,BETA2,B(1C1),B2(101),C0
* CCMNCN /CSVP/(1C1),C2,CWATER(5000),DRIV1,DMAX,FZ,FRO,FZ,FZ
* R1(RA1,EEA2,BRH,C1,FHO2,RMAX,THETA,XK6,THETA,XK4,XX10,
* XX11,XX12,BDR,Z1YR1,Z1YR2,ZR,ZS,ZSV2(101),ZAEYL

```

```

C   ***CALCULATE VERTICAL STEP SIZE
C   D2 = ZLYR2 / FLOAT (N)
C   ***CALCULATE NUMBER OF GRID POINTS IN WATER COLUMN
C   NWMAX = INT ((ZLYR1/DZ)+0.5)
C
C   ***CALCULATE SOUND SPEED AT ALL GRID POINTS IN WATER COLUMN
C   L = 1
C   DO 20 I=1,NWMAX
C       ZI = I*D2
C       LP1 = L+1
C       ***NEED TO UPDATE PROFILE ENDPOINTS?
C       IF (ZI.LE.ZSVP(IP1)) GO TO 10
C       ***YES
C       L = L+1
C       LF1 = I+1
C       CWATER (I) = CSVP(L)+ (CSVP(LP1)-CSVP(L)) * (ZI-ZSVP(L)) /
C
C   10  *      CCCONTINUE
C
C   20  *      CCCONTINUE
C
C   C   RETURN
C
C   CCCCC
C   C   SUBROUTINE INITIAL
C   C   {1}  THIS SUBROUTINE INITIALIZES CONSTANTS AND VARIABLES
C   C   {2}  VALUES ARE TRANSFERRED TO/FROM MAIN PROGRAM VIA COMMON
C   C   BLOCK.
C
C   C   CCMHCN /IN/ IA,IBOT1,IFACE,IP2,ISLOPE,ISTEP,IW2,N,NA,NBCI,NM1,
C   C   NSSTEP,MAXNXLFS
C   *  CCMHCN /REAL/ ALPHA1,AT(5000),BETA2,B(101),C(101),D(101),E(101),
C   *  F(101),G(101),H(101),I(101),J(101),K(101),L(101),M(101),N(101),
C   *  O(101),P(101),Q(101),R(101),S(101),T(101),U(101),V(101),
C   *  W(101),X(101),Y(101),Z(101),MAXL,DRIVL,DRIVR,FRAC,XX4,XX10,
C   *  XLAM,XX6,XMAX,XLAM,XX7,XLAM,XX8,XLAM,XX9,XLAM,XX10,
C   *  X1,X2,X3,X4,X5,X6,X7,X8,X9,X10,X11,X12,X13,X14,X15,X16,X17,X18,
C   *  X19,X20,X21,X22,X23,X24,X25,X26,X27,X28,X29,X2A,X2B,X2C,X2D,X2E,
C   *  X2F,X2G,X2H,X2I,X2J,X2K,X2L,X2M,X2N,X2O,X2P,X2Q,X2R,X2S,X2T,X2U,
C   *  X2V,X2W,X2X,X2Y,X2Z,X2AELIR
C
C   C   *** IF CO NOT SPECIFIED SET CO TO AVERAGE SPEED IN WATER COLUMN
C   C   *** (USING MAX FILE FROM FILE)
C   *  IF (CO .NE. 0.0) GO TO 11
C   *  EC 10  I=2,ZSVP
C   *      CO=CO+(ZSVP(I)-CSVP(I-1))*(CSVP(I-1))
C
C   10  *      CCCONTINUE

```

```

11      CO = C0/ZSVF(NSVP)
C      CONTINUE
C      ***
C      *** INITIALIZE RANGE
C      RA1 = 0.0
C      ***
C      *** INITIALIZE POINTER THAT POINTS TO BCT0 IN FECFILE PCINT
IECT1 = 0
C      ***
C      *** COMPUTE REFERENCE WAVE NUMBER
XRF0 = 2.0*FI*FRQ/C0
C      ***
C      *** COMPUTE REFERENCE WAVELENGTH
XLAMDA = CC/FRQ
C      ***
C      *** IF DRVL=0 SET DRVL EQUAL TO 1/2 REFERENCE WAVELENGTH
IF (DRVL.EQ.0.0) DRVL = 0.5 * XLAMDA
C      ***
C      *** IF DRMAX=0 SET DRMAX EQUAL TO REFERENCE WAVELENGTH
IF (DRMAX.EQ.0.0) DRMAX = XLAMDA
C      ***
C      *** IF DRVL GREATER THAN DRMAX SET DRVL EQUAL TO DRMAX
IF (DRVL.GT.DRMAX) DRVL = DRMAX
C      ***
C      *** COMPUTE ATTENUATION - SACLANT MEMO SH-121 (JENSEN + FERIA)
*** MODIFIED AS FOLLOWS:
*** IF INPUTTED BETA IS LT 0.0, ALPHA IS COMPUTED IN DB/METER
*** AND USED FOR BETA
ALPHA = FRQ*FRQ*(-.007 + (.155*1.7)/(1.7*1.7 + FRQ*FRQ*.000001))
*     *1.0E-09
C      ***
C      *** INITIALIZE POINTER THAT POINTS TO INTERFACE GEM PCINT
IFACE = IN1 (BZ(1)/DZ + 0.5)
C      ***
C      *** RELEASE INTERFACE
IFACE = IN1 (BZ(1)/DZ + 0.5)
C      ***
C      *** INITIALIZE MATCCN

```

THIS SUBROUTINE CALCULATES VARIOUS VARIABLES NEEDED TO COMPUTE
 THE DIAGONAL MATRIX ELEMENTS. THESE VARIABLES BEGINNING WITH XX HAVE
 NO SPECIAL PHYSICAL SIGNIFICANCE BUT THEY CONTRIBUTE TO
 COMPUTATIONAL EFFICIENCY.
 CCNFILE XN1

```
CCFILEX A142 C CCR CTHC, EYE, XHS XRI, XRI2,  
** XX1, XX2, XX3, XX4, XX5, XX6, XX7, XX8, XX9, XX10, XX11  
** YL1, YL2, YL3, YL4, YL5, YL6, YL7, YL8, YL9, YL10, YL11, YR12,  
** U12, U13, U14, U15, U16, U17, U18, U19, U20, U21, U22, U23, U24, U25,  
** INSTEP, ISLOPE, ISTEP, IW2, N, NA, NBC1, NBC1,  
** INSTEP, ISLOPE, ISTEP, IW1, N, NA, NBC1, NBC1,  
** CCMCN /  
** BEAL/ALEPHAT(5600), BETA2(B(101)/B(102)), CO(FBQ/FDR/ED2),  
** CSVP(101), C2(CMAX(Z(NMAX)(Z(NMAX)/PR14)), XX10),  
** R1(RA(151)/C1(HHO2/RMAX(XK0)), RMAX(XK0), ZS(ZSVB(T(101)),  
** XX11, XX12, XX13, XX14, XX15, XX16, XX17, XX18, XX19, XX20, XX21),  
** CPLEX(XL1, XL2, XL3, XL4, XL5, XL6, XL7, XL8, XL9, XL10), CR(5000), CI(5000),  
** EYE, XX1, XX2, XX3, XX4, XX5, XX6, XX7, XX8, XX9, XX10, XX11, XX12, XX13, XX14, XX15, XX16, XX17, XX18, XX19, XX20, XX21, XX22, XX23, XX24, XX25, XX26, XX27, XX28, XX29, XX30, XX31, XX32, XX33, XX34, XX35, XX36, XX37, XX38, XX39, XX40,  
IPD05190  
IPD05200  
IPD052100  
IPD052200  
IPD052300  
IPD052400  
IPD052500  
IPD052600  
IPD052700  
IPD052800  
IPD052900  
IPD053000  
IPD053100  
IPD053200  
IPD053300  
IPD053400  
IPD053500  
IPD053600  
IPD053700  
IPD053800  
IPD053900  
IPD054000  
IPD054100  
IPD054200  
IPD054300  
IPD054400  
IPD054500  
IPD054600  
IPD054700  
IPD054800  
IPD054900  
IPD055000  
IPD055100  
IPD055200  
IPD055300  
IPD055400  
IPD055500  
IPD055600  
IPD055700  
IPD055800  
IPD055900  
IPD05600  
IPD056100  
IPD056200  
IPD056300  
IPD056400  
IPD056500  
IPD05660  
  
C EYE = CMPLX(0.0,1.0)  
C  
C XX1 = CMPLX( C-0 , + 0.25/(DZ*DZ*XK0) )  
C XX2 = 2.0 * { X1 - 0.25 * CMPLX( CO/C2 ,  
C *** COMPUTE COEFFICIENT A IN SEDIMENT LAYER  
C *** FIRST CALCULATE REAL INDEX OF REFRACTION  
C XN = CO/C2  
C *** THEN CALCULATE COMPLEX INDEX OF REFRACTION SQUARED  
C XX1 = CMPLX( SREAGE2-11/IN TR(6659),  
C *** XN1 = CMPLX( -XN*XN , XN*XN*BETA2/27 . 287527 )  
C *** CALCULATE A2  
A2 = 0.5 * EYE * XK0 * (XN1-1.0)  
C  
C XX3 = 0.5 * A2 - IX2  
C XX4 = 1.0 + RH(1/XH02)  
C XX5 = XX2*(1.0/XX4-1.0) + A2/ (2.0*(RH(1/XH01 + 1.0))  
C XX6 = IX2/IX4 * IX6  
C XX7 = RH01/RH02 * IX6  
C XX8 = CMPLX( 0.0 , -DZ*XK0 )  
C XX9 = 1.0 / { X8  
C XX10 = RH01 + RH02  
C XX11 = RH01 - RH02  
C XX12 = 4.0 * X1  
  
*** THIS SECTION PERTAINS TO POINTS IN WATER COLUMN  
DO 10 I=1,NMAX  
** CALCULATE REAL INDEX OF REFRACTION IN WATER  
** XN = CO/CWAIE(I)  
*** CALCULATE ATTENUATION AS PER COMMENTS IN SUBROUTINE  
*** INITIAL  
** IF(BETA1-1.1-0.0) BETA1 = ALPHA*CWAIE(I)/FBO  
*** CALCULATE COMPLEX INDEX OF REFRACTION SQUARED  
89 C
```

```

C      *** XN1 = CHEX { XN*XN   XN*XN*BE TA1/27.2E7527 )
C      *** CALCULATE COEFFICIENT A(I)
C      *** A(I) = 0.5 * FIVE * XK0 # (XN1- 1.0)
C      *** CALCULATE XN1H
C      XN1H(I) = 0.5 * A(I) - XX2
C
C      RETURN CONTINUE
C      END
C
C      SUBROUTINE SFIELD(FRQ,C0,ZS,N,DZ,U)
C
C      *** THIS SUBROUTINE IS IDENTICAL TO SUBROUTINE SFIELD AS PER
C      *** NUSC TECHNICAL REPORT 6659.
C
C      *** **** FIELD - SEE NORDA TECH NCIE 12 BY H.-K. BROCK
C      *** **** **** **** **** **** **** **** **** **** **** ****
C
C      *** CALLING ROUTINE SUPPLIES:
C      *** FRQ - FREQUENCY IN HZ
C      *** C0 - REFERENCE SECUND SPEED - METERS/SEC
C      *** ZS - DEPTIC OF SOURCES IN METERS.
C      *** N - NUMBER OF POINTS IN ARRAY U
C      *** LZ - DEPTIC INCREMENT - METERS
C      *** SFIELD SUBROUTINE SUPPLIES:
C      *** U - COMPLEX STARTING FIELD
C      *** **** **** **** **** **** **** **** **** **** **** ****
C
C      CCNFILEX U(1) 15926535/
C      DATA FI/3./
C
C      *** FILE FIELD IS DEFINED AS GAUSSIAN BEAM AT RANGE = C.
C      *** ICAL VARIABLES - GA GAUSSIAN AMPLITUDE
C      *** XK0=2.0*PI*FRQ/C0
C      *** GW=2.*C/XK0
C      *** GA={C/(GW)}/GW
C      *** DC=10 I=1, N
C      *** ZH=I*LZ
C      *** FB=GAUSS{GA ZM,2S, GW} - GAUSS (GA, -ZN, ZS, GW)
C      *** U(I)=CMPLX (PR, 0.0)
C      *** CONTINUE
C      *** RETURN
C      *** FUNCTION GAUSS (GA, Z, GD, GW)

```

```

      C INPUT - GAUSSIAN AMPLITUDE - V EXP(-(Z - GD) / GM)* *2)
      C OBJECT - GAUSS = GAUSS* EXP(-((Z - GD) / GM))
      C TELESCOPIC VARIABLE - V
      C V = (Z - GD) / GM
      C I = -(V*V)
      C GAUSS = GAUSS* EXP(V)
      C RETURN
      C END

```

STRUCTURE WRITE1

(1) THIS SUBROUTINE OUTPUTS UNFORMATTED DATA TO A FILE
 THAT IS USED BY THE PLOTTING ROUTINE.
 (2) THE FILENAME CORRESPONDS TO UNIT FILE NUMBER: NOU = 52
 {3} THE FILENAME AND FILETYPE FOR THIS FILE ARE:
 FILECUT FLCITER

```

CCFILEX A4 A2 C4 CR CTCWC/EYE, YMS, XRI, XRI2,
*     XX1, XX12, XX15, XX16, XX17, XX18, XX19, XX1A, XX1B
*     YI, YI1, YI12, YI15, YI16, YI17, YI18, YI19, YI1B, YRIZ,
*     D1225, 1226, 1227, 1228, 1229, 1230, 1231, 1232, 1233, 1234, 1235, 1236, 1237, 1238, 1239, 1240
*     CCMMCN /IN/ 1IBOT1, 1FACE1, IPY4, ISLOPE, ISTEP, IW2, N, NA, NBCT, NB1,
*     INSTEP, 1STEP1, ASVE, NMAY, NYLFS
*     CCMMCN /CSVP/ 101, C1, C2, C3, C4, C5, C6, C7, C8, C9, C10, C11, C12, C13, C14, C15, C16, C17, C18, C19, C20, C21, C22, C23, C24, C25, C26, C27, C28, C29, C30
*     R11RA, 1228, 1229, 1230, 1231, 1232, 1233, 1234, 1235, 1236, 1237, 1238, 1239, 123A, 123B, 123C, 123D, 123E, 123F, 123G, 123H, 123I, 123J, 123K, 123L, 123M, 123N, 123O, 123P, 123Q, 123R, 123S, 123T, 123U, 123V, 123W, 123X, 123Y, 123Z
*     CCMMCN /CPLY/ 1, 2, 3, 4, 5, 6, 7, 8, 9, 10, 11, 12, 13, 14, 15, 16, 17, 18, 19, 20, 21, 22, 23, 24, 25, 26, 27, 28, 29, 30
*     C1, C2, C3, C4, C5, C6, C7, C8, C9, C10, C11, C12, C13, C14, C15, C16, C17, C18, C19, C20, C21, C22, C23, C24, C25, C26, C27, C28, C29, C30
*     DATA NOU/52/
*** WRITE MAXIMUM RANGE
      C   WRITE(NUO,*) RMAX
*** INITIALIZE RANGE VARIABLE AT WHICH SOLUTION IS TO BE RECORDED
      C   XMAX = RA1 + RIR
*** COMPUTE RECEIVER DEPTH TO NEAREST DZ
      C   IF (2R,LT,12) ZD = DZ
      C   IWZ = 2R/DZ + 0.5
      C   2R = 16Z*DZ

```

```

C *** WRITE STARTING VALUE
C      WRITE(NOUT,*) R1, ZE, U(IWZ)
C
C      RETURN
C      END

```

SUBROUTINE PRINT1

```

(1) THIS SUBROUTINE OUTPUTS FORMATTED DATA TO A FILE
    WHICH IS READY TO BE SENT TO THE PRINTER.
(2) THE FILE CORRESPONDS TO UNIT FILE NUMBER = NPOU1 = 55
(3) THE FILENAME AND FILETYPE FOR THIS FILE ARE:
        IPRINT PRINTER

DIMENSION ID(17)
CCHMCN /IN/ IA
CCHMCN /NSIEP/ STEP1, ISVE, NWMAXLFS, LISTEP, IW2, N, NA, NECT, NE1,
* CCHMCN /REAL/ ALTEHA, ATT(5000), BETA1, BETA2, B(1C1), B2(101), CO
* CSVP(101), C2, CWATER(5000), DREDRIV1, DRMAX, FRO, FRC, FRZ,
* R1, RA(1FA), RHC1, RHC2, RMAX, THETA, XK0, XLANDA, XPR, XK14, XK10,
* XX11, XME, ZDR, ZLYR1, ZLYR2, ZR, ZS, ZSVP(101), ZAEYR
* FAIA, NPOU1/5/
*      *** FROMPT USE FOR RUN IDENTIFICATION
*      WRITE(6,990)
*      READ(5,891) (ID(I), I=1, 16)
*      *** PRINT SELECTED PARAMETERS OF INTEREST
*      WRITE(NPOU1,900) (ID(I), I=1, 16), ZFRO, ZSF, ZDZ, ZK0, XK0,
*      XLANDA, RMAX, DRIVL, DRMAX, WDE, ZABILY, N
*      *** PRINT SOUND SPEED PROFILE IN WATER
*      WRITE(NPOU1,904)
DC 5 1=1 N=5
*      WRITE(NFCUT,905) ZSVP(I), CSVP(I)
CONTINUE
5
*      *** PRINT MORE SELECTED PARAMETERS OF INTEREST
*      WRITE(NPOU1,901) ZLYR1, RHO1, BETAI, ZLXK2, EHO2, BETA2, C2
*      *** PRINT EOTICE PROFILE
*      WRITE(NPOU1,902)
NEOTH { = NECT-1

```

```

10      DC 10 I=1 XEOTM1
          WRITE(MFCUT,903) ER(I), BZ(I)

C      *** COMPUTE DEPTH PRINT INCREMENT TO NEAREST D2
C      IFZ = INT( PDZ/DZ+0.5 )
C      IF ( IFZ-E0 ) IPZ = 1

C      *** INITIALIZE RANGE VARIABLE AT WHICH SOLUTION IS TO BE PRINTED
C      XFR = EA1+FIR

C      890  ECFMAT(16A4,'ENTER RUN IDENTIFICATION: ')
C      891  ECFMAT(16A4,'//',IPD PRINTED OUTPUT' // 1X, '6 UN 1.D. : ', )
C      892  ECFMAT(16A4,'//',7X,'GAUSSIAN STARTING' // 1X, '6 UN 1.D. : ', )
C      *      'SEE FURTHER INFORMATION ON CN VARIABLES'.
C      *      'SEE MAIN IPD PROGRAM LISTING') //'
C      *      7X, 'FREQUENCY
C      *      7X, 'SOURCE DEPTH
C      *      7X, 'RECEIVER DEPTH
C      *      7X, 'DEPTH INCREMENT
C      *      7X, 'REF SCND SPEED
C      *      7X, 'REF SCND SPEED
C      *      7X, 'REF WAVELENGTH
C      *      7X, 'PAX RANGE OF SOLUTION
C      *      7X, 'RANGE STEEP CN HORIZONTAL SECTION
C      *      7X, 'MAXIMUM RANGE STEEP
C      *      7X, 'RECORDED RANGE STEEP
C      *      7X, 'DEPTH OF DEEPER SEIGNE ART ATTENU LYR
C      *      7X, '#VERTICAL EFCINTS IN GRID
C      *      7X, 'LAYER MAX DEPTH(N)
C      *      7X, 'PAT(DB/KI) SCND SPEED, //'
C      *      7X, 'WATER F13-14X-15X-13X-65X 'SEE PROFILE AOVE.
C      *      901  ECFMAT(16A4,'//',SELDIMENT PRofile // F13-14X-64X F13-15X-13X-65X 'SEE PROFILE AOVE.
C      *      902  FORMAT(16A4,BOTICH PRofile // F13-14X-64X F13-15X-13X-65X 'SEE PROFILE AOVE.
C      *      903  ECFMAT(20X,F10.5,SCND SPEED PROFILE IN WATER: //,DEPTH', //')
C      *      904  ECFMAT(10X,F10.5,SCND SPEED PROFILE IN WATER: //,DEPTH', //')
C      905  ECFMAT(14X,F10.5, 'H. 6X, 10.2, ' H/S', //')

C      RETURN
C      END

C      SLERCUTINE NEWSEG

```

THIS SUBROUTINE IS CALLED AT THE START OF EACH NEW BOTTOM
 SEGMENT. THE SUBROUTINE DOES THE FOLLOWING TASKS FOR EACH
 EFFECTIVE SEGMENT:
 (1) UPDATES BOTTOM PROFILE POINTERS: IBCT1 & IEOT12
 (2) COMPUTES SLOPE: THETA1
 (3) COMPUTES NUMBER OF RANGE STEPS IN SEGMENT: NSTEP
 (4) COMPUTES RANGE STEP: DR
 (5) SETS SLICE FLAG: ISLOPE
 (6) ISLOPE = 1 - BOTTOM SLOPES DOWN
 (7) ISLOPE = 2 - BOTTOM LEVELS
 (8) ISLOPE = 3 - BOTTOM SLOPES UP
 (9) ISLOPE = 4 - BOTTOM SLOPES DOWN, MODIFY BC1ION
 (10) ISLOPE = 5 - BOTTOM SLOPES UP, MODIFY EDITION
 (11) INITIALIZES RANGES: RA1 & RA2
 (12) CHECKS THAT RANGE STEP IS LESS THAN DRMAX
 (13) ISSUES ERROR OR WARNING MESSAGES AS APPROPRIATE

```

COMMON /IN/ IA,IBOT1,IFACE,IPZ,ISLOPE,ISTEP,IWZ,N,NA,NBCT,NH1,
      NSLIP,NSLIP1,NSVE,NWMAX,NXFLS
* COMMON /REAL/ ALPHAB(500),BETA1,BETA2,BR(101),C0
*           CSVP(101),C2,CWATER(500),DR,DRMAX,DR(101),E2(101),F0
*           R1,R2,FEA2,RRHC1,RHO2,RMAX,XLAM,XX4,XX10,
*           XX11,X16,WR,214E1,Z1VZ2,ZR,ZS,ZSVP(101),ZAEVK
* DATA IPOINT/55/

```

```

C     *** UPDATE BOTTOM PROFILE PCINTER
C     *** IEOT1 = IBCT1 + 1
C     *** IEOT2 = IBCT1 + 1
C     *** GET STARTING AND ENDING RANGES AND DEPTHS FOR THIS SEGMENT
C     G1 = EB(IBCT1)
C     Z1 = B2(IBCT1)
C     Z2 = B2(IBCT12)
C     Z2 = B2(IBCT12)
C     *** ERRORCHECK
C     *** IF (R2-IE, R1) GO TO 100
C     *** PUT Z1 AND Z2 CN NEAREST GRID PCINTS
C     ITTEMP = INT(Z1/DZ + 0.5)
C     Z1 = D2 * FLOAT(ITEMP)
C     ITTEMP = INT(Z2/D2 + 0.5)
C     Z2 = D2 * FLOAT(ITEMP)
C     *** COMPUTE SLICE
C     FEITA = SATAN2(Z2-Z1/R2-R1)
C     DCES BCTOB(SLOPE DCN LEVEL OR UP?
C     IF (THETA-G1-0.0) GO TO 10
C     IF (THETA-II-0.0) GO TO 20
C
C     *** BOTTOM IS LEVEL NUMBER OF RANGE STEPS FOR SEGMENT
  
```

```

      NSTEPE = INT( (R2-R1) / DRFLVL + 0. 99999 )
      C
      C      *** DETERMINE RANGE STEP
      C      *** DR = (R2-R1) / FLOAT(NSTEP)
      C      SET ISLOPE = 2
      C      GO TO 80
      C
      C      *** BOTTOM SLOPES DCWN NUMBER OF RANGE STEPS
      C      NSTEPE = INT( (Z2-Z1+0.05) / DZ )
      C      *** DETERMINE RANGE STEP
      C      DR = (R2-R1) / FLOAT(NSTEP)
      C      SET ISLOPE = 1
      C      ISLOFF = 1
      C      GO TO 30
      C
      C      *** BOTTOM SLOPES UP
      C      *** DETERMINE NUMBER OF RANGE STEPS
      C      NSTEPE = INT( (Z1-Z2+0.05) / DZ )
      C      *** DETERMINE RANGE STEP
      C      DR = (R2-R1) / FLOAT(NSTEP)
      C      SET ISLOPE = 1
      C      ISLOFF = 3
      C
      C      CCCONTINUE STEP TOO LARGE?
      C      *** IF ( DR.LE.DRMAX ) GOTO 80
      C      *** YES, BOTTOM MUST BE MODIFIED
      C      SET ISLOPE = 4
      C
      C      IF( ISLOPE.LT.0.0 ) ISLOPE = 5
      C      *** DETERMINE NUMBER OF RANGE STEPS REQUIRED TO MOVE UP
      C      CRDCWN CNE GRIL FCINT
      C      NSTEP1 = INT( DR/DRMAX + 0. 99999 )
      C      *** DETERMINE RANGE STEP
      C      DR = DR / FLOAT(NSTEP1)
      C      *** DETERMINE NUMBER OF RANGE STEPS
      C      CRDCWN CNE GRIL FCINT
      C      NSTEP1 = NSTEP * NSTEP1
      C      *** COMPUTE SLOPE OF SLOPING SECTION
      C      COMPUTE ATAN2(DZ,DR)
      C      *** COMPUTE LOCATION OF NEXT LEVEL SECTION FOLLOWING A
      C      NXLFS = NSTEP1/2 + 2
      C      *** SLICING SECTION
      C      *** INDICATE TO USER THAT BOTTOM HAS BEEN MODIFIED
      C      TEMP = C5 * DZ
      C      WRITE(6,903) R1, R2, TEMP
      C      WRITE(6,903) R1, R2, TEMP
      C

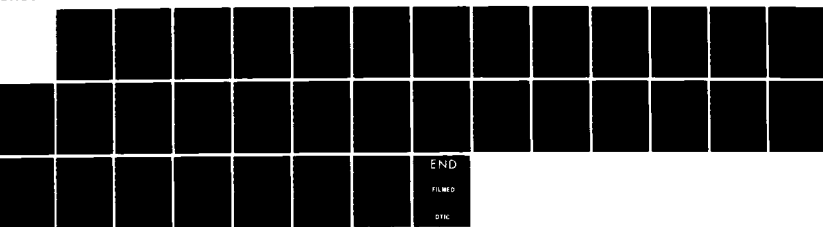
```

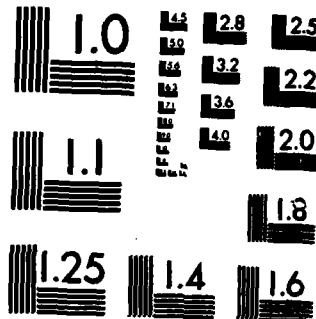
AD-A150 784 THE IMPLICIT FINITE-DIFFERENCE (IFD) ACOUSTIC MODEL IN 2/2
A SHALLOW WATER ENVIRONMENT(U) NAVAL POSTGRADUATE
SCHOOL MONTEREY CA M E KOSNIK JUN 84

UNCLASSIFIED

F/G 20/1

NL





MICROCOPY RESOLUTION TEST CHART
NATIONAL BUREAU OF STANDARDS-1963-A

```

C 80  CC CALLING INITIALIZE FA1 & FA2
      RA1 = R1
      RA2 = RA1+LF
C     *** INDICATE TO USER HOW FAR SOLUTION FIELD HAS PROGRESSSED
      WRITE(6,902) R1
C     *** IF RANGE STEP GREATER THAN 1 (?) WAVELENGTH WHILE WARNING
      IF (DR.LE.XLAMDA) GO TO 90
      WRITE(6,901) R1, F2, DR, XLAMDA
      WRITE(NEUT,901) R1, R2, DR, XLAMDA
C
C 90  RETURN
C     *** ERROR EXIT IBOT1 IBOT2 IBOT1
      WRITE(NEOUT,900) IBOT2, IBOT1
C
C     STOP
C
C 900  * FC5MAT //, 1X 'ERROR: THE RANGE AT BOTTOM PROFILE PCINT NUMBER '
      * '12, IS LESS. THAN THE RANGE AT BOTOM PROFILE PCINT. //'
      * 'NUMBER ,12, //, 1X, EXECUTION TERMINATE. //'
C
C 901  * FC5MAT //, 1X 'WARNING: THE HORIZONTAL RANGE STEP BETWEEN RANGE R = ' F8. 1, //
      * ' AND RANGE R = ' F8. 1. '(METERS)' P5. 1 ' METERS. //'
      * ' . THE REFERENCE WAVELENGTH THIS IS ' F8. 1, ' METERS.' )
      * ' FC5MAT //, 1X 'THE PROGRAM HAS REACHED RANGE R = ' F8. 1, ' AND RANGE ' //
      * ' F8. 1. NOTE: THE BOTTOM BETWEEN RANGE ' F8. 1, ' AND RANGE ' //
      * ' F8. 1. HAS BEEN MODIFIED BECAUSE OF THE VERY SMALL ' //
      * ' SLCPE. ' 8X ' THE DIFFERENCE BETWEEN THE MOLIFIED ' //
      * ' BOTTOM AND YOUR ' 8X ' INPUT BOTTOM IS NEVER GREATER ' //
      * ' THAN ' F8. 2, ' METERS. //'
C
C 902  * FC5MAT //, 1X 'WARNING: THE HORIZONTAL RANGE STEP BETWEEN RANGE R = ' F8. 1, //
      * ' AND RANGE R = ' F8. 1. '(METERS)' P5. 1 ' METERS. //'
      * ' . THE REFERENCE WAVELENGTH THIS IS ' F8. 1, ' METERS.' )
      * ' FC5MAT //, 1X 'THE PROGRAM HAS REACHED RANGE R = ' F8. 1, ' AND RANGE ' //
      * ' F8. 1. NOTE: THE BOTTOM BETWEEN RANGE ' F8. 1, ' AND RANGE ' //
      * ' F8. 1. HAS BEEN MODIFIED BECAUSE OF THE VERY SMALL ' //
      * ' SLCPE. ' 8X ' THE DIFFERENCE BETWEEN THE MOLIFIED ' //
      * ' BOTTOM AND YOUR ' 8X ' INPUT BOTTOM IS NEVER GREATER ' //
      * ' THAN ' F8. 2, ' METERS. //'
C
C 903  * FC5MAT //, 1X 'WARNING: THE HORIZONTAL RANGE STEP BETWEEN RANGE R = ' F8. 1, //
      * ' AND RANGE R = ' F8. 1. '(METERS)' P5. 1 ' METERS. //'
      * ' . THE REFERENCE WAVELENGTH THIS IS ' F8. 1, ' METERS.' )
      * ' FC5MAT //, 1X 'THE PROGRAM HAS REACHED RANGE R = ' F8. 1, ' AND RANGE ' //
      * ' F8. 1. NOTE: THE BOTTOM BETWEEN RANGE ' F8. 1, ' AND RANGE ' //
      * ' F8. 1. HAS BEEN MODIFIED BECAUSE OF THE VERY SMALL ' //
      * ' SLCPE. ' 8X ' THE DIFFERENCE BETWEEN THE MOLIFIED ' //
      * ' BOTTOM AND YOUR ' 8X ' INPUT BOTTOM IS NEVER GREATER ' //
      * ' THAN ' F8. 2, ' METERS. //'
C
C 96   END
C
C
C 9999  SUBROUTINE NEWMAT
C
C THIS SUBROUTINE IS CALLED AT THE START OF EACH NEW EDITION
C SEGMENT. THE SUBROUTINE DOES THE FOLLOWING TASKS:
C (1) COMPUTES TRIDIAGONAL MATRIX ELEMENTS FOR MATRIX Y
C (A) MATRIX Y IS AT RANGE WHERE FIELD IS KNOWN: RANGE=RA1
C (B) MATRIX Y MATRIX CN RHS OF EQUATION

```

- (2) USES Y MATRIX ELEMENTS AND KNOWN FIELD AT RANGE RA1 TO
 COMPUTES RHS VECTOR C(1,4) ELEMENTS (SEE TRIDG AND TEXT)
 (3) COMPUTES TRI DIAGONAL MATRIX ELEMENTS FOR MATRIX X
 {A} X MATRIX VALUES STORED IN C(I,1) & C(I,2) AND C(I,3)
 {B} X MATRIX AT RANGE: RA2 = RA1 + DR
 {C} X MATRIX AT RANGE: RA2 = RA1 + DR

TRIDIAGONAL MATRIX ELEMENTS ARE REPRESENTED BY VARIABLES BEGINNING WITH X OR Y. FOR VARIABLES BEGINNING WITH X OR Y THE LETTERS IN THE VARIABLE NAME HAVE THE FOLLOWING SIGNIFICANCE:

X	- ELEMENT IN X MATRIX
Y	- ELEMENT IN Y MATRIX
Z	- ELEMENT ON MAIN DIAGONAL
R	- ELEMENT TO LEFT OF MAIN DIAGONAL
S	- ELEMENT TO RIGHT OF MAIN DIAGONAL
I	- ELEMENT IN ROW AT WATER INTERFACE
M	- ELEMENT IN ROW AT SEDIMENT INTERFACE
N	- ELEMENT IN ROW IN SEDIMENT LEVELING INTERFACE
P	- INTERFACE ELEMENT ON SLOPING INTERFACE

COMPLEX DEFLATION BEING 1, GAMMA 1, BETA 2, GAMMA 2, 221, 222, Z23, Z24

```

CCDEFIX A12 C12 R12 S12 X12 Y12 Z12 I12 M12 N12 P12
*** CCOMCN /NS1EP /REAL /CP1 /CSVP /C2 /ATT(500) /DR14 /BR(101) /BZ(101) /C0
*** R11 /I15 /E14 /R10 /H10 /DR5 /BZ5 /T1 /XK0 /X10 /PR(X4,X10).
*** X11 /X16 /A12 /DR2 /I12 /C5000 /C4 /C(500,0,4) /Z5 /V10 /AEL1A
*** CCMMCN /CP1X /CPIX /CPIX /CPIX /CPIX /CPIX /CPIX /CPIX /CPIX /CPIX
*** R11 /I15 /E14 /R10 /H10 /DR5 /BZ5 /T1 /XK0 /X10 /PR(X4,X10).
*** X11 /X16 /A12 /DR2 /I12 /C5000 /C4 /C(5000) /CT16(5000).
*** U(5000) /225.226.227.228.229.2210(5000) /YRI /YIV /YRZ .
*** CCMMCN /BEDA2 /GAMMA2 /BEDA2 /GAMMA2 /NS1 /NS2 /NS3 /NS4 /NS5 /NS6 /NS7 /NS8
*** *** COMPUTE MAIN DIAGONAL ELEMENT, Y MATRIX, IN SEDIMENT
*** YES=1. 0+DR*XX3
*** COMPUTE OFF-DIAGONAL ELEMENTS, Y MATRIX, IN WATER & SEDIMENT
*** YRWS=DR*XX1
*** COMPUTE MAIN DIAGONAL ELEMENT, X MATRIX, IN SEDIMENT
*** XES=2. 0-YWS
*** COMPUTE OFF-DIAGONAL ELEMENTS, X MATRIX, IN WATER & SEDIMENT
*** IFD09030
*** IFD09040
*** IFD09050
*** IFD09060
*** IFD09070
*** IFD09080
*** IFD09090
*** IFD09100
*** IFD09110
*** IFD09120
*** IFD09130
*** IFD09140
*** IFD09150
*** IFD09160
*** IFD09170
*** IFD09180
*** IFD09190
*** IFD09200
*** IFD09210
*** IFD09220
*** IFD09230
*** IFD09240
*** IFD09250
*** IFD09260
*** IFD09270
*** IFD09280
*** IFD09290
*** IFD09300
*** IFD09310
*** IFD09320
*** IFD09330
*** IFD09340
*** IFD09350
*** IFD09360
*** IFD09370
*** IFD09380
*** IFD09390
*** IFD09400
*** IFD09410
*** IFD09420
*** IFD09430
*** IFD09440
*** IFD09450
*** IFD09460
*** IFD09470
*** IFD09480
*** IFD09490
*** IFD09500

```

```

C     *** XIRHS = -YIRHS ELEMENT IN RHS COLUMN VECTOR
C     YIRHS(1) = U(1)*YIRHS(1) + U(2)*YIRHS
C     C(1,4) = U(1)*YIRHS(1) + U(2)*YIRHS
C     *** CCMPUTE ELEMENTS IN FIRST ROW ON LHS
C     C(1,2) = T20*YIRHS(1)
C     C(1,3) = XIRHS(1)
C     *** CCMPUTE REMAINING ELEMENTS ON BOTH RHS & LHS FOR ROWS IN WATER
C     DC 10 I=2,IFACE1
C     *** FIRST WORK WITH RHS
C     YIRHS(1) = U(1)*YIRHS(1) + U(2)*YIRHS(1) + U(3)*YIRHS
C     *** WORK WITH LHS
C     C(1,1) = XIRHS
C     C(1,2) = 2.0 - YIRHS(1)
C     C(1,3) = XIRHS
C     C(1,4) = U(1)*YIRHS(1) + U(2)*YIRHS(1) + U(3)*YIRHS
C
10   *** CCNINUE CCMPUTE LHS & RHS ELEMENTS IN SEDIMENT
C     IFACEP = IFACE + 1
C     NM1 = N - 1
C     DC 20 I=IFACEP,NM1
C     *** RHS
C     C(1,4) = U(1)*YIRHS + U(2)*YIRHS + U(3)*YIRHS
C     *** LHS
C     C(1,1) = XIRHS
C     C(1,2) = XIRHS
C     C(1,3) = XIRHS
C
C     CCNINUE
C
C     *** IF ENTIRE SEGMENT LEVEL GO TO 50
C     IF ( ISLOPE.EQ.2 ) GOTO 50
C
C     *** INTERFACE SLOPES FITTER UP OR DOWN MATRIX ELEMENTS
C     CALCULATE CONSTANTS FOR COMPUTING MATRIX ELEMENTS
C     FEETA = ABS(THETA)
C     SINE = SIN(THETA)
C     CCSE = COS(THETA)
C     DELTA = XX10 + XX11*(XX8+XX9)*SINE*COS
C     DELTA = 1 - C/DELTA
C     DELIN = DELIN * XX12 * RHO1
C     GAMMA1 = DELIN * (XX12*RHO2*COS*COSE + RHO1*SINE*SINE) +
C
C     EIDA2 = DELIN * (XX12*RHO1*COS*CCSE + RHO2*SINE*SINE) +
C     GAMMA2 = DELIN * (RHO1*SINE*CCSE/D2) * RHO2
C     221 = DELIN * (RHO1*SINE*XX11) * RHO2*SINE*CCSE +
C           XX8*SINE*CCSE*XX11)

```

```

* 222 = DELINE * (RHC1*B2 - (COSF-XX8*SINE) * XX9*XX11*EYE*XK0*
* 223 = DELINE * (A2 * ( RHO1*COSF*CCSE + RHO2*SINE*SINE
* + XX8*SINE*CCSE * XX11)
* (CCSE + XX8*SINE) * XX9*XX11*EYE * XK0*SINE )
* 225 = 1.5*D5*Z1
* 226 = 1.0 + 0.5*D6* (ZZ2-BEDA1-GAMMA1)
* 227 = -0.5*D7*ZZ3
* 228 = 1.0 - 0.5*D8* (ZZ4-BEDA2-GAMMA2)
* 229 = 2.0 - 228
* 2210 = 2.0 - 226

C *** IF BOTTON SLOPES UP, GO TO 40
C IF (TISLOPE-EC-3*CR. ISLOPE-EQ.5 ) GC TC 40
C *** BOTTON SLOPES DOWN
C IFACE2 = INTERFACE
C *** COMPUTE OFF-DIAGONAL X MATRIX ELEMENTS ON INTERFACE
C YLI = 0.5* DR * GAMMA1
C YRI = 0.5 * DR * BEDA1
C *** COMPUTE MAIN DIAGONAL, X MATRIX ELEMENT ON INTERFACE
C YNI = A(IFACE1)*ZZ5 + ZZ6
C *** COMPUTE INTERFACE ELEMENT IN RHS COLUMN VECTOR
C C(IFACE,4) = U(IFACEP)*YRI
C *** COMPUTE X MATRIX ELEMENTS ON INTERFACE
C XLI = -0.5* DR * GAMMA2
C XNI = A(IFACE2)* ZZ7 + ZZ8
C *** IF MODIFIED BOT THEN NO NEED TO ADJUST LBS
C *** IF (ISLCE-EQ.4 ) GO TO 45
C C(IFACE1) = XLI
C C(IFACE2,2) = XNI
C C(IFACE2,3) = XRI
C *** COMPUTE X MATRIX ELEMENTS ONE ROW ABOVE INTERFACE
C C(IFACE,1) = XIRHS
C C(IFACE,2) = 1.0 - DR * X1M(IFACE)
C C(IFACE,3) = XIRHS
C GO TO 60

C *** BOTTOM SLOPES UP
C 40
C IFACE2 = INTERFACE
C *** COMPUTE OFF-DIAGONAL X MATRIX ELEMENTS ON INTERFACE
C YLI = 0.5* DR * GAMMA2
C YRI = 0.5 * DR * BEDA2
C *** COMPUTE MAIN DIAGONAL, X MATRIX ELEMENT ON INTERFACE
C YNI = - A(IFACE) * ZZ7 + ZZ9
C *** COMPUTE INTERFACE ELEMENT IN RHS COLUMN VECTOR

```

```

C      C(INTERFACE,4) = U(IPACEF)*YLI + U(IFACE)*YRI +
C      *** COMPUTE X MATRIX ELEMENTS ON INTERFACE
C      YLI = -0.5*DR*GAMMA1
C      YRI = -0.5*DR*BEDA1
C      *** IF MODIFIED BOTTOM THEN NO NEED TO ADJUST LHS
C      IF(IISLCF.EQ.5) GO TO 45
C      C(IFACE2,1) = YLI
C      C(IFACE2,2) = YMI
C      C(IFACE2,3) = YRI
C      *** COMPUTE X MATRIX ELEMENTS ONE ROW BELOW INTERFACE
C      C(IFACE,1) = YLRUS
C      C(IFACE,2) = YNS
C      C(IFACE,3) = YLRUS
C      GO TO 45
C
C      *** SAVE INTERFACE VALUES ON SLOPING SECTION
C      YLIZ = YLI
C      YRIZ = YRI
C      XLIZ = YLI
C      XRIZ = YRI
C
C      *** SEGMENT LEVEL COMPUTE MATRIX ELEMENTS ON INTERFACE
C      IFACE2 = IFACE
C      YLI = DR*XX6
C      YRI = 1.0 + DR*(XX1H(IFACE)/XX4 + XX5)
C      YRI = DR*XX7
C      C(IFACE,4) = U(IPACE)*YLI + U(IFACE)*YRI + U(IFACEF)*YRI
C      C(IFACE,1) = -YLI
C      C(IFACE,2) = 2.0 - YRI
C      C(IFACE,3) = -YRI
C      *** SAVE INTERFACE VALUES ON LEVEL SECTION
C      YLIIV = YLI
C      YRIV = YRI
C
C      CONTINUE
C
C      *** COMPUTE ARTIFICIAL ATTENUATION MATRIX
C      *** SEE AESD PFMODEL EYBROCK - NORDA TE CH NOTICE 12 - JAN 78
C      *** CALCULATE GRID POINT AT TOE OF ART ATTENUATION LAYER
C      IA = INT((ZABLE5/DZ + 0.01)
C      *** CALCULATE NUMBER OF GRID POINTS IN ART ATTENUATION LAYER
C      NA = N - IA
C      *** CALCULATE ATTENUATION MATRIX
C      DO 70 J=1,NA
C      AT(J) = EXP(-(J-NA)*DR*EXP(-(TEMP*TEFF)))
C
C      45
C      50
C      60

```

```

C      *** SCALE FOR SOLUTION FIELD AT RANGE RA2
C      CALL TRIDG (C,U,N,CRC,TWO)
C      *** APPLY ARTIFICIAL ATTENUATION
C      CALL ATTEND (U,ATT,IA,NA)

C      RA2F = RA2 + 0.5
C      *** TIME TC WRITIE?
C      IF( RA2P.GE.IWR ) CALL WRITE2
C      *** TIME TC PRINT?
C      IF( RA2P.GE.XPR ) CALL PRIM12
C      *** UPDATE INTERFACE ECINTER
C      IFACE = TIPACE2

        END
      END
    
```

SUBROUTINE TRIING (C,U,N,CR,CTWO)

*** THIS SUBROUTINE SOLVES A SET OF $N - 1$ (NN1) LINEAR
 *** SIMULTANEOUS EQUATIONS HAVING A TRIDIAGONAL COEFFICIENT
 *** MATRIX. MATRIX ELEMENTS IN THE LOWER DIAGONAL, MAIN DIAGONAL
 *** AND UPPER DIAGONAL ARE STORED IN C(I,1), 'C(I,2)' AND C(I,3)
 *** RESPECTIVELY. THE RHS COLUMN VECTOR IS STORED IN U(I).
 *** THE SOLUTION FIELD IS STORED IN U(I).
 *** (1) THE INDEX I REFERS TO ROW NUMBER I.
 *** (2) WE NEED ONLY ECLIVE AN NN1 SYSTEM. (RATHER THAN
 *** AN NNXNN SYSTEM) BECAUSE U(N) IS KNOWN.
 *** (3) THIS SUBROUTINE IS A MODIFIED VERSION OF SUBROUTINE
 *** TRIING FROM:
 *** "APPLIED NUMERICAL ANALYSIS" (SECOND EDITION)
 *** BY CURTIS F. GEARLD PUBLISHED BY ADDISON-WESLEY PUBLISHING CO. 1980
 *** PUBLISHED BY ADDISON-WESLEY PUBLISHING CO. 1980
 *** PUBLICED:
 *** (A) INTRODUCING ARRAYS CTWO AND CR TO PRESERVE THE
 *** ORIGINAL VALUES IN C(I,2) AND TO MAKE THE ROUTINE
 *** MORE EFFICIENT. THIS RESULTS IN A CCNSIDERABLE
 *** SAVINGS IN EXECUTION TIME FOR THE CASE OF A
 *** HORIZONTAL BOTTOM (SEE SUBROUTINE TRIDL)
 *** (B) MODIFYING THE ROUTINE TO SOLVE AN NM1 X NM1
 *** SYSTEM.

C *** (5) SEE PAGES 129 AND 133 IN THE TEXT FOR FURTHER INFO.

```

C     CCFILEX C(5000,4), U(5000), CR(5000), CTWO(5000)
C
C     N=1 = N - 1
C     N=N-1
C     CTWO(1)=2, NM1=1
DO 10 I=2,NM1
      CR(I)= C(I,1) / CTWO(I-1)* C(I-1,3)
      CTWO(I)= C(I,2) / CR(I) * C(I-1,4)
10   CCFILEX

```

```
      U(N) = 0.0
```

*** NOW PERFORM BACK SUBSTITUTION

```

      D(1,20)=1/NM1 / CTWO(NM1)
      D(2,20)=NM1 - I
      U(N)= ( C(I,4)-C(I,3)*U(N+1) ) / CTWO(I)
20   CCFILEX
      RETURN
      END
```

20

SUBROUTINE TRILG (C,U,N,CR,CTWO)

*** THIS SUBROUTINE IS A MODIFIED VERSION OF SUBROUTINE TRILD
*** FROM THE TINY PROGRAM. SUBROUTINE TRILD IS IN TURN A MODIFIED
*** VERSION OF TRILG AS FER THE REFERENCE BELOW.
*** THE SUBROUTINE SOLVES A SET OF N-EQUATIONS HAVING A TRIANGULAR COEFFICIENT
*** MATRIX. ELEMENTS HAVING ROW NUMBER I ARE STORED IN C(I,1). MAIN DIAGONAL
*** AND UPPER DIAGONAL ELEMENTS STORED IN C(I,2) AND C(I,3)
*** RESPECTIVELY. THE RES COLOUN VECTORS STORED IN C(I,4).
*** THE SOLUTION VECTOR IS STORED IN U(I).
*** INDEX I REFERS TO ROW NUMBER I.
*** (1) WE NEED ONLY SOLVE AN NXNX SYSTEM (RATHER THAN
*** AN NXN SYSTEM) BECAUSE U(N) IS KNOWN: U(N)=0.0
*** (2) THE SUBROUTINE IS A MODIFIED VERSION OF IFD SUB-
*** ROUTINE TRILG WHICH IN TURN IS A MODIFIED VERSION
*** OF SUBROUTINE TRILG AS PERIODIC PERIODIC ANALYSIS.
*** (3) APPLIED NUMERICAL ANALYSIS" (SECOND EDITION)
*** EY: CURTIS P. GERALD

*** (4) THIS ONLY IDENTIFICATION TO IPD SUBROUTINE TRIG, IS
 THAT TRIDIAGONAL NOT RECALCULATE ACTIVELY AND CROUT BUT
 BUT RATHER TRIDIAGONAL USES THE ARRAY VALUES CALCULATED
 BY TRIG. THIS RESULTS IN A CONSIDERABLE SAVINGS
 IN EXECUTION TIME FOR THE CASE OF A HORIZONTAL
 BOTTOM.

CCMPLEX C(5000,4), U(5000), CR(5000), CTWO(5000)

NN1 = N - 1
NN2 = N - 2

DO 10 I=2, NN1
C(I,4) = C(I,4) - CR(I) * C(I-1,4)

10 CCMTIME
U(N) = 0.0
*** NOW PERFORM EACH SUBSTITUTION

U(NN1) = C(NN1,4) / CTWC(NN1)
DC 20 I=1, NN2
U(N) = (C(N,4) - C(N,3)*U(N+1)) / CTWO(N)
20 CCMTIME
RETURN
END

SUBROUTINE DOWN

THIS SUBROUTINE UPDATES THE RHS & LHS OF THE EQUATION AND
 SCIENCES FOR THE SOLUTION VECTOR AT RA2.
 {1} THE RHS COLUMN VECTOR VALUES ARE STORED IN C(I,4)
 {2} THE INTERFACE AT RANGE RA1 IS AT GRIDPOINT INTERFACE
 {3} THE INTERFACE AT RANGE RA2 IS AT GRIDPOINT INTERFACE
 { WHERE IPACE2 = IPACE + 1 }

CCMPLEX A2, C, CR, CTWC, E1E,
 X11, X12, X13, X14, X15, X16, X17, X18, X19, X110, X111,
 Y11, Y12, Y13, Y14, Y15, Y16, Y17, Y18, Y19, Y110, Y111,
 U22, U23, U24, U25, U26, U27, U28, U29, U210,
 CCMHON / NSIEP, STEP1, IPACE, IPZ, LSLOPE, LISTEP, INAY, NLIPS,
 NSVE, INAY, NBCI, NBI.

```

CCMNCN /REAL/ ALPHABET(5000) BETA1(8 DRMAX){101} BZ(101) C0 FDZ
      C1R1/1512RH/C1EHO21RMAX 'DRMAX' XMAX{101} PRX14.114.
      R111/X1512DR21YR12ZB.ZS '25VP' XMAX{101} ZAEIYR
      CCNCK /CPLX/ A15000/A26(X15000/4) 'CB1(5000)' CTWC(5000).
      BXE,X11,X12,X13,X14,X15,X16,X17,X18,X19,X20,X21,X22,X23,X24,X25,X26,Z27,Z28,Z29,Z210
      U(5000),225,226,227,Z27,Z28,Z29,Z210

C     *** UPDATE IPACE2
C     *** UPDATE Y MATRIX + 1
C     *** YH = A(IPACE)*225 + ZZ6
C     *** UPDATE Y MATRIX, HAIN DIAGONAL, WATER ELEMENT, ONE ROW
C     *** AFACE INTERFACE = 1.0 + DR * XX1H(IPACE-1)
C
C     *** UPDATE RHS
C     CALL RHS
C     *** UPDATE LHS
C     *** UPDATE X MATRIX ELEMENTS ONE ROW ABOVE INTERFACE
C     C{IPACE,1} = XMAX
C     C{IPACE,2} = 1.0 - DR*XX1H(IPACE)
C     *** UPDATE X MATRIX ELEMENTS ON INTERFACE
C     C{IPACE,1} = XMAX
C     C{IPACE,2} = A(IFACE2) * 227 + 228
C     C{IPACE,3} = XH1
C
C     *** SOLVE THE TRIDIAGONAL SYSTEM
C     CALL TRDG(C,U,N,CR,CTWO)
C     *** UPDATE IPACE2
C     IPACE = IPACE2
C     RETURN
C
C     SUBROUTINE UP
C
C THIS SUBROUTINE UPDATES THE RHS & LHS OF THE EQUATION AND
C SOLVES FOR THE SOLUTION FIELD AT RA2.
C {1} THE RHS COLUMN VECTOR VALUES ARE STORED IN C(I,4)
C {2} THE INTERFACE AT RANGE RA1 IS AT GRIDPCINT1(IFACE2)
C {3} THE INTERFACE AT RANGE RA2 IS AT GRIDPCINT1(IFACE2
C WHERE IPACE2 = IPACE - 1

```

```

C  CCMFILE X11,X12,C,CR,CTWC,EYE,XHS,XRI,XRIZ,
C  X11,X12,X13,X14,X15,X16,X17,X18,X19,X1,X1H
C  Y11,Y12,Y13,Y14,Y15,Y16,Y17,Y18,Y19,Y1,X1H
C  U11,U12,U13,U14,U15,U16,U17,U18,U19,U1,X1H
C  D11,D12,D13,D14,D15,D16,D17,D18,D19,D1,X1H
C  I11,I12,I13,I14,I15,I16,I17,I18,I19,I1,X1H
C  P11,P12,P13,P14,P15,P16,P17,P18,P19,P1,X1H
C  R11,R12,R13,R14,R15,R16,R17,R18,R19,R1,X1H
C  CCNHCN /INSLP,/NSV1,BETA1,BETA2,BR{101}B2{101}CO
C  CREAL,CSVP,{1C1},C2CHACAT,(500),DR,DRIVX,DZ,PRC,EDR,FSZ,
C  B11,B12,B13,B14,B15,B16,B17,B18,B19,B1,X1H
C  CCNHCN /CPLX,X11,A15000,A15112,A15124,A15134,A15144,A15154,A15164,A15174,A15184,A15194,A15000),
C  X11,X12,X13,X14,X15,X16,X17,X18,X19,X11H(5000),
C  U11,U12,U13,U14,U15,U16,U17,U18,U19,U1,X1H
C  *** UPDATE IPAC12
C  IPACE2 = IPACE - 1
C  *** DEDATE Y HAIRIX, * MAIN DIAGONAL, INTERFACE ELEMENT
C  Y11 = -A(IPACE)
C  *** DEDATE RHS
C  CALL RHS
C  *** UPDATE LHS
C  *** UPDATE X MATRIX ELEMENTS ONE ROW BELOW INTERFACE
C  C(IPACE,1) = XIRWS
C  C(IPACE,2) = XIRWS
C  *** UPDATE X MATRIX ELEMENTS ON INTERFACE
C  C(IPACE,1) = XLI
C  C(IPACE,2) = -A(IPACE2)
C  C(IPACE,3) = XRI
C  *** SOLVE THE TRIANGULAR SYSTEM
C  CALL TRDG(C,U,N,CR,CTWO)
C  *** DEDATE IPACE
C  IPACE = IPACE2
C  RETUR
C  END
C
C  SUBROUTINE SSLCF
C
C  *** THIS SUBROUTINE IS CALLED TO ADVANCE THE SOLUTION FIELD
C  *** FOR THE CASE OF A MOLEIFIED BOTTOM.

```



```

C      *** MAIN DIAGONAL IN WATER ONE ROW ABOVE INTERFACE
C      IF (ISLOPE.EQ.-5) GO TO 25
C      YMM (IFACE-1) = 1.0 + DR * XX1M (INTERFACE-1)
C      *** UPDATE RHS INTERFACE ELEMENTS
C      YLI = YLIV
C      YNI = 1.0 + DR * ( XX1M (IFACE)/XX4 + XX5 )
C
C      *** UPDATE RHS
C      C (IFACE,1) = -YLI
C      C (IFACE,2) = 2.0 - YMI
C      C (IFACE,3) = -YNI
C      *** SOLVE SYSTEM
C      CALL RHS
C      CALL TB1D (C, U, N, CR, CTW0)
C      GC TO 50
C
C      *** STOPPING SECTION
C      *** UPDATE INTERFACE ELEMENTS
C      YLI = YLIZ
C      XLI = XLIZ
C      XRI = XRIZ
C      *** SOLVE SYSTEM AS APPROPRIATE
C      IF (ISICE.EQ.:4) CALL DOWN
C      IF (ISICPE.EQ.:5) CALL UP
C
C      CCNTINUE
C      RETURN
C      END
C
C      SUBROUTINE RHS
C
C THIS SUBROUTINE MULTIPLIES TRIDIAGONAL MATRIX Y TIMES SCUTION
C FIELD U TO OBTAIN AN UPDATED RHS
C (1) THE RHS COLUMN VECTOR VALUES ARE STORED IN C(I,4) .
C
C CCMFIX X11,X12,X13,X14,X15,X16,X17,X18,X19,X1Z,X1Y,X1Z,X1Y,X1Z,
C      X11,X12,X13,X14,X15,X16,X17,X18,X19,X1Z,X1Y,X1Z,X1Y,X1Z,
C      X11,X12,X13,X14,X15,X16,X17,X18,X19,X1Z,X1Y,X1Z,X1Y,X1Z,
C      U125,U126,U127,U128,U129,U130
C      CCEHNCN /IN/141BOT1.1FACE1NP2/ISLOPE,1STEP,1NSVPSMAX,NLFS,
C      NSIEP,1STEP,1NSVPSMAX,NLFS,1STEP,1NSVPSMAX,NLFS,1STEP,1NSVPSMAX,NLFS,
C      CCEHNCN /REAL/ALPHA1,BETA1,BETA2,BR1C1)B2(10),C0,DR,DRIVL,DRMAX,DZ,FRQ,DR,EEZ.
C      CSVP(101),C2,CWATER(5000),DR,DRIVL,DRMAX,DZ,FRQ,DR,EEZ.

```

```

* B11RA165BHC1BHO2BRMAX THETA(XX0,XX2,XX4,XX10,
* XX11,XX12,XX13,XX14,XX15,XX16,XX17,XX18,XX19,XX20,
* CPLEX /CPLX /A15000 /A2S(5000,4) /CR(5000),CTW(5000),
* EX1,XR1,XR12,XR13,XR14,XR15,XR16,XR17,XR18,XR19,XR10,
* Y11,Y12,Y13,Y14,Y15,Y16,Y17,Y18,Y19,Y10,
* U(5000),225,226,227,228,229,2210,
* C *** UPDATE IPACEN & IFACEPP
*      IPACEN = IFACE - 1
*      IFACEP = IFACE + 1
*      DATE RHS
*      C(I4) = U(1) * YMH(I) + U(2) * YMWS
*      DC10 I=2,IPACEN = U(I) * YMH(I) + (U(I-1)+U(I+1)) * YMWS
*      C(I4) = U(I) * YMH(I) + (U(I-1)+U(I+1)) * YMWS
*      COUNT(NBE,4) = U(IPACEN)*YLI + U(IFACE)*YMI + U(IFACEF)*YFI
*      DC20 I=IPACEP NN1
*      C(I4) = U(I)*YMS + (U(I-1)+U(I+1)) * YMWS
*      COUNT(NBE
* C RETURN
* END
* C
* CCCCCC SUBROUTINE LEVEL
* THIS SUBROUTINE UPDATES THE RHS OF THE EQUATION AND SOLVES
* FOR THE SOLUTION FIELD A RANGE RA2.
* {1} THE RHS COLUMN VECTOR VALUES ARE STORED IN C(I4)
* {2} FOR THE LEVEL INTERFACE THE LHS TRIDIAGONAL MATRIX
* ELEMENTS NEED NOT BE UPDATED.
* CCFILEX A12 CCB CTHC EYE
* X1,X12,X13,X14,X15,X16,X17,X18,X19,X112,X11M
* X11,X110,X111,X112,X113,X114,X115,X116,X117,X118,X119,X11M
* U225 I=226 IP2 Z228 Z229 Z210
* ISLOPE,1STEP.
* CCNHCN /1STEP. MSTEP1,NSVE,NMAX,NXIFS
* CCNHCN /REAL/ ALPHABET(5000),BET(5000),DRIVL,DMAX,F2,F0,F2Z,
* CSVP /IC1/ C2CHATER(5000),DRIVL,DMAX,F2,F0,F2Z,
* B11RA165BHC1BHO2BRMAX THETA(XX0,XX2,XX4,XX10,
* XX11,XX12,XX13,XX14,XX15,XX16,XX17,XX18,XX19,XX20,
* CPLEX /CPLX /A15000 /A2S(5000,4) /CR(5000),CTW(5000),

```

```
*** XX1,XX2,XX3,XX5,XX6,XX7,XX8,XX9,XX10,XX11(5000),YRI,XX14(5000),YRI,  
C U(5000),Z25,Z26,Z27,Z28,Z29,Z210,XX15(5000),YRI,XX16(5000),YRI.
```

```
*** UPDATE RHS  
CALL RHS
```

```
*** SOLVE THE TRIDIAGONAL SYSTEM  
CALL TRIDDL (C,U,N,CR,C TWO)  
RETURN
```

```
C C CCCCCCCCC
```

SUBROUTINE PRIM12

- (1) THIS SUBROUTINE IS EFFECTIVELY THE CONTINUATION OF SUBROUTINE PRINT1.
- (2) THE PPII CREATED CORRESPONDS TO UNIT FILE NUMBER: NPCUT = 55.
- (3) THE FILENAME AND FILETYPE FOR THIS FILE ARE: IPICUT PTRINTER

```
DIMENSION FRIAG(5000), PIRD(121,121)  
CCEFILEX A2,CRACT,6 PFILE, XMS,XRI,XRIZ,  
* X1,X2,X3,X4,X5,X6,X7,X8,X9,X10,X11,  
* X12,X13,X14,X15,X16,X17,X18,X19,X10,X11,  
* X12,X13,X14,X15,X16,X17,X18,X19,X10,X11,  
* X12,X13,X14,X15,X16,X17,X18,X19,X10,X11,  
* U11,I1,I2,I3,I4,I5,I6,I7,I8,I9,I10,I11,  
* CCNNCN /IN/ ,T1,BOT1,1STEP,1W2,N,NA,NBOT,NN1,  
* INSIEP,AIEPA,ATT(500),BETA2,BR(101),BZ(101),CO  
* CCNNCN /REAL/AIEPA,ATT(500),BETA1,DRDRIV1,DHMAX,FZ,PRC,EG,EC,  
* CSVP,(IC1),C2,CRA1ER(500),  
* R1,I1,I2,I3,I4,I5,I6,I7,I8,I9,I10,I11,I12,I13,I14,I15,I16,I17,  
* I1,I2,I3,I4,I5,I6,I7,I8,I9,I10,I11,I12,I13,I14,I15,I16,I17,  
* R1,I1,I2,I3,I4,I5,I6,I7,I8,I9,I10,I11,I12,I13,I14,I15,I16,I17,  
* PIRD,CSVP,CPLEX,A2,A(5000),A2,C(5000),CR(5000),CTWO(5000),  
* EY1,EY2,EY3,EY4,EY5,EY6,EY7,EY8,EY9,EY10,EY11,EY12,EY13,EY14,EY15,EY16,EY17,  
* Y11,Y12,Y13,Y14,Y15,Y16,Y17,Y18,Y19,Y110,Y111,Y112,Y113,Y114,Y115,Y116,Y117,Y118,Y119,  
* R1,I1,I2,I3,I4,I5,I6,I7,I8,I9,I10,I11,I12,I13,I14,I15,I16,I17,I18,I19,I110,I111,I112,I113,I114,I115,I116,I117,I118,I119,I120,  
* DATA POUT(55),
```

```
*** ELINT RANGE  
IF(RA2.LT. 1398.0) - CR-(RA2 .GT. 2002.0)) GO TO 30  
IPD15260
```

```
C C
```

```

C      WRITE(NPOUT,900) RA2
C      I5 = 1E+15
C      *** COMPUTE AND PRINT PROPAGATION LOSS AT EACH IPZTH DEPTH
C      WRITE(NPOUT,901)
C      I1 = 0
C      DC 20 I=IPZN,IPZ
C      Z1 = I*D2
C      I211 = LAT(Z1,YE1)
C      PLF = CAFS(D1,I)
C      IF (PLF .LT. 0.0) GO TO 10
C      PL = -20.0*ALOG10(PL) + 10.0*ALOG10(R12)
C      GO TO 15
C      PL = 999.9
C      CONTINUE
C      PRMAG(I1) = CAB5(U(I1))
C      IF(Z1 .GT. 1210) GO TO 20
C      WRITE(Z1,902) Z1, PL, PRMAG(I1)
C      TIPI = I1 + 1
C      DIFD(I1,IR) = PI
C      PIFD(I1,IR) = PRMAG(I1)*100
C      CONTINUE
C      IF(RA2.GT.1990.0) WRITE(31,36) (ATT(I),I=1,4000)
C      FCENAT(7F10.5)
C      *** DETERMINE NEXT RANGE AT WHICH TO PRINT SOLUTION
C      IER = XPR+FIR
C      30
C      36
C      900
C      ECENAT(15X,'5X'RANGE='F9.36' 'H'14') , 'PRMAG(I)',/
C      901
C      ECENAT(10X,F10.2,36,F10.2,13X,E12.5)
C      902
C      ECENAT(15X,'5X'DEPTH='LSS(0B)' 'H'14') , 'PRMAG(I)',/
C
C      RETURN
C
C      SUBROUTINE WRITE2
C
C      (1) THIS SUBROUTINE IS EFFECTIVELY THE CONTINUATION OF
C          SUBROUTINE WRITE1
C      (2) THE SUBROUTINE WRITES RECEIVED DEPTH AND U(I)
C          WHEN CALLED. IT THEN UPDATES THE NEXT RANGE (XWR).
C          (3) THE FILE WRITTEN INTO CORRESPONDS TO UNIT FILE NUMBER:
C              NOU = I5743

```


RETURN
END

SUBROUTINE END (RA2)

THIS SUBROUTINE IS CALLED WHEN THE SOLUTION FIELD HAS REACHED THE MAXIMUM RANGE SPECIFIED (RMAX). THE SUBROUTINE SENDS APPROPRIATE MESSAGES TO THE TERMINAL AND STOPS EXECUTION.

WRITE(6,899) R12
WRITE(6,900)
WRITE(6,901)

C
899 FORMAT(1X,'THE PROGRAM HAS REACHED RANGE R = ',F8.1,' METERS.')
900 FCENAT(1X,'END OF RUN')
* * * * *
* 1C1* (A) OUTFILE IS FORMATTED. OUTPUT HAS BEEN GENERATED. //.
* 1C1* (B) THIS FILE IS READY TO BE SENT TO THE PRINTER. //.
* 1C1* (C) THE FILENAME AND FILETYPE FOR THIS FILE ARE: //.
* 1C1* (D) OUTFILE IS FORMATTED. OUTPUT HAS BEEN GENERATED. //.
* 1C1* (E) THIS FILE CONTAINS INPUT DATA FOR THE PLOT ROUTINE. //.
* 1C1* (F) THE FILENAME AND FILETYPE FOR THIS FILE ARE: //.
* 1C1* (G) THE FILENAME AND FILETYPE FOR THE PLOT ROUTINE ARE: //.
* 1C1* (H) THE PLOTTYPE AND FORTRAN //.
* 1C1* (I) THE PLOTTYPE AND FORTRAN //.
* 1C1* (J) THE PLOTTYPE AND FORTRAN //

RETURN
END

THEN FOLLOW PROGRAM PROMPTS. //

APPENDIX B
TL CONICUR PLCT PROGRAM LISTING

```
*****PL000010
*****PL000020
*****PL000030
*****PL000040
*****PL000050
*****PL000060
*****PL000070
*****PL000080
*****PL000090
*****PL000100
*****PL000110
*****PL000120
*****PL000130
*****PL000140
*****PL000150
*****PL000160
*****PL000170
*****PL000180
*****PL000190
*****PL000200
*****PL000210
*****PL000220
*****PL000230
*****PL000240
*****PL000250
*****PL000260
*****PL000270
*****PL000280
*****PL000290
*****PL000300
*****PL000310
*****PL000320
*****PL000330
*****PL000340
*****PL000350
*****PL000360
*****PL000370
*****PL000380

*** THE FOLLOWING IS A GRAPHICS PACKAGE TO DC CONTOURING

*** 11 MARK E. KOSNIK
*** U.S. NAVAL ECST GRADUATE SCHOOL
*** MCENTERY, CA 93943

*** ALPHABETICAL LISTING OF VARIABLES
*** DATA - ARRAY TO STORE VALUES TO BE CONTOURED
*** DATA - ARRAY TO STORE VALUES READ IN FROM LIFE PROGRAM
*** N - INTEGER VALUE FOR NUMBER OF DEPTH INCREMENTS

DIMENSION VARIABLES MUST USE A SQUARE ARRAY FOR PROPER CONTOURING)
REAL DATA(121,121),A(121,121),
INTEGER N,121,I,J

C COMMON   WC6K(200 00)
C
C READ IN TL VALUES GENERATED BY THE IFD.
C READ(1,600){DATA(I,J),I=1,N},J=1,N
600  FCBKA{1,600}{DATA(I,J),I=1,N},J=1,N
      READ(2,600){DATA(I,J),I=1,N},J=1,N

C PAMULATE ARRAY IN PROPER FORMAT TO BE CONTOURED.
DC 10 I = 1,N
DC 11 = N - (1-1)
DC 2 C J = (1-1)
```

20

```
    C CM41DE = DATA (11,J)
    C CCATINDE
    C ECTING/GRAPHICS ROUTINE.
    C CALL TEK618
    C CALL CCMPRS
    C CALL FAGE(11,0,{E,5})
    C CALL FLOWUP({1,-C,-5})
    C CALL AREA2D({8,C,6,0})
    C CALL FEIGHT({-2})
    C CALL XNAME({{B} ANGE {{}} M {{}} S!;100})
    C CALL SWISSHE({90,-30,-1,0,0,2,1})
    C CALL FEIGHT({-30,{ST!}}
    C CALL FASALE({-5,{AND}})
    C CALL MIXALN({-11,C)ONTOURS},100,1.,1)
    C CALL FEIGHT({-2})
    C CALL MESSAGE({{F} FIGURE 1{{}} 100,3.5-10-75})
    C CALL MESSAGE({{F} 100,1,4,6,40),100,1,4,6,40)
    C CALL YAXANG({0,0})
    C CALL FEIGHT({0,0})
    C CALL RESET({S1155M})
    C CALL GRAP({400,0,100,0,2000,0,121,-20,0,1,0})
    C CALL ECODOM({20,0,0,0})
    C CALL FEIGHT({0,-125})
    C CALL CONMAK({A},{N,1})
    C CALL CONLIN({O},{offb},{LABELS},1,10)
    C CALL CCNANG({90,-30,-1})
    C CALL FASPLN({2,-C})
    C CALL LINEAR(1,'IAEELS','DRAW')
    C CALL CCNTUR(1,'IAEELS','DRAW')
    C CALL LOTD(11)
    C CALL GRID(16,1)
    C CALL ENDPL(16)
    C CALL LONEPI
    EN
```

114

APPENDIX C
RUNNING THE CONTOUR PLOT ON THE NPS COMPUTER

A. INTRODUCTION

This Appendix describes a procedure for running the TL contour plot on the NPS computer. Detailed instructions for running the IFD program can be found in Jaeger(1983).

B. COPYING THE FILE FOR USE

Once the TL values have been generated by the IFD program, all that is needed to produce a TL contour plot is the file PICTS FORTRAN. This file is shown in Appendix E and can be copied from a computer account maintained by the Underwater Acoustics Curriculum. To link with this account and obtain a copy of the file, the user should proceed as follows:

- (1) Log on terminal.
- (2) Enter: CP LINK 0160P 191 195 &R .
- (3) When prompted for the read password enter: UX .
- (4) Enter: ACC 195 C .
- (5) Enter: COPY PICTS FORTRAN C = A .

At this point the PICTS FORTRAN file should reside on the user's A disk.

C. RUNNING THE PROGRAM

Before running the program the user must obtain the TL values from the IFD program. These TL values must be sent to

a data disk in order for the FICIS program to be able to use them. This can be done by placing a WRITE statement in the IFD program that sends the values to a data disk. The modified IFD depicted in Appendix A uses this technique and can be used as a guide.

Once the data disk has been created, the user must assign temporary disk space (IDISK) to give the program sufficient room to generate the IL contours. For more information on how to assign temporary disk space, see NPS Technical Note TN-VM-C1 which is available in the computer consultant's office.

With these initial steps completed, all that remains is to compile and run the program. The program can be compiled by:

Enter: FCRTGI PLOTS .

The program must be run at the TEK618 graphics terminal under DISSPLA. This can be done by:

Enter: DISSPLA .

The user will then be prompted for the compiled Fortran program name and the file definitions for the data disk, before the program will run.

APPENDIX D

SOURCE DEPTH SENSITIVITY ANALYSIS

During the laboratory experiment, two supplemental sets of measurements were taken to obtain an indicator of the sensitivity of the pressure amplitude to changes in the source depth. The first set of measurements was obtained by varying the source depth with the receiver fixed at 1.0X (4.8 cm from the beach), and lowered in depth to the bottom. For the second set of measurements, the receiver was fixed at the third dump distance (14.4 cm from the beach), and measurements were taken with the source fixed at 5, 7, 9, 11, 13, 15, 17, 19, 21, 23, 25, 27, 29, and 31 cm from the surface.

The results of the first analysis are shown in Figure D.1. In the figure, pressure was normalized by dividing by the maximum pressure and depth was normalized by dividing by the depth of the water column. Although theory predicts only one propagating mode at this distance, the results show modal phase interference.

The results of the second analysis are shown in Figure D.2 through Figure D.6. In the figures, each curve represents a set of measurements taken with the source fixed at a specific depth. For convenience, more than one curve is shown on a given figure. All pressure values were normalized by dividing by the maximum pressure in the field. The depth values were normalized by dividing by the maximum water depth.

In general, at 1.0X there appears to be modal phase interference which is influenced by source depth. Given the roughness of this analysis, the details of this interference are obscure. However, the modal interference does not appear

to be inconsistent with either the placement of the source
or with the previous experimental measurements.

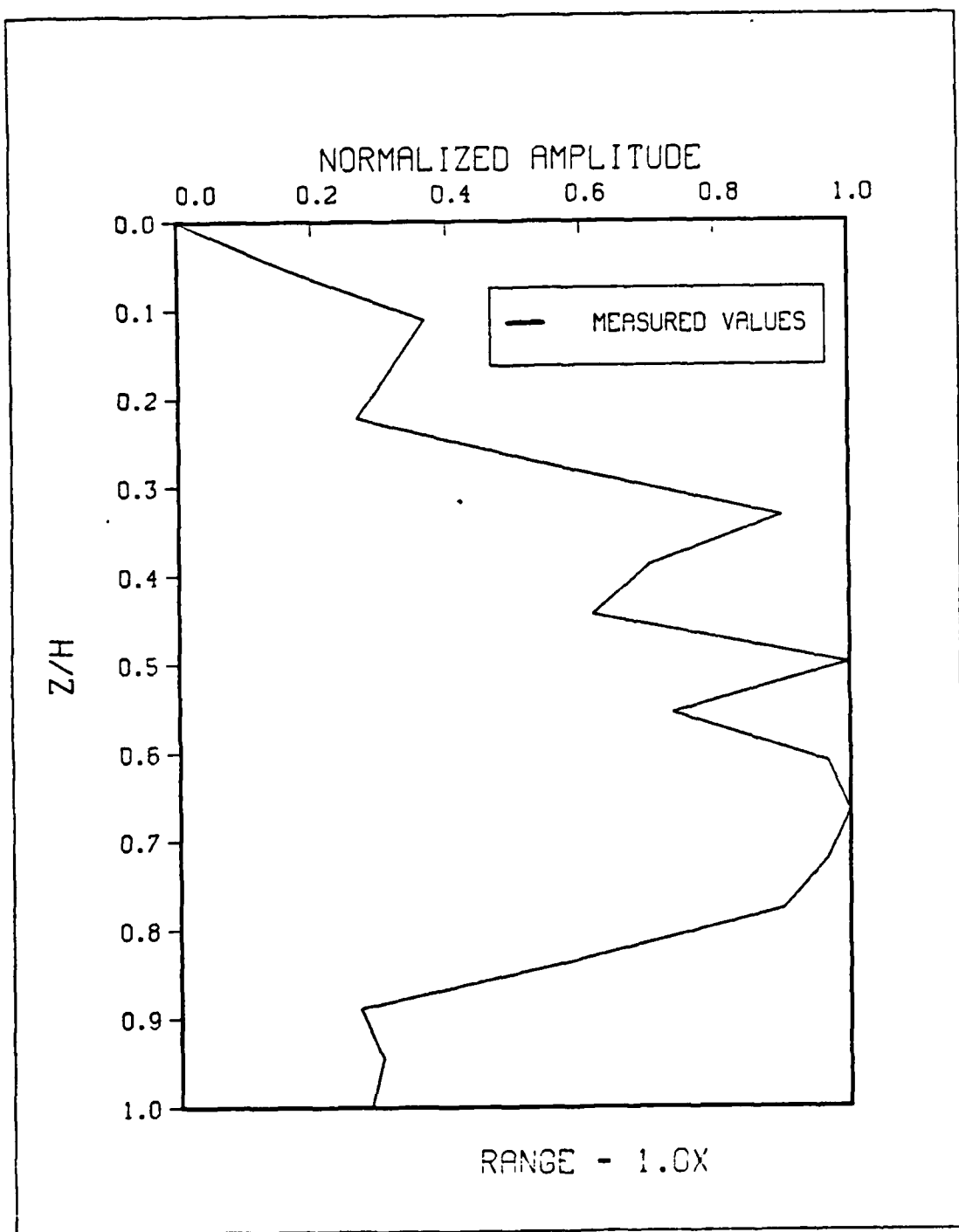


Figure D.1 Source Sensitivity Analysis at 1.0X.

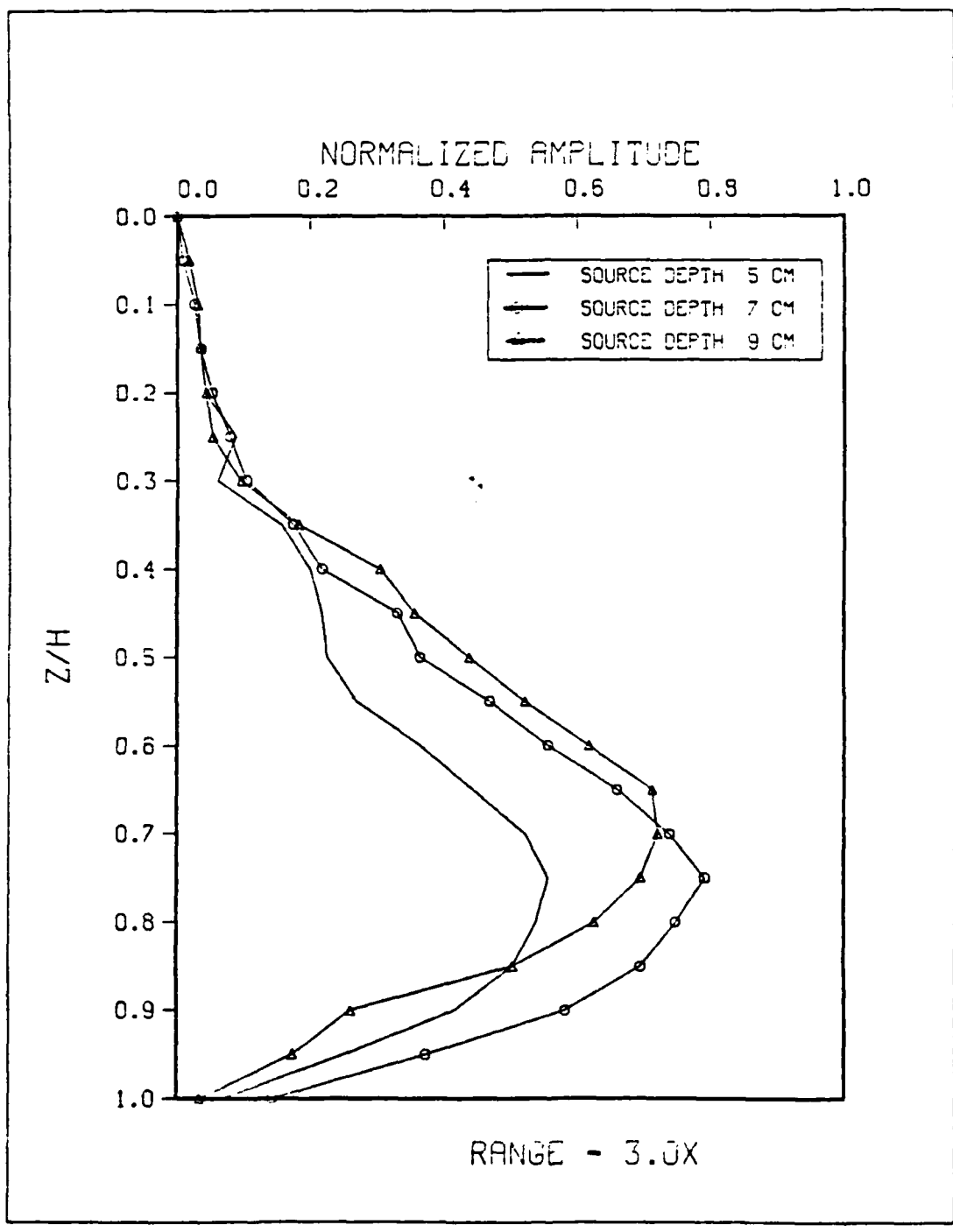


Figure D.2 Measurements with Source Depth of 5, 7, and 9 Cm.

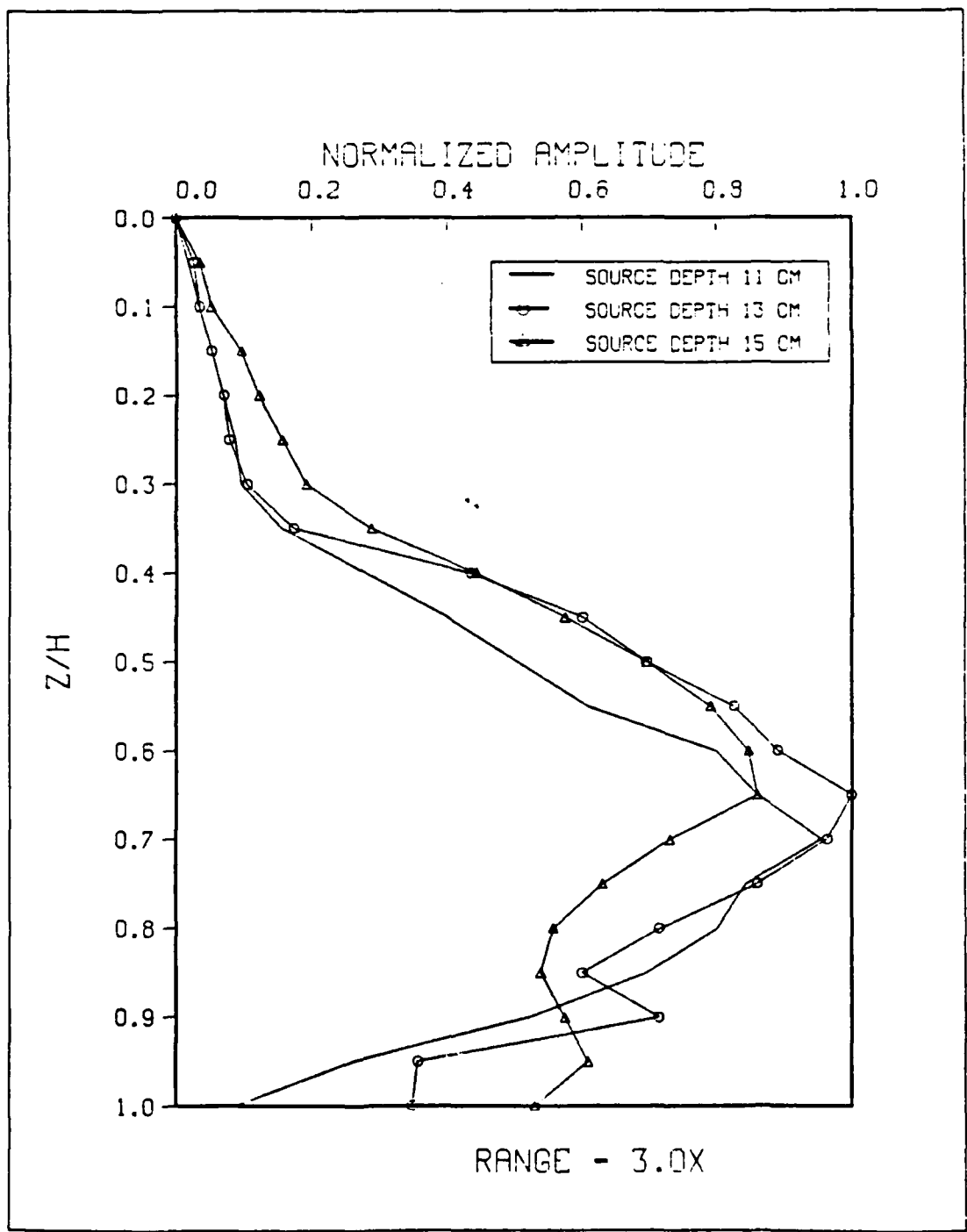


Figure D.3 Measurements with Source Depth of 11, 13, and 15 cm.

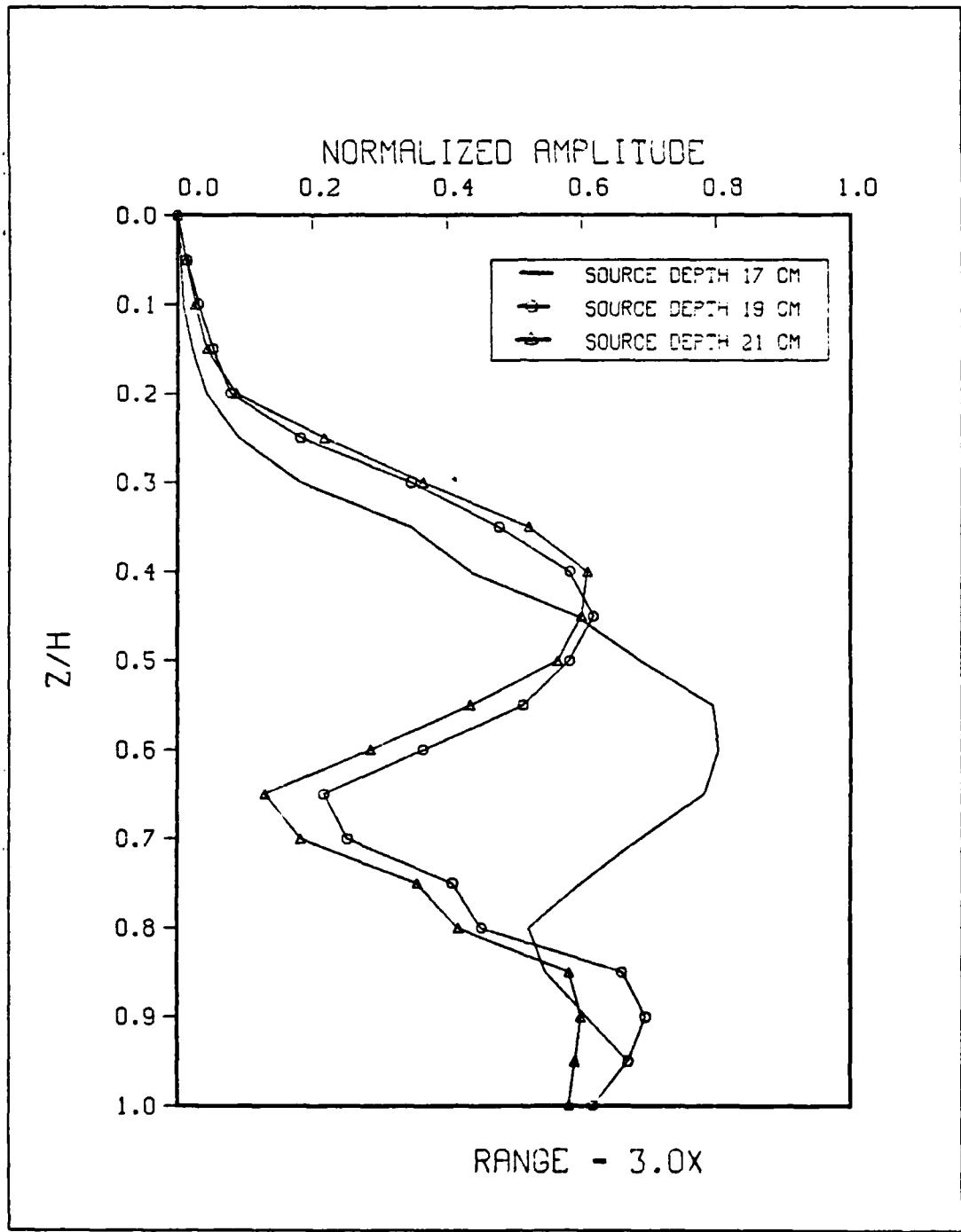


Figure D.4 Measurements with Source Depth of 17, 19, and 21 Cm.

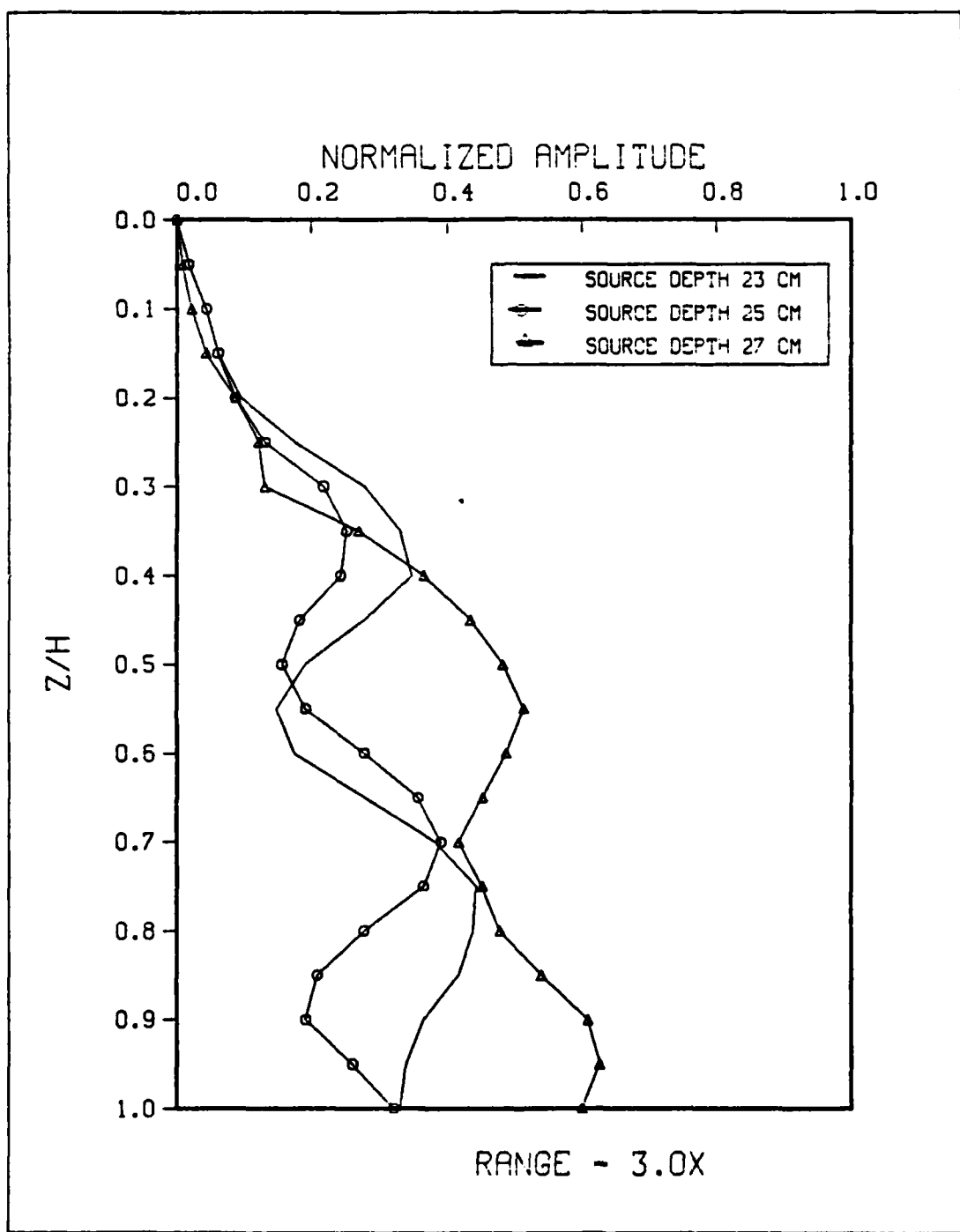


Figure D.5 Measurements with Source Depth of 23, 25, and 27 Cm.

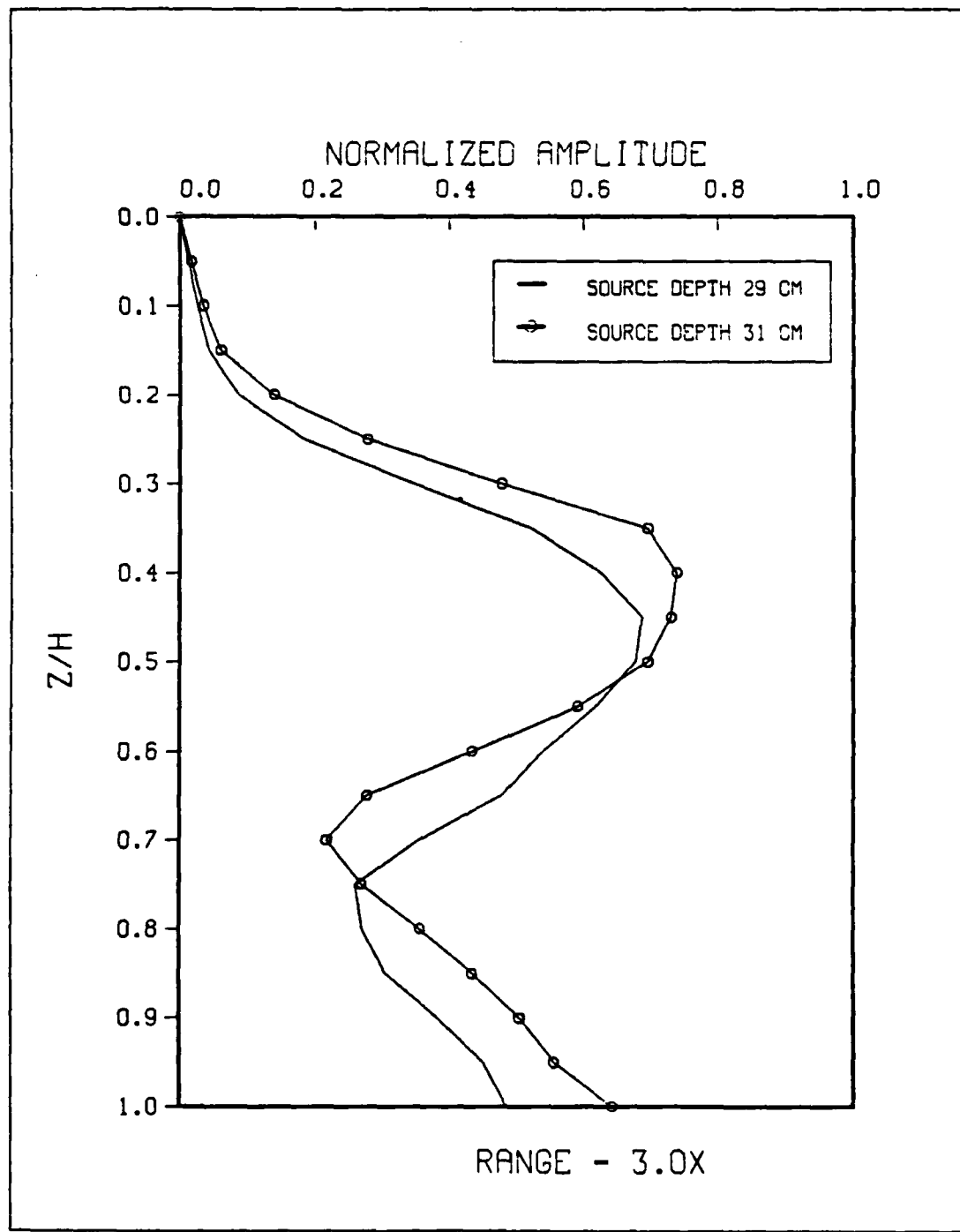


Figure D.6 Measurements with Source Depth of 29 and 31 Cm.

BIBLIOGRAPHY

- Anderson, C.L., and Liebermann, R.C., "Sound Velocities In Rocks And Minerals," Physical Acoustics, IV-B, Edited by K.P. Maran, Academic Press, 1968.
- Faek, C.K., The Accustic Pressure In A Wedge-Shaped Water Layer Overlying A Fast Fluid Bottom, Master's Thesis, Naval Postgraduate School, March, 1984.
- Fradshaw, J.A., Laboratory Study Of Sound Propagation Into A Fast Fluid Medium, Master's Thesis, Naval Postgraduate School, June, 1981.
- Frock, H.K., The AESD Parabolic Equation Model, NCSDA Technical Note 12, January, 1978.
- Coppens, A.E., Humphries, and Sanders, J.V., "Propagation Of Sound Out Of A Fluid Wedge Into An Underlying Fluid Substrate Of Greater Sound Speed", Accepted for Publication by JASA, May 1984.
- Coppens, A.E., and Sanders, J.V., "Propagation Of Sound From A Fluid Wedge Into A Fast Bottom," PLENUM, 1980.
- Coppens, A.E., Sanders, J.V., Iannou, G.I., and Kawamura, M., Two Computer Programs For The Evaluation Of The Accustic Pressure Amplitude And Phase At The Bottom Of A Wedge Shaped Fluid Layer Overlaying A Fast Fluid Half Space, Naval Postgraduate School Technical Report NPS-61-75-002, December, 1978.
- Graves, R.F., Nagel, A., Überall, H., and Zauer, G.I., "Range Dependent Normal Modes In Underwater Sound Propagation: Application To A Wedge Shaped Ocean," JASA, Vol. 58, December 1975.
- Hardin, R.H., and Tappert, F.D., "Applications Of The Split Step Fourier Method To The Numerical Solution On Nonlinear And Variable Coefficient Wave Equations," SIAM Review, Vol. 15, 1973.
- Jaeger, L.E., A Computer Program For Solving The Parabolic Equation Using An Implicit Finite-Difference Solution Method Incorporating Exact Interface Conditions, Master's Thesis, Naval Postgraduate School, September, 1983.
- Jensen, F.B., and Kuperman, W.A., Environmental Accustical Modeling At SACLANTCEN, SACLANTCEN Report SH-34, November, 1979.
- Jensen, F.B., and Kuperman, W.A., "Sound Propagation In A Wedge-Shaped Ocean With A Penetrable Bottom," JASA, Vol. 67, May, 1980.
- Jenser, F.B., and Krol, H., The Use Of The Parabolic Equation Method In Sound Propagation Modelling, SACLANTCEN Memorandum SH-72, August, 1975.
- Kawamura, M., and Iannou, J., Pressure On The Interface Between A Converging Fluid Wedge And A Fast Fluid Bottom, Master's Thesis, Naval Postgraduate School, December, 1978.

Kinsler, L.F., Frey, A.R., Coppens, A.B., AND Sanders, J.V.,
Fundamentals Of Acoustics, Third Edition, John Wiley and
Sons, 1972.

Lee, I., and Botseas, G., IEC: An Implicit Finite-Difference
Computer Model For Solving The Parabolic Equation, NTSC
Technical Report 6659, May, 1982.

Lee, I., Botseas, G., and Papadakis, J.S., "Finite-Difference
Solution To The Parabolic Equation," JASA, Vol. 70,
September, 1981.

Lee, I., and McDaniel, S.T., "A Finite-Difference Treatment
Of Interface Conditions For The Parabolic Equation: The
Irregular Interface," JASA, Vol. 73, May, 1983.

Lee, D., and Papadakis, J.S., Numerical Solutions Of
Underwater Acoustic Wave Propagation Problems, NTSC
Technical Report 5929, February, 1979.

IeSesre, F., Personal Communication, 11 May 1984.

McDaniel, S.T., and Lee, D., "A Finite-Difference Treatment
Of Interface Conditions For The Parabolic Equation: The
Horizontal Interface," JASA, Vol. 71, April, 1982.

INITIAL DISTRIBUTION LIST

	No. Copies
1. Defense Technical Information Center Cameron Station Alexandria, Virginia 22314	2
2. Library, Code 0142 Naval Postgraduate School Monterey, California 93943	2
3. Commanding Officer ATIN: LT Mark E. Kosnik SWCS CCOM SWC Delt HD Class 85, CICVN 1 OCT 84 Newport, Rhode Island 02841	2
4. Superintendent ATIN: Mr. J.V. Sanders, Code 61 Sd Naval Postgraduate School Monterey, California 93943	8
5. Superintendent ATIN: Mr. A.B. Cappens, Code 61 Cz Naval Postgraduate School Monterey, California 93943	2
6. Superintendent ATIN: LCDR C.R. Lunlap, USN(Ret), Code 68 DJ Naval Postgraduate School Monterey, California 93943	3
7. Superintendent ATIN: Dr. C.K. McCoers, Code 68 MR Chairman, Department of Oceanography Naval Postgraduate School Monterey, California 93943	1
8. Chief of Naval Research ATIN: Mr. Michael McKissick 200 N. Quincy St. Arlington, Va 22217	1
9. Eugene W. Brown NAVCCEANO Code 7300 Bay St. Louis, MS 39522	1
10. Commanding Officer ATIN: Mr. James Andrews Naval Ocean Research and Development Activity NSRI Station Bay St. Louis, MS 39522	1
11. Commanding Officer ATIN: Mr. T.N. Lawrence, Code 323 Naval Ocean Research and Development Activity NSRI Station Bay St. Louis, MS 39522	1

12. Commanding Officer
Attn: Mr. Robert Gardner
Naval Ocean Research and Development Activity
NSRDA Station
Bay St. Louis, MS 39522

1

END

FILMED

3-85

DTIC